

1988

Application of pulsed amperometric detection to reversed phase high performance liquid chromatography of some sulfur-containing pesticides

Aporn Ngoviwatchai
Iowa State University

Follow this and additional works at: <https://lib.dr.iastate.edu/rtd>

 Part of the [Analytical Chemistry Commons](#)

Recommended Citation

Ngoviwatchai, Aporn, "Application of pulsed amperometric detection to reversed phase high performance liquid chromatography of some sulfur-containing pesticides " (1988). *Retrospective Theses and Dissertations*. 9704.
<https://lib.dr.iastate.edu/rtd/9704>

This Dissertation is brought to you for free and open access by the Iowa State University Capstones, Theses and Dissertations at Iowa State University Digital Repository. It has been accepted for inclusion in Retrospective Theses and Dissertations by an authorized administrator of Iowa State University Digital Repository. For more information, please contact digirep@iastate.edu.

INFORMATION TO USERS

The most advanced technology has been used to photograph and reproduce this manuscript from the microfilm master. UMI films the original text directly from the copy submitted. Thus, some dissertation copies are in typewriter face, while others may be from a computer printer.

In the unlikely event that the author did not send UMI a complete manuscript and there are missing pages, these will be noted. Also, if unauthorized copyrighted material had to be removed, a note will indicate the deletion.

Oversize materials (e.g., maps, drawings, charts) are reproduced by sectioning the original, beginning at the upper left-hand corner and continuing from left to right in equal sections with small overlaps. Each oversize page is available as one exposure on a standard 35 mm slide or as a 17" x 23" black and white photographic print for an additional charge.

Photographs included in the original manuscript have been reproduced xerographically in this copy. 35 mm slides or 6" x 9" black and white photographic prints are available for any photographs or illustrations appearing in this copy for an additional charge. Contact UMI directly to order.



300 North Zeeb Road, Ann Arbor, MI 48106-1346 USA



Order Number 8625425

**Application of pulsed amperometric detection to reversed
phase high performance liquid chromatography of some
sulfur-containing pesticides**

Ngoviwatchai, Aporn, Ph.D.

Iowa State University, 1988

U·M·I
300 N. Zeeb Rd.
Ann Arbor, MI 48106



**Application of pulsed amperometric detection
to reversed phase high performance liquid chromatography
of some sulfur-containing pesticides**

by

Aporn Ngoviwatchai

**A Dissertation Submitted to the
Graduate Faculty in Partial Fulfillment of the
Requirements for the Degree of
DOCTOR OF PHILOSOPHY**

**Department: Chemistry
Major: Analytical Chemistry**

Approved:

Signature was redacted for privacy.

In Charge of Major Work

Signature was redacted for privacy.

For the Major Department

Signature was redacted for privacy.

For the Graduate College

**Iowa State University
Ames, Iowa**

1988

TABLE OF CONTENTS

	Page
I. INTRODUCTION	1
II. REVIEW OF PERTINENT LITERATURE	5
A. Classification of Sulfur-containing Pesticides	5
1. Introduction	5
2. Classification	6
B. Oxidation of Sulfur-containing Pesticide	14
1. Chemical oxidation	14
2. Photooxidation	19
3. Electrochemical oxidation	20
C. Pesticide Analytical Methodology	22
1. Introduction	22
2. Classical methods	23
3. Gas Chromatography	25
4. High Performance Liquid Chromatography	26
D. Electrochemical Detection of Sulfur Compounds at Gold Electrode	29
1. Investigation of the electrochemical oxidation of sulfur compounds at gold electrodes	29
2. Electrochemical detection of sulfur-containing pesticides following HPLC separations	34
3. Theory and applications of pulsed amperometric detection	38

II. EXPERIMENTAL	44
A. Chemical	44
B. Instrumentation	44
1. Voltammetric studies	44
2. Coulometric studies	45
3. Flow-injection studies	51
4. High Performance Liquid Chromatography (HPLC)	54
IV. CYCLIC VOLTAMMETRY OF SULFUR COMPOUNDS AT GOLD ELECTRODES IN ALKALINE SOLUTIONS	61
A. Introduction	61
B. Concentration Dependence	61
C. Rotation Speed and Scan Rate Dependence	65
D. Effect of Negative Potential Scan Limits	65
E. Proof of Adsorption	66
F. Conclusion	72
V. CHRONOCOULOMETRIC STUDY OF SULFUR COMPOUNDS AT A GOLD ELECTRODE IN A THIN-LAYER CELL	73
A. Introduction	73
B. Determination of the cell Volume	78
C. Determination of the Number of Electrons Transferred	86
D. Identification of the Oxidation Products	104
E. Determination of the Adsorption Isotherm	109
F. Coulometric Study of some other Sulfur Compounds	110
G. Conclusion	115

VI.	FLOW-INJECTION ELECTROCHEMICAL DETECTION OF SULFUR COMPOUNDS IN ALKALINE SOLUTIONS	117
A.	Introduction	117
B.	Flow-injection Electrochemical Detection of Sodium Thiophosphate	118
C.	Calibrations	124
D.	Dependence of the Peak Shape on Waveform and Analyte Concentration	128
E.	Conclusion	134
VII.	CYCLIC VOLTAMMETRY OF SULFUR-CONTAINING PESTICIDES IN 50% ACETONITRILE/ACETATE BUFFER AT GOLD ELECTRODES	135
A.	Introduction	135
B.	Acetate Buffer with Acetonitrile Added	136
C.	50% Acetonitrile/Acetate Buffer with Pesticides Added	140
D.	Dependence on Rotational Speed and Potential Scan Rate	145
E.	Proof of Adsorption of Dimethoate on Gold	148
F.	Conclusion	153
VIII.	FLOW-INJECTION DETECTION OF SULFUR-CONTAINING PESTICIDES WITH PULSED AMPEROMETRIC DETECTION AT GOLD ELECTRODES	157
A.	Introduction	157
B.	Optimization of 2-step PAD Waveform	158
C.	Calibrations	162
D.	Limits of Detection for Selected Pesticides	162
E.	Electrode Fouling at Continuous Flow of Analytes	167
F.	Conclusion	171

IX.	HIGH PERFORMANCE LIQUID CHROMATOGRAPHY WITH PULSED AMPEROMETRIC DETECTION OF SULFUR-CONTAINING PESTICIDES	172
A.	Introduction	172
B.	Chromatography	175
C.	Analysis of a Real-life Sample	179
D.	Conclusion	179
X.	C-18 REVERSED PHASE TRACE ENRICHMENT OF PESTICIDES	183
A.	Introduction	183
B.	Determination of the Capacity of the Forecolumn	186
C.	Preconcentration and Calibration	187
D.	Determination of Forecolumn Efficiency	195
E.	Conclusion	198
XI.	SUMMARY	200
XII.	SUGGESTED FUTURE RESEARCH	203
XIII.	BIBLIOGRAPHY	206
XIV.	ACKNOWLEDGEMENTS	214

LIST OF FIGURES

Figure III-1.	Coulometric gold thin-layer cell	46
Figure III-2.	Coulometric flow system	49
Figure III-3.	Gold flow-through cell	52
Figure III-4.	Preconcentration flow system	56
Figure III-5.	Closed-loop system for determination of absolute efficiency of the forecolumn	58
Figure IV-1.	Current-potential curves for sodium thiophosphate by cyclic voltammetry at a gold RDE in 0.1 M NaOH as a function of added sodium thiophosphate	62
Figure IV-2.	Current-potential curves for sodium thiophosphate as a function of negative potential limits by cyclic voltammetry at a gold RDE in 0.1 M NaOH	67
Figure IV-3.	Current-potential curves for sodium thiophosphate demonstrating adsorption on a gold RDE by cyclic voltammetry in 0.1 M NaOH	70
Figure V-1.	Current-potential curve for $\text{Fe}(\text{CN})_6^{3-}/\text{Fe}(\text{CN})_6^{4-}$ system by cyclic voltammetry in 0.1 M NaOH at a gold electrode in a thin-layer cell	79
Figure V-2.	Current-time curves for electrolysis of $\text{Fe}(\text{CN})_6^{4-}$ solutions at a gold electrode in a thin-layer cell	82
Figure V-3.	Coulometric data for $\text{Fe}(\text{CN})_6^{4-}$ as a function of concentration at a gold electrode in a thin-layer cell	84
Figure V-4.	Current-potential curves for sodium thiophosphate by cyclic voltammetry at a gold electrode in a thin-layer cell	87
Figure V-5.	Current-time curves for sodium thiophosphate by double-potential step coulometry at a gold electrode in a thin-layer cell	92

Figure V-6.	Current-time curves for sodium thiophosphate demonstrating determination of Q_{total} and Q_{ads} by coulometry at a gold electrode in a thin-layer cell	95
Figure V-7.	Plots of $\log Q$ vs. $\log N_{total}$ for sodium thiophosphate in 0.1 M NaOH	99
Figure V-8.	P-31 NMR chemical shifts for standard SPO_3^{3-} , PO_4^{3-} and PO_3^{3-} and the product solution after exhaustive electrolysis of 0.5 mM sodium thiophosphate at a gold electrode	106
Figure V-9.	Adsorption isotherm for sodium thiophosphate on gold in 0.1 M NaOH	111
Figure VI-1.	Comparison of DC, 2-step and 3-step PAD for sodium thiophosphate	120
Figure VI-2.	Calibration plots (i_p vs. C^b) for sodium thiophosphate by PAD and DC	125
Figure VI-3.	Dependence of the peak width on waveform for detection of 3.0 mM sodium thiophosphate in 0.1 M NaOH	129
Figure VI-4.	Dependence of the peak width on concentration for 3-step PAD of sodium thiophosphate in 0.1 M NaOH	132
Figure VII-1.	Current-potential curves at RDE for acetate buffer at pH 5.0 as a function of added acetonitrile	137
Figure VII-2.	Current-potential curves at RDE for 50% acetonitrile in acetate buffer at pH 5.0 as a function dimethoate added	146
Figure VII-3.	Current-potential curves at RDE for dimethoate in 50% acetonitrile in acetate buffer at pH 5.0 as a function of potential scan rate	148
Figure VII-4.	Current-potential curves at RDE for dimethoate in 50% acetonitrile in acetate buffer at pH 5.0 as a function of the negative potential scan limit	151

Figure VII-5.	Current-potential curves in flow-injection cell with potential scans interrupted at -800 mV, during the injection of dimethoate, as a function of delay time after the sample plug has passed by the electrode	154
Figure VIII-1.	Optimization of two-step potential waveform for FI-PAD	159
Figure VIII-2.	Representative flow-injection detection of selected sulfur-containing pesticides by two-step PAD	163
Figure VIII-3.	Calibration plots for dimethoate by FI/PAD	165
Figure VIII-4.	FI/PAD of dimethoate with consecutive injections and continuous flow	169
Figure IX-1.	Chromatogram of a mixture of eight standard pesticides using HPLC/PAD	177
Figure IX-2.	Chromatograms of a lake water sample with and without spiking with pesticides using HPLC/PAD	180
Figure X-1.	Break-through curve for dimethoate on C-18 reversed-phase forecolumn using PAD	188
Figure X-2.	Detection of dimethoate using PAD with and without preconcentration	191
Figure X-3.	Preconcentration calibration plots for dimethoate using PAD	193
Figure X-4.	Reproducibility of efficiency of the forecolumn by PAD after preconcentrations of same absolute amount of dimethoate at different concentrations and sample loading times	196

LIST OF TABLES

Table II-1.	Common sulfur-containing pesticides	7
Table II-2.	General formulas for organothiophosphate pesticides	8
Table II-3.	General formulas for thiocarbamate pesticides	11
Table II-4.	Common organosulfur pesticides	13
Table V-1.	Numerical experimental data for coulometry of sodium thiophosphate	102
Table V-2.	Coulometric results for selected sulfur compound	114
Table VII-1.	Representative sulfur-containing pesticides showing anodic responses by cyclic voltammetry at a gold RDE in 50% acetonitrile in acetate buffer pH 5.0	141
Table VIII-1.	Limits of detection of selected sulfur-containing pesticides by FI/PAD	168

I. INTRODUCTION

The development of agriculture over the last 1,000 years or more has had a great impact on man and his environment. During the evolution of early agriculture, man developed relatively stable agrosystems. This was achieved more by necessity and chance than by design. Man obviously harvested those plants which survived pest damage and, thereby, unconsciously selected plants for highest pest resistance. Agriculture, throughout its history, has been beset by severe pest outbreaks. Through the centuries, many cultural and physical practices were developed by man for protection of crops. These practices evolved many centuries before the emergence of the crop protection sciences and even before the biology of insect, weeds and the causal agents of plant disease were understood. Various chemicals were recommended for the control of insects and diseases as early as the 18th century. Recently, the first known recording of pesticide chemistry was discovered on the wall of an ancient temple of the pharaohs in Upper Egypt.

The agricultural revolution of the 20th century has further disrupted and complicated the stability of the pest species in our agrosystems. This was brought about by the runaway population growth of the world and man's need for food and fiber, and also the advancement of scientific agricultural technology. To attain the potential yields of

new cultivators, pesticides were used extensively to protect them from pests.

Many of the problems encountered with some of the early commodity pesticides were due to the fact that, while these materials were not acutely toxic, they persisted in the environment, often accumulated in food chains, and sometimes posed risks of long-term health effects. Many of these early commodity pesticides were of the structural family of chlorinated hydrocarbon (e.g., DDT). As regulatory pressure on these sort of materials mounted, different chemicals came to the forefront - most notably the organophosphate and carbamate pesticides. These materials generally provided the advantages of posing fewer and smaller risks of long term human health and environmental effects. They were frequently, however, more acutely toxic than the organochlorine pesticides they replaced. The presence of pesticide residues in food, wildlife and the environment is, consequently, of growing concern. To meet modern pesticide regulatory requirements there is a growing demand for data on the metabolism and degradation of pesticides, and, most of all, there is a need for simplified analytical procedures for both qualitative and quantitative determination of these pesticide residues.

Over the past three decades, many advances have been made in pesticide residue analysis. Owing to the variety of

sensitive and selective detectors developed for use with gas-liquid chromatography (GLC), this technique has been the predominant analytical tool for pesticide residue analysis over the past 20-25 years. However, many pesticides of current interest are not well suited for GLC analysis owing to factors such as thermal degradation, involatility or undesirable adsorptive effects. High performance liquid chromatography (HPLC) provides a suitable alternative for the analysis of many such compounds, but its usefulness for the determination of pesticide residues at ppm levels or less in environmental samples has been limited by the lack of detectors with adequate sensitivity and/or selectivity.

The interest in developing inexpensive, economical fuel cells produced intensive studies in the electrochemical oxidation of organic substances. Several reviews on electrochemical oxidation of organic compounds have been published which recognize the importance of the literature on the oxidation of sulfur-containing organic materials (1-6). Although electrochemical detectors have been developed and applied to many classes of analytes in recent years, not many of them are applicable for sulfur-containing compounds. Detection at noble-metal electrodes suffers from poor performance because of the loss of electrode activity due to adsorbed carbonaceous radicals and polymeric films with most severe loss of activity observed for sulfur-compounds (7).

Initial work was performed to alleviate this problem by devising a solid electrode with continuous reactivation of the anode surface through the use of wiper blades (8). In recent work, pulsed amperometric detection (PAD) has made use of periodic polarity-reversal techniques to recondition the electrode surface and reactivate it after passivation has occurred. Since high performance liquid chromatography and electrochemical detection are very compatible, combination of these two techniques has opened up a whole new field of analytical possibilities for pesticide residue analysis.

This dissertation describes the use of a two-step pulsed potential waveform which results in the reactivation of the gold electrode as well as the amperometric detection of sulfur-containing pesticides within the execution of this simple waveform. The compatibility of high performance liquid chromatography and pulsed amperometric detection will be demonstrated for the analysis of some typical sulfur-containing pesticides. A simple on-line sample preconcentration prior to HPLC separation is demonstrated to increase the sensitivity of the chromatographic technique.

II. REVIEW OF PERTINENT LITERATURE

A. Classification of Sulfur-containing Pesticides

1. Introduction

Natural organosulfur compounds are known to be widely distributed throughout the plant kingdom. These compounds often make important contributions to the odor and flavor of many of the cosmetibles. In some instances these sulfur compounds may also serve by their odor and taste to repel predators or act for the plant as resistance factors against infection by microorganisms. In other words, these compounds are acting as natural pesticides.

Most sulfur-containing natural pesticides exert their toxic action by tying up or inhibiting certain important enzymes cholinesterase (ChE), of the nervous system. Throughout the nervous system in vertebrates, as well as insects, are electrical switching centers, synapses, where the electrical signal is carried across a gap to a muscle or another nerve fiber (neuron) by a chemical, in many instances acetylcholine (ACh). After the electrical signal (nerve impulse) has been conducted across the gap by ACh, the ChE enzyme moves in quickly and destroys the ACh so the circuit will not be "jammed". These chemical reactions happen extremely rapidly and go on constantly under normal conditions. When sulfur-containing pesticides enter the

scene, they attach to the ChE in a way that prevents the removal of the ACh. The accumulation of ACh interferes with neuromuscular function, causing rapid twitching of voluntary muscles and finally paralysis. The target animal is dead due to improper functioning of the respiratory system.

Table II-1 gives examples of many of the sulfur-containing pesticides which are currently in use or have been used. It is clear that the types of functionalities present, e.g., organophosphate derivatives, chlorocarbons, sulfonamides, dithiocarbamates, oxime derivatives and cyclic esters. Despite the dissimilarity of their structures, these pesticides have the same mode of reaction as the natural sulfur-containing pesticides - anticholinesterase.

2. Classification

Due to various combinations of oxygen, carbon, phosphorous and sulfur, sulfur-containing pesticides have different identities which can be structurally divided into four major classes - organothiophosphates, thiocarbamates, organosulfurs and miscellaneous. General formulas and typical examples for each class are given as follows.

a. Organothiophosphates This sulfur analog of organophosphorous pesticides constitutes the biggest class of sulfur-containing pesticides. Table II-2 depicts three subclasses of organothiophosphates along with their general formulas. In general, the organothiophosphorous pesticides

Table III-1. Common sulfur-containing pesticides

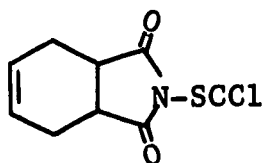
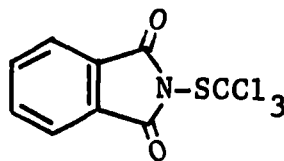
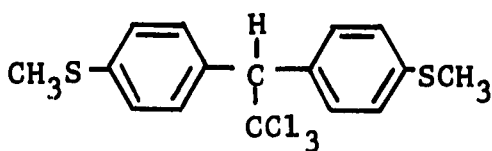
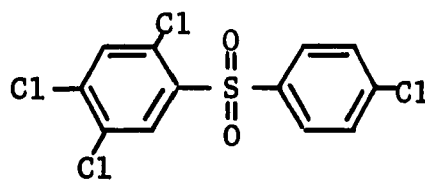
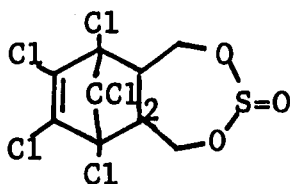
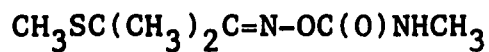
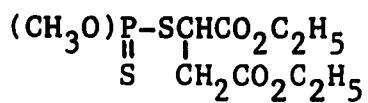
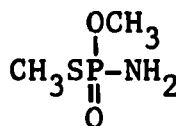
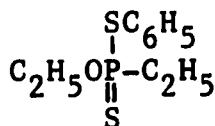
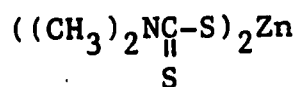
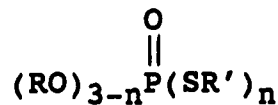
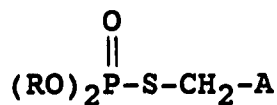
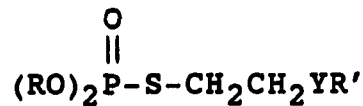
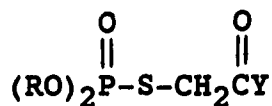
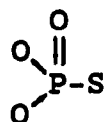
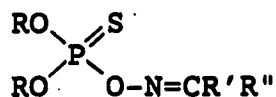
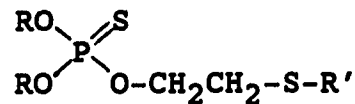
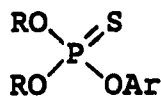
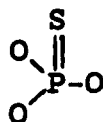
CAPTANFOLPETMETHIOCHLORTETRADIFONENDOSULFANALDICARBMALATHIONMETHAMIDOPHOSFONOFOSZIRAM

Table II-2. General formulas for organothiophosphate pesticides

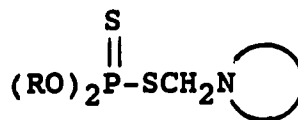
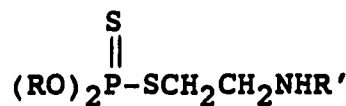
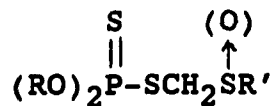
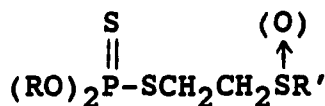
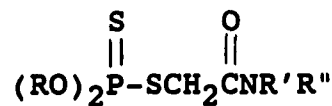
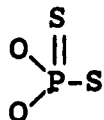
PHOSPHOROTHIOATE



PHOSPHOROTHIONATE



PHOSPHOROTHIOLATHIONATE



are relatively poor inhibitors of acetylcholinesterase but are converted by cytochrome p-450-containing monooxygenase enzyme systems in insects and mammals to the corresponding phosphate triesters that are potent inhibitors of the acetylcholinesterase. Introduction of a thiono-sulfur in an organophosphorous pesticides has advantages and disadvantages. From a favorable viewpoint, compared to phosphate esters, the phosphorothionates are generally more stable to hydrolysis and, therefore, may have greater insecticidal activity. Perhaps the most important contribution which a thiono-sulfur atom may make is the "delay factor" provided by P=S to P=O activation. This factor gives mammals the opportunity to detoxify the toxicant, and in many cases, phosphorothionate is substantially less toxic to warm-blooded animals than the corresponding phosphate ester. A classical example of the "delay factor" is found in the safe organo-phosphorous insecticide, malathion, for which it was demonstrated over two decades ago that slow in vivo oxidation to the anticholinesterase malaaxon provided the opportunity for detoxifying enzymes in mammals, most likely a carboxylesterase, to degrade malathion to non-toxic metabolic products (9). The mouse LD₅₀ of purified malathion is 3,200 mg/Kg, compared to 75 mg/Kg for malaaxon (10).

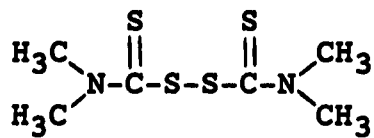
Typical examples of phosphorothionates are ethyl parathion and methyl parathion. These two compounds are the most popular organothiophosphorous pesticides applied to a variety of crops including green vegetables.

Azinphosmethyl, widely used as an insecticide, and acaricide is a typical example of phosphorothiolothionate pesticides. The compound is usually referred to as "Guthion", the trademark name assigned by Mobay Chemical Co. Similar to phosphorothionates, the toxic effect of the compound is attributable to its oxygen analog formed in vivo which inhibits brain acetylcholinesterase.

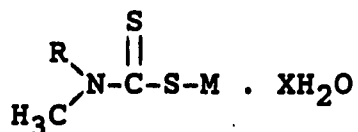
b. Thiocarbamates Thiocarbamates are the derivatives of thiocarbamic acids (HOOCNH_2). General formulas and typical examples are given in Table II-3.

Among the different classes of organic insecticides presently in use, the methylcarbamate esters rank at or near the top in acute mammalian toxicity, and in many cases the methylcarbamates are as toxic to mammals as they are to insects (11). The principal reason for the high toxicity of methylcarbamates to both mammals and insects probably is attributable to the absence of a "delay factor" such as that provided by the thiosulfur in phosphorothionate insecticides. Thus, most methylcarbamate insecticides are direct inhibitors of either insect or mammalian acetylcholinesterase. During the past two decades, a wide

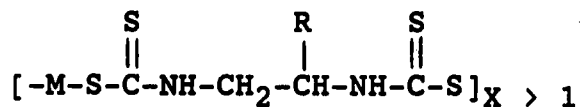
Table II-3. General formulas for thiocarbamate pesticides



I (thiram)



- II: M = Na, R = H, X = 2 (metham - Na)
 III: M = NH₄, R = CH₃, X = 2 (diram)
 IV: M = 1/2 Zn, R = CH₃, X = 0 (ziram)
 V: M = 1/3 Fe, R = CH₃, X = 0 (ferbam)



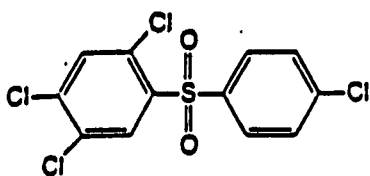
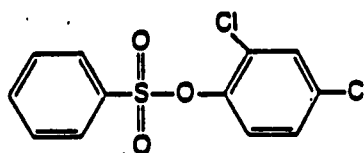
- VI: M = 2 Na, R = H, X = 1 (nabam)
 VII: M = Zn, R = H, X > 1 (zineb)
 VIII: M = Mn, R = H, X > 1 (maneb)
 IX: M = Mixt. of Zn and Mn, R = H, X > 1 (mancozeb)
 X: M = Zn, R = CH₃, X > 1 (propineb)

variety of new derivatized carbamates have been discovered, and several of them are currently undergoing development to improve properties of selectivity and toxicology. Of the various groups examined, those leading to derivatives which contain an N=S linkage have generated the largest number of new compounds with improved properties of selectivity. Since the first insecticides of this type were discovered in the early 1970s (12,13), examination of other types of derivatives containing an N=S linkage has been stimulated extensively. In general, these thiocarbamate derivatives are described as having strong insecticidal, acaricidal and nematocidal activity, along with high specificity and low mammalian toxicity.

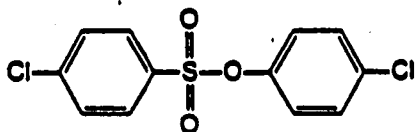
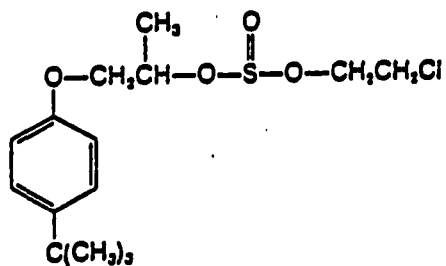
c. Organosulfur-pesticides The organosulfur-pesticides have sulfur as their central atom. They resemble the DDT structure in that most have two phenyl rings. Typical examples of the pesticides of this type are shown in Table II-4.

Dusting sulfur by itself is a good acaricide (miticide), particularly in hot weather. The organosulfurs, however, are far superior and require much less material to achieve control. Of greater interest is that the organosulfurs have very low toxicity to insects. As a result, they are used only for mite control with one valuable property: they are usually ovicidal, as well as

Table II-4. Common organosulfur pesticides

TETRADIFON (Tedlon[®])*p*-chlorophenyl 2,4,5-trichlorophenyl sulfoneGENITE[®]

2,4-dichlorophenyl benzenesulfonate

OVEX (Ovotran[®])*p*-chlorophenyl *p*-chlorobenzenesulfonateARAMITE[®]2-(*p*-*tert*-butylphenoxy)-1-methylethyl
2-chloroethyl sulfite

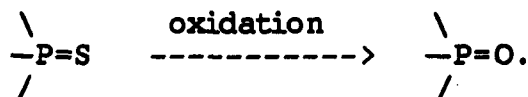
being toxic to the young and adult mites.

d. Miscellaneous There are some other sulfur-containing pesticides that do not fall into any of the above major classes. These pesticides contain sulfur as a sulfide linkage in part of the molecular structure of organophosphates, carbamates and other pesticide compounds. Typical examples are aldecarb ($\text{CH}_3\text{-S-C(CH}_3)_2\text{-CH=N-OOC-NHCH}_3$) and methomyl ($\text{CH}_3\text{-S-C(CH}_3)=\text{N-O(O)CNHCH}_3$). Toxicology and selectivity of these pesticides are described by their major functionalities of the molecules.

B. Oxidation of Sulfur-containing Pesticides

1. Chemical oxidation

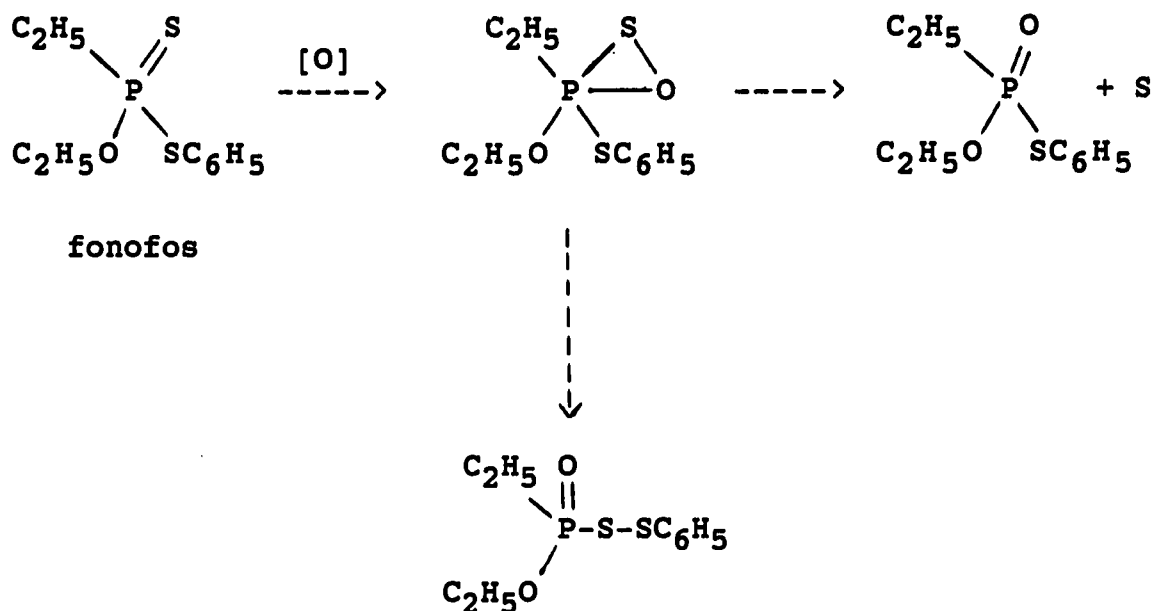
Except for organothiophosphorous pesticides, the literature is devoid of studies on the chemical oxidation of sulfur-containing pesticides. Oxidation of neutral organothiophosphorous esters usually involves the sulfur atoms of thiophosphoryl and thioether group in the molecule, which generally makes the organothiophosphorous pesticides more reactive, i.e., stronger inhibitors of esterase. The thiophosphoryl group is oxidatively desulfurized to phosphoryl group with various oxidants,



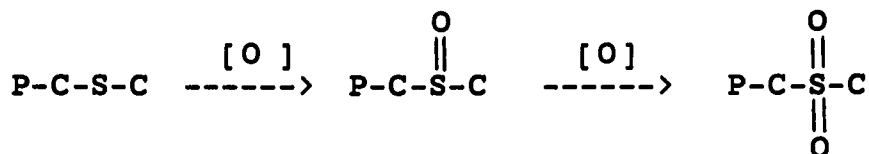
Nitric acid and dinitrogen tetraoxide are utilized to produce the corresponding oxo-analogs from phosphorothionates. Bromine water is often used for the conversion of inactive phosphorothionate insecticide into potent anticholinesterase, mainly for analytical purposes. Peroxy acids are also used for the same purpose.

The oxidation products of phosphorothionate esters are not always the corresponding oxo-analogs; the oxidation initiates further degradation of the esters and any susceptible groups in the side chain suffer the effects of the oxidants. For example, dimethoate does not transform to its oxo-analog, dimethoxon, by the action of bromine. In fact, as many as five unknown esterase inhibitors that are less polar than dimethoxon are found in the reaction mixture (14).

An attempt to isolate an oxidation intermediate which decomposes to an oxo-analog and a cleavage product was undertaken by McBain et al. (15). By careful treatment with *m*-chloroperbenzoic acid under anhydrous conditions, fonofos was converted to the oxo-analog (22%) and an oxygenated product (30%). The oxygenated product which originally was supposed to be the hypothetical oxidation intermediate was later characterized as the phosphinyl disulfide (16).

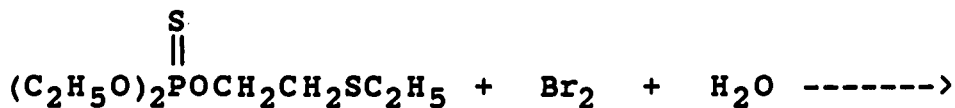


The thioether group in the side chain is oxidized to sulfoxide and then sulfone:

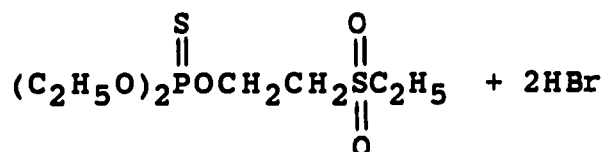


A thioether group is more susceptible to oxidation than a thiophosphoryl group. Thus, fenthion is oxidized to the sulfoxide with hydrogen peroxide and to the sulfone with potassium permanganate without alteration of the thiophosphoryl group (17). Similarly, demeton-O is oxidized

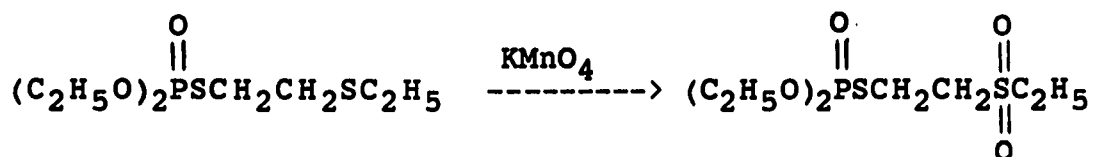
to its sulfoxide with a restricted amount of bromine in water or with 30% hydrogen peroxide at room temperature.



dementon-O



Both sulfur atoms are oxidized with excess amount of bromine or with nitric acid. Phosphorothiolate sulfur atom greatly resists oxidation. Thus, demeton-S is oxidized to its sulfone with potassium permanganate, keeping the thiolate sulfur atom intact (18).

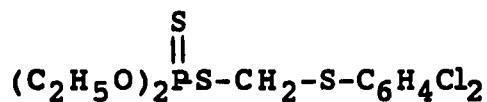


dementon-S

Phorate is oxidized to its sulfoxide and phorate O-analog sulfoxide with hydrogen peroxide, and to its sulfone and o-analog sulfone with peroxy acid or potassium permanganate

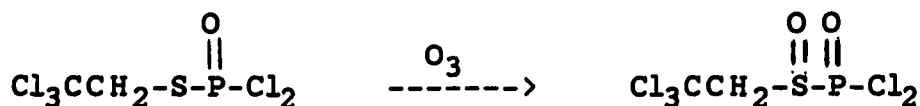
(17). Carbophenothion is similarly oxidized with peracetic acid, forming the sulfoxide and sulfone of the O-analog and additional three anticholinesterase (19).

In certain cases, thiolate sulfur can be oxidized. By the reaction with bromine in acetic acid, phenkapton is decomposed and the sulfur atom linked to the aromatic ring is converted to aryl sulfonic acid, while both the thiono and thio sulfur atoms are oxidized to sulfuric acid (20).



phenkapton

Under the same reaction conditions, O,O-diethyl phosphorodithioic acid gives two moles of sulfuric acid, whereas O,O,S-triethylphosphorodithioate gives only one mole of the acid. Therefore, the thio sulfur atom of phenkapton probably is oxidized after the hydrolytic cleavage of the PS-CS bond. The thiolate sulfur atom of S-trichloroethyl phosphorodichlorodithioate is oxidized without bond-cleavage by ozone to the sulfinylphosphoric dichloride, which was patented for preparation of pesticides (21).



The S-alkyl thiolate sulfur atom in partial esters of phosphorothioic acid is very susceptible to oxidation, which is in contrast with that in neutral ester, probably due to high electron density of the ions. Thus, S-alkyl and O,S-dialkyl phosphorothiolates are readily decomposed oxidatively by the action of iodine (22-24).

2. Photooxidation

Among the physical forces that are responsible for the chemical change of pesticides in the environment, solar radiation is the most powerful. Although the atmosphere effectively absorbs ultraviolet light of short wavelength (< 290 nm), sufficient energy exists within the range of ultraviolet sunlight wavelength (290-450 nm) to bring about many chemical transformations of organothiophosphorous pesticides (22): oxidation of thiophosphoryl and thioether groups, cleavage of ester and other linkages, thiono-thiolo and cis-trans isomerizations, and polymerization. The products of photochemical reactions and rate of their formation are greatly affected by many factors such as light intensity, the wavelength of light, irradiation time, the state of the chemical, the kind of supporting medium and solvent, pH of solution, and the presence of water, air, and photosensitizers.

Irradiation by ultraviolet light causes many organophosphorothionates to be converted to more potent enzyme inhibitors (23,24), due to photooxidation and photoisomerization. The photochemical conversion of thiophosphoryl group has been demonstrated with methyl parathion, dimethoate and EPN. Okada and Uchida reported that the esterase-inhibiting photoproduct of dimethoate was chromatographically different from dimethoxon (25). Dauterman described the conversion of dimethoate to dimethoxon by exposing the thin film to air even in the absence of ultraviolet light (26).

The thioether group in the side chain is photocatalytically oxidized to sulfoxide and sulfone. The photooxidation is observed with dialkyl thioethers (phorate, disulfoton, thiometon), alkyl aryl thioethers (fenthion, carbophenothion), and diaryl thioethers (abate) (27,28). This appears to occur more rapidly than the oxidative desulfuration of the thiophosphoryl group. It was concluded that, with fenthion on plants, photooxidation takes place at the thioether group while oxidative desulfuration of the phosphoryl group is caused by enzymatic oxidation (29).

3. Electrochemical oxidation

Unlike chemical and photochemical oxidations, most studies on electrochemical oxidation of sulfur-containing pesticides have been performed on dithiocarbamate

pesticides. The first electrochemical oxidation of dithiocarbamate pesticides was observed by Stricks and Chakravarti (30) in early 1960s. Polarographic study had shown that oxidation of these compounds produces mercury compounds via reaction analogous to those of mercaptans.

In acidic solutions, dithiocarbamate pesticides decompose readily into the corresponding amines and carbon disulfide. Polarographic study had been employed to determine the kinetic parameters of these reactions (31-33). The plot of the log of the rate of decomposition vs. pH exhibits a break at the same pH as the plot of the submit potential vs. pH for pyrrolidinedithiocarbamate. In strongly basic solutions, however, Halls and co-workers (34) have shown that the products of the oxidation at mercury electrodes were unstable and a different reaction sequence was proposed.

The adsorption prewaves which appear in the anodic polarograms of dithiocarbamate pesticides have been studied carefully by Kitagawa and Taku (35). Surface excess of 5.8×10^{-10} mole/cm² was found for the ligand which forms a HgL₂ adsorption complex.

At solid electrodes, oxidation of dithiocarbamate pesticides generally gives disulfide dimers. Cauquis and Lachenal (36) isolated pure disulfide in a nearly quantitative yield by oxidation at platinum electrode in

acetonitrile. The rate of the electron transfer step (k_s) was found to be 3×10^{-2} cm/sec, and the chemical dimerization (k_f) was found to be 2×10^5 /m/sec at room temperature using the current-potential curves at a rotating platinum disk electrode. Similar polarographic behavior was observed by Bond and Cassey for some organothiophosphate pesticides containing dialkyldithiophosphate anions (37). Two polarographic oxidation waves were found which correspond to the formation of the tris- and bis-mercury (II) complexes. By performing wave-shape analysis as a function of ligand concentration, they found later that both waves are reversible for these system in acetone (38).

C. Pesticide Analytical Methodology

1. Introduction

A pesticide residue analysis usually consists of five steps: sampling, extraction of the residue from the sample matrix, removal of interfering co-extractives ("clean-up"), identification and estimation of the quantity of residue in the clean-up extract, and, finally, confirmation of the presence and identity of the residues.

Since the quantity of residue in the clean-up extract is usually at a very low amount (e.g., 10^{-12} to 10^{-9} g), selective determinative methods are usually required to obtain this sensitivity. Chromatographic methods are by far

the most widely used for determination of pesticide residues, followed by spectrometric and biological methods. The latter, which includes bioassay and enzymatic techniques, is simple, since it does not involve clean-up. However, the method is non-specific. Enzyme inhibition, when used as a detection procedure after thin-layer chromatography (TLC), is sensitive (low ng detection limits) and selective for certain organophosphorous and carbamate pesticides.

2. Classical methods

Spectrometric methods are generally less sensitive and less selective than gas or thin layer chromatography and are ancillary techniques to gas chromatography used for confirmation of residue identity or quantitation of individual pesticides. If selectivity and sensitivity are adequate, colorimetric methods can be advantageously adapted to automated processes. Fluorescent pesticides and their metabolites may be determined by fluorimetry, which is more sensitive than visible, UV or IR methods. Since relatively few pesticides are naturally fluorescent, fluorimetry can be highly selective; however, removal of fluorescent impurities is often necessary and, in many cases, this can be difficult.

Paper chromatography provided the analyst in the late 1950s with the first multi-residue method for separation and identification of pesticides. Paper chromatography has

been largely superseded by gas chromatography, as the primary determination procedure, and by thin layer chromatography, for screening, semi-quantitation, and confirmation. Compared to paper chromatography, thin layer chromatography (TLC) offers generally increased resolution, shorter development time, and increased sensitivity. Most TLC pesticide analysis has been performed on 0.25 mm layers of alumina or silica gel, but polyamide and cellulose also are used. Many organophosphorous pesticides and carbamate pesticides are detectable at low ng levels by enzyme inhibition techniques or at higher levels by numerous chromogenic reagents.

Gel permeation chromatography has proved to be a highly valuable tool for the isolation of pesticides. The method has been improved considerably by the use of Bio Beads SX-3 and ethyl acetate-toluene (39,40). Johnson et al. (41) confirmed that a broad range of organophosphate pesticides could be recovered from fats and oils in good yields. Determination of dimethoate in waste water, soil and sediment, using gel permeation chromatography for sample clean-up, was performed by Kjolholt (42). Separation of dimethoate from other compounds was achieved using gel permeation chromatography with Bio-Beads SX-3, followed by determination of dimethoate by capillary gas chromatography with nitrogen-phosphorous detectors. The method was claimed

to be the first selective method for determination of dimethoate in complex environmental samples at the pptr-level.

3. Gas Chromatography

Gas chromatography is by far the most widely used for pesticide residue analysis. Thermally and chemically stable stationary phases, designed especially for gas liquid chromatography, such as the commercial "OV" series, are finding increasing use. The rate of appearance of "new" stationary phases appears to be declining. Electron-capture detectors continue to dominate in organochlorine determinations. Thermionic or halide-flame detectors have been refined for greater stability, but flame photometric detectors are becoming more favored. Greenhalgh and Nelson (43) described optimization techniques for flame photometric detector in both phosphorous and sulfur modes, a timely study to assist a tedious operation.

Mass spectrometry as a detector for gas liquid chromatography is expensive for routine work, but is unique in its capability for specific identification of chromatographic analytes. Luke and Dahl (44) identified different organophosphates in residue analysis by gas chromatography/mass spectrometry (GC/MS).

With an electron capture detector, the detector that gives the highest sensitivity of any contemporary gas

chromatographic detectors, detection limits in low pg (10^{-12} g) amounts can be obtained. However, for complex environmental samples at pptr-levels, rigorous clean-up of pesticide extracts and/or derivatizations are usually required to enhance the selectivity and sensitivity of the gas chromatographic methods (45).

4. High Performance Liquid Chromatography

Most of the pesticides used formerly were thermally stable and their residue on food products could be determined readily by gas liquid chromatography. However, during the past 20 years, there has been a trend toward the use of pesticides which would degrade more readily and, thus, be less detrimental to the environment. Many of these newer pesticides are thermally labile and/or non-volatile and, thus, are not directly amenable to determination by gas liquid chromatography.

High performance liquid chromatography (HPLC) has proven to be an excellent technique for determination of many of the new types of pesticides, as is reported by the review by Lawrence and Turton (46). The advent of techniques and the use of bonded phases in reversed phase HPLC has permitted the development of sensitive analytical procedures for the direct determination of organic compounds in water without derivatization.

a. Columns Reversed phase high performance liquid chromatography on C-18-bonded packing materials owes its great popularity to its ability to separate non-ionic, ionic, and ionizable substances in partition, ion-suppression, or ion-pairing modes (47), the stability of the bonded phase column, and the simple, inexpensive solvent systems utilized. A detailed review of HPLC columns for pesticides has been published (48)

b. Eluents A widely versatile set of solvents with a wide range of chromatographic properties includes hexane, methylene chloride, diethyl ether, acetonitrile and methanol. These solvents are usually used in mixtures with a solvent composition and strength that optimize capacity and selectivity.

c. Detectors The most common detector for HPLC is the ultraviolet (UV) absorbance detector. The original UV detector used a low pressure mercury lamp with a filter that emitted light of very high intensity, predominantly at a wavelength of 254 nm. Many aromatic compounds absorb strongly at or near this wavelength and can be detected with good sensitivity. It is advantageous however, to have a variable wavelength spectrophotometric detector so that the analyst is able to select the wavelength of maximum sensitivity for each compound, to increase selectivity of detection of the analyte over interferences, and to use

absorbance ratio at several wavelengths to improve identification of peak. Detection limits in the low ng-range are reported for most of the carbamate pesticides when monitored with the state-of-the-art UV detectors at wavelengths of optimum response (typically 190-210 nm) (49).

Fluorescence detectors are highly sensitive and selective because of the flexibility to control excitation and emission wavelengths in the detection process. An especially promising approach for trace analysis is the use of high intensity laser sources. Although a number of pesticides have been reported to fluoresce naturally (50-53), and several authors have recently used HPLC with fluorescence detectors to selectively determine pesticide residues (54-56), many pesticides are not naturally fluorescence and derivatization (pre- or post-column) of the pesticides of interest often is performed for increased selectivity and/or sensitivity of detection. Only slightly better detection limits are obtained by derivatization in fluorometric detection, with reported detection limits typically between 1-10 ng for dansyl chloride derivatives (57,58).

Refractive index detectors are either of the optical deflection or the prism type. These detectors are universal, relatively insensitive detectors that require close temperature control ($\pm 0.5\%$) and cannot be used with

solvent programming. They have had little or no use in pesticide residue analysis.

**D. Electrochemical Detection of Sulfur Compounds
at Gold Electrodes**

1. Investigation of the electrochemical oxidation of sulfur compounds on gold electrodes

This review is limited to anodic oxidation of sulfur-compounds on gold electrodes. For reviews of anodic detection on platinum (Pt) and mercury (Hg) electrodes, see Polta (59) and Udin (60).

Of the noble metals, gold (Au) is the most convenient for studying electrochemical processes such as the oxidation of dissolved sulfur compounds, because there is an extensive potential range over which there is no significant background current from surface oxide formation.

Unfortunately, detailed studies of the reactions of sulfur species on this noble metal are particularly sparse, probably because sulfur deposited on Au does not display electrochemical activity such as that found when sulfur is deposited on Pt.

The oxidation of sulfur dioxide in sulfuric acid solutions was investigated by Samec and Weber (61,62) at stationary and rotating gold disk electrodes. An oxidation mechanism was concluded to involve rapid reaction of H_2O

with adsorbed SO_2 to give HSO_4^- , and the oxidation is accelerated by an unidentified reduced species formed on the negative potential scan.

Wierse, Lohrengel and Schultze (63) investigated the reactions of sulfur formed by oxidation of sulfide and polysulfide ions in alkaline solutions. It was concluded that the oxidation of sulfide ions on gold was limited only by diffusion and that the adsorption of the sulfur formed upon oxidation was restricted to sub-monolayer quantities. Related studies were performed by Van Huong et al. (64) who found that sulfur deposited in the gas phase onto Au is stable over a wide potential range in neutral solution. A thorough investigation of the deposition and reactions of sulfur on Au electrodes was undertaken by Hamilton and Woods (65) who postulated polysulfides as intermediate products in the reaction producing sulfur and its reverse reaction, with S_2^{2-} as the predominant species. Sulfur was found to be completely oxidized to sulfate, although the electrode was inhibited by the presence of a layer of adsorbed sulfur.

The electrochemistry of thiocyanate was studied at Au electrodes in acetonitrile and dimethylsulfoxide solutions by Martins et al. (66,67). More recently, a study for thiocyanate anion was reported by Itabashi (68) for the oxidation at gold electrodes in aqueous perchloric solutions. Both of the above groups of study claimed that

trithiocyanate $(\text{SCN})_3^-$ is formed as the reaction product.

Recently, Moscardo-Levelut and Plichon (69,70) studied the electrochemical behavior of sulfide, polysulfide, and the sulfur oxyanions at gold electrode in aqueous sodium hydroxide solutions. The oxidation of sulfide was found to proceed in two steps with the first leading to S_2^{2-} , S_3^{2-} and molecular sulfur, S^0 ; and the second oxidizes these intermediates to SO_3^{2-} . With the exception of S_2^{2-} and S_3^{2-} , no other polysulfide anions were discovered under these conditions. In addition, it was reported that sulfate and sulfite are not electroactive on gold in basic solutions and that thiosulfates can be oxidized, but not reduced under these conditions.

A few studies of the electrooxidation of sulfur-containing organic compounds have been reported. Koryta and Pradac (71) extended the investigations of the electrochemical behavior of the common sulfur-containing amino acids with the study of cystine on a Au electrode. In comparison to Pt, they found that the rate of adsorption of cystine is larger and the quantity of adsorbed material is smaller at a Au electrode. The principal oxidation product was speculated to be cysteic acid and a mechanism involving participation of surface oxide was proposed. Oxidation of sulfur-containing amino acids also was studied by Reynaud, et al. (72), and Safronov et al. (73), in order to gain a

preliminary understanding of the electrochemical behavior of protein components.

Zakharov et al. (74) investigated the electrochemical oxidation of thiourea on a Au electrode in sulfuric acid solutions. Two anodic processes were observed: the initial step involved a diffusion-controlled oxidation followed by a further oxidation step, having diffusion and adsorption-controlled character, to various oxygen-containing products. This two-step mechanism also was found to explain the oxidation of diethyldithiocarbamate on Au electrodes (75).

In a recent publication (76), Buckley et al. reported on the S^{2-}/S^0 system on Au electrodes. Sulfur deposited on Au by the anodic oxidation of S^{2-} species in solution was studied by X-ray photoelectron spectroscopy. The initial layer was claimed to behave as gold sulfide. Multilayers of sulfur had a lower volatility and a small electron binding energy than bulk elemental sulfur, which indicate that there is interaction with the underlying gold or gold sulfide. The anodic oxidation of S^{2-} to S^0 , and the reverse process, were investigated also on Au electrodes using the rotating ring-disc electrode technique. Polysulfide ions (S_x^{2-}) were found as intermediates in both processes. Polysulfides also are produced by chemical reaction of deposited sulfur with S^{2-} species in solution.

Finally, blocking oriented monolayers of alkyl mercaptans on gold electrodes was investigated by Finklea et al. (77). Alkyl mercaptans with long hydrocarbon chains (C_{12} , C_{14} , C_{16} and C_{18}) are formed spontaneously into organized monolayers on Au during adsorption from solution. The oriented monolayers were found to be stable over a wide potential range of the electrode submerged in aqueous solution due to high affinity of sulfur for gold. Upon the use of this coated Au electrode, suppression of Au oxide formation was observed which was concluded to imply that water is blocked effectively from the Au surface. The mercaptan monolayers were concluded also to be effective at blocking the access of a variety of redox molecules to the electrode in water, since permeation through the monolayer was not evident. On the other hand, acetonitrile appeared to render the monolayer permeable to ferrocene. It was hypothesized that the strong hydrophobic repulsion of the hydrocarbon tails from water resulted in a tightly packed and, therefore, impermeable coating, while the presence of slight solvation was sufficient to loosen the packing and allow penetration to occur. Hence, the permeability of a monolayer can be adjusted by mixtures of organic and aqueous electrolyte as the contacting phase.

2. Electrochemical detection of sulfur-containing pesticides following HPLC separations

Although High Performance Liquid Chromatography (HPLC) continues to find a useful place as an analytical tool for the separation and determination of pesticide residue, one short-coming of this technique has been the lack of specific and sensitive detectors. Compatibility between HPLC and electrochemical detection makes it very challenging for chemists to combine these two techniques.

The suitability of electrochemical detection to a given problem ultimately depends on the voltammetric characteristics of the molecule(s) of interest in a suitable mobile phase and at a suitable electrode surface. All detectors limit the available choices of mobile phase composition to some degree; however, in electrochemical detection one must be conscious of the fact that a complex surface reaction is involved which depends on the medium. Therefore, some effort is required to simultaneously optimize both the column and detector performance. Fortunately, it is possible to make a few generalizations. For all practical purposes, direct electrochemical detection is not likely to be useful in normal phase adsorption separation since non-polar organic solvents are not well-suited to many electrochemical reactions. The HPLC stationary phases of choice clearly include all ion-exchange

and reverse-phase materials, since these are compatible with polar solvents containing some dissolved ionic material. The ionic strength, pH, electrochemical reactivity of the solvent and electrolyte, and the presence of electroactive impurities (e.g., dissolved oxygen, halides, trace metals) are all important considerations.

The choice of electrode material is more critical in HPLC with electrochemical detection than for the usual electroanalytical experiments, primarily due to the ruggedness and long-term stability required. Electrodes subject to complicated surface renewal problems (i.e., Pt, glassy carbon, Au and Hg films) many work well in some cases and be disastrous in others.

The first electrochemical detector for HPLC utilized polarography (Hg electrode). Koen et al. (78,79) reported a rapid method for quantitative determinations of pesticides by liquid chromatography with polarographic detection. Application for parathion and methyl parathion on crops was demonstrated to be successful, with the limits of detection of 0.03 ppm and 0.1 ppm, respectively. The sensitivity of the detector resulted from the arrangement of the detector body, which forced the eluent from the liquid chromatographic column to flow through a 1 mm x 1 mm space around the Hg drop, which was produced in micro size at the end of a 0.07-mm i.d. glass capillary tube. Separation was

achieved by pumping an oxygen-free eluent through the analytical column. Extended studies have been performed utilizing DC polarography for the determination of parathion (80,81) and dithiocarbamate fungicides (82-84), and AC polarography for the determination of dithiocarbamate fungicides (85). However, precision and recoveries reported in these studies are lower than those desired for routine monitoring of pesticide levels.

Recently, comparison of ultraviolet and reductive amperometric detection for determination of ethyl and methyl parathion was reported by Clark et al. (86). Comparison was performed for the determination of parathions on vegetable material and surface water samples using reversed phase HPLC with UV-electrochemical detection at glassy carbon electrode. The selectivity of electrochemical detection made it unnecessary to chromatographically resolve the plant components from the pesticides which were electrochemically active and, thereby, allowed rapid analysis. The electrochemical detector was proved to be more sensitive than the UV-detector for parathions. However, the UV-detector gave a greater long-term stability and was easier to prepare for use than was the electrochemical detector, where electrode fouling was observed to be a problem. The development of reductive detection has been slow because of difficulties in preparing

convenient and reliable working electrodes for use with HPLC. Hence, extensive examinations of reductive electrochemical detection for pesticide residues have not appeared.

While direct oxidative electrochemical detection has not been demonstrated for sulfur-containing pesticides, oxidative electrochemical detection following UV irradiation has been reported for organothiophosphate compounds, including the parathions, by Ding and Krull (87). Photolytic derivatization of the analyte in the HPLC effluents occurred within a 10-12 ft, 1/6-inch o.d., 0.8-mm i.d., Teflon tube followed by electrochemical detection at a glassy carbon electrode. These authors are presently trying to demonstrate the nature of the species being photolytically generated by using photolytic-cyclic voltammetric technique. For later reference, detection limits obtained from the injections of 20- μ l sample are given below for some organothiophosphate pesticides:

<u>compound</u>	<u>limit of detection (ppm) (87)</u>
ehthyl guthion	0.31
guthion	0.20
malathion	0.50
parathion	0.20
ethion	1.25
thimet	0.63

3. Theory and applications of pulsed amperometric detection (PAD)

Pulsed amperometric detection is a new technique developed in the early 1980s by Hughes, Meschi and Johnson (88), who observed that the surface activity of Pt electrodes could be restored by alternate anodic and cathodic polarization of the electrode. These authors incorporated this pretreatment into a three-step potential waveform which integrated sequentially the processes of detection and reactivation.

Conventional pulsed amperometric detection now involves the measurement of the analytical signal at a precisely controlled delay time (t_d) following application of the detection potential (E_{det}). A positive potential pulse to an oxidative cleaning potential (E_{clean}) is subsequently applied at a value in the vicinity of anodic oxygen evolution. Finally, a negative step to E_{ads} is made at a value near the vicinity of cathodic hydrogen evolution to remove the surface oxide that is formed during the application of E_{clean} , i.e., recondition the electrode surface. In many cases, adsorption of analyte also occurs at E_{ads} . Generally, potentials in the pulsed waveform can be predicted from the cyclic voltammogram with and without the analyte present. However, the optimum pulsed potential waveform is experimentally obtained only at actual flow

injection analysis. This potential waveform having a frequency of ca. < 1 Hz allows the technique to be employed in conjunction with flow-injection and high performance liquid chromatography analysis with sufficient time resolution to accurately describe peak shapes.

The first successful examples of pulsed amperometric detection was illustrated for the anodic detection of methanol, ethanol, ethylene glycol and formic acid at Pt electrodes in aqueous acid solutions (88). Hughes and Johnson extended this initial study to the detection of polyalcohols and carbohydrates in standard solutions (89); and the detection of carbohydrate in beverages (90) and other food products (91), using HPLC. Detection limits of ca. 0.1-1 ppm were reported for monosaccharides.

Capability of the technique to the detection of carbohydrates also was reported by Edwards and Haak (92), and Rocklin and Pohl (93). The application of pulsed amperometric detection at gold electrodes was illustrated for eleven carbohydrates which had been separated in less than fifteen minutes. Detection limits were reported as low as 30 ppb for sugar alcohols and monosaccharides and ca. 0.1 ppm for oligosaccharides.

Recently, a comparison of the pulsed amperometric detection of carbohydrates at Au and Pt electrodes was reported by Neuburger and Johnson (94). It was concluded

that Au electrodes have the advantage of high sensitivity and lower detection limits in comparison to Pt electrodes. Detection limits were claimed to be ca. five times better for glucose, fructose, sorbitol and sucrose using a three-step pulsed amperometric detection at Au electrodes. A two-step potential waveform was proposed later for the detection of carbohydrates at gold electrodes by the same authors (95), and pulsed amperometric detection of carbohydrates based on a three-step waveform was extended to potentiostats capable of programming an asymmetric square waveform (e.g., normal pulse voltammetric waveforms) to give approximately the same sensitivities and detection limits as obtained by the three-step method.

Pulsed amperometric detection also has been applied to detection of other classes of compounds. Polta and Johnson (96) reported the detection of aliphatic amines, including essential amino acids, using pulsed amperometric detection at Pt electrode in alkaline solutions. A representative chromatogram was shown for the separation of seven amino acids by high performance liquid chromatography in ca. fifteen minutes. Detection limits at the ppm levels were reported. The mechanism of oxidation was concluded to involve electrocatalytic oxygen transfer, and hydroxylamines were speculated as being the initial products at the electrode reactions. It was noted that the analytical

response was dependent upon the adsorption isotherm of the amino acid being detected; hence, linear calibration plots of current vs. concentration were obtained only at low surface coverage of analyte. These authors also reported the detection of aminoglycosides at platinum electrodes (97). The response was concluded to correspond to oxidation of the amine groups and not the alcohol groups.

Rocklin (98) reported that formaldehyde, acetaldehyde, propionaldehyde, butylaldehyde and formic acid can be determined in a single analysis by ion chromatography with pulsed amperometric detection at a Pt electrodes. The separation was accomplished in ca. twenty minutes with detection limits ranging from 1 to 3 ppm. It was noted that the presence of methanol and ethanol interfered with the analysis.

Adsorbed electroinactive species also can be detected using pulsed amperometric detection at Pt electrodes. Polta and Johnson (99) illustrated this technique using chloride and cyanide. It was observed that the adsorption of the anions alters the rate of surface oxide formation, thus enabling an indirect detection of the electroinactive species by monitoring the current due to oxide formation on the electrode surface. Sensitivity was found to be high and calibration curves were approximately consistent with adsorption control according to the Langmuir isotherm.

Pulsed amperometric detection was applied to the detection of pesticides for the first time by Thomas and Sturrock (100) who described the reversed phase chromatographic separation of carbamate pesticides with pulsed amperometric detection at a platinum electrode. Limits of detection on the order of 0.1 ng were reported. Other application of the technique was reported recently by Ohsawa et al. (101) for the determination of xylitol in human serum and saliva following separation by an ion chromatograph.

Pulsed amperometric detection was demonstrated to be useful for the reproducible anodic detection of numerous sulfur compounds as reported by Polta and Johnson (102). The results presented for thiourea were characteristic of all sulfur compounds studied. Linear calibration plots of i_p vs. C were obtained for low concentrations and short adsorption times. For high concentrations and long adsorption time, linear calibration curves were obtained by plotting $1/i_p$ vs. $1/C$. Detection limits were claimed to be better for the signals obtained by using pulsed amperometric technique than for other methods. Related study was performed also by the same authors where the matter of analytical calibration in pulsed amperometric detection was examined (103). A mathematical equation was manipulated and applied to predict the response of pulsed amperometric

detection as a function of adsorption time for thiourea at Pt electrodes. The rate constants governing adsorption and desorption of the analyte were estimated along with the maximum surface coverage by adsorbed thiourea.

Recently, starch and carbohydrates were determined using flow injection analysis system comprised of a glucoamylase immobilized reactor followed by pulsed amperometric detection by Larew et al. (104). Glucoamylase, immobilized onto porous silica and packed into a short column, was capable of nearly quantitative (98.2%) conversion of the starch to glucose. The sensitivity of pulsed amperometric detection of soluble starch was increased 26-fold by first passing the starch through the immobilized glucoamylase reactor. Finally, Welch et al. reported the comparison of pulsed amperometric detection and conductivity detection for carbohydrates (105). Pulsed amperometric detection at a Au electrode was shown to be more sensitive than conductivity detection in alkaline solutions of $\text{Ba}(\text{OH})_2$. However, a linear response to higher concentrations was obtained using conductivity detection as compared to pulsed amperometric detection. The response of conductivity detection in series with pulsed amperometric detection was claimed to be linear for glucose over the range of 6×10^{-7} to 1×10^{-2} M.

III. EXPERIMENTAL

A. Chemicals

All chemicals were reagent grade (from Fisher, Aldrich or Alfa). Standard pesticides were obtained from the Environmental Protection Agency (EPA, Research Triangle Park, NC). All pesticides were used without further purification. Water was deionized and filtered through a Barnstead NANOPURE II water system.

Dissolved oxygen was removed from solutions in voltammetric studies at rotating electrodes by saturation with nitrogen. A blanket of nitrogen was maintained above the solution at all times throughout experimentation. All eluents used for HPLC were passed through a 0.45- μ m filter and were degassed under vacuum prior to use.

B. Instrumentation

1. Voltammetric studies

a. Electrodes, rotator and recorder The Model DD20 gold disc electrode was from Pine Instrument Company (Grove City, PA.). The geometric area of the electrode was 0.458 cm². The rotator was Model ASR (Pine Instrument Co.). Electrode rotation speed could be set from 100 to 10,000 rev/min within 1% accuracy. Current-potential curves were recorded on a Model 7035B X-Y recorder (Hewlett-Packard, San

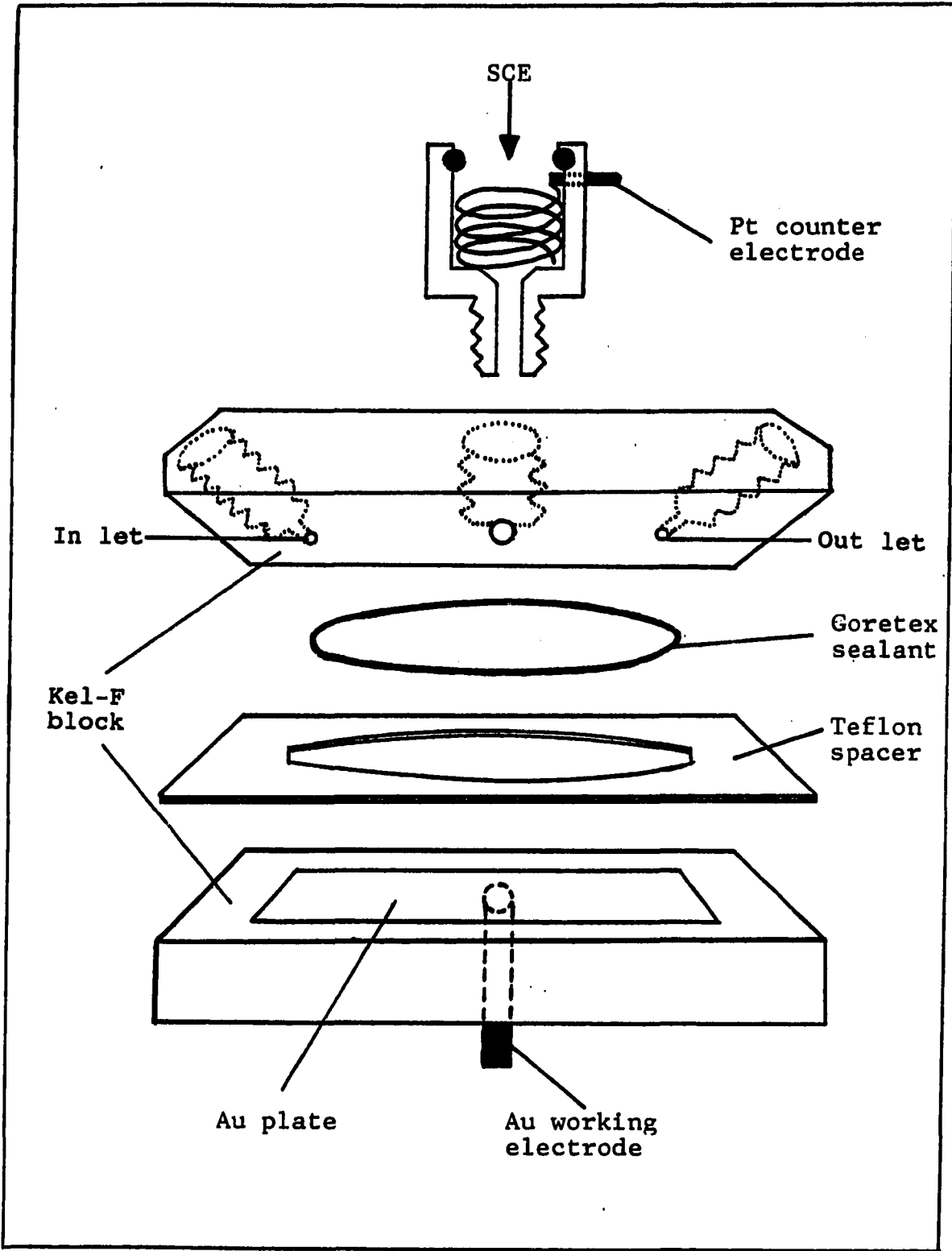
Diego, CA) or a Model 100 Omnigraphic recorder (Houston Instruments, Bellaire, TX).

b. Potentiostat Potentiostatic control for cyclic and linear scan voltammetry was achieved by a Model RDE-3 potentiostat (Pine Instrument Co.). Potentiostatic control for pulsed voltammetry was achieved by a Model UEM Pulsed Amperometric Detector (Dionex Corp., Sunnyvale, CA). A miniature saturated calomel electrode (SCE) was used as the reference electrode. All potentials are reported as volts (V) versus SCE.

2. Coulometric studies

a. Thin-layer cell Coulometric study at a Au electrode was achieved at a thin-layer cell constructed in the machine shop of the Department of Chemistry, Iowa State University. An exploded view of the cell body is shown in Figure III-1. All electrodes were mounted in Kel-F blocks in a sandwich-type arrangement. The working electrode made of a gold plate was removable for replacement or polishing. A miniature SCE was snugly fitted into a Plexiglas fitting with the aid of a rubber gasket. A platinum wire served as a counter electrode was coiled around the SCE inside the Plexiglas fitting, which was sealed into place in the cell body by a tapered screw. The working electrode and the reference electrode were separated by a Teflon spacer of

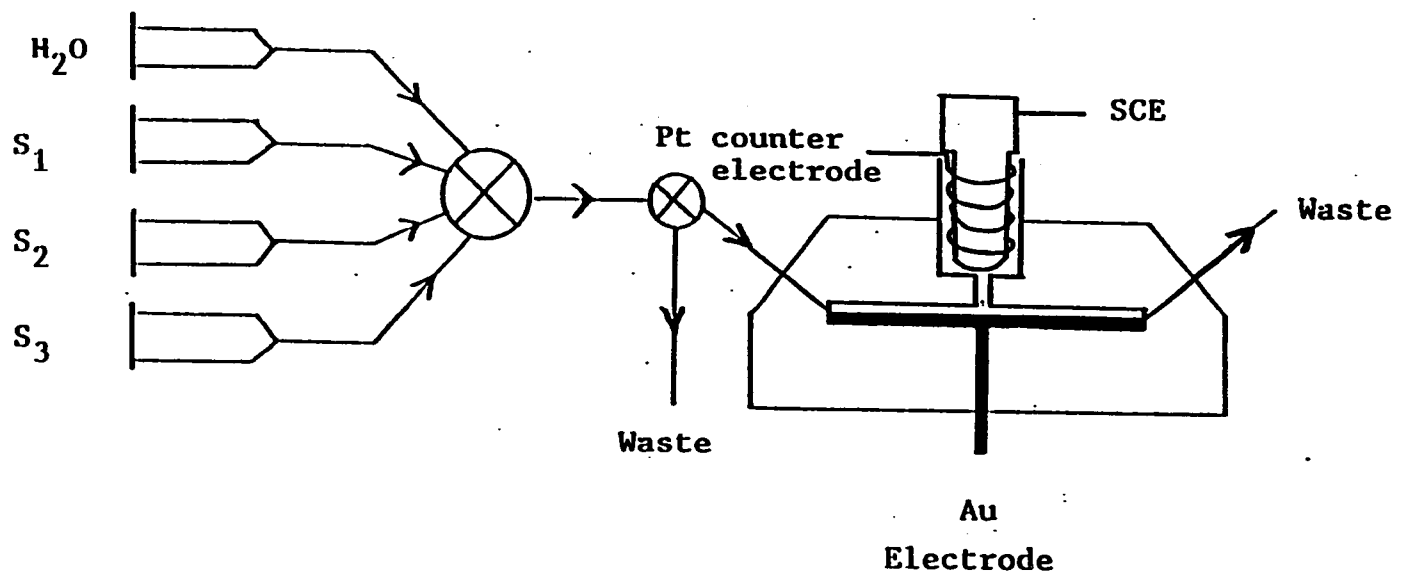
Figure III-1. Coulometric gold thin-layer cell



50 μm thickness. The geometric area of the working electrode was determined by the size of the hole on the spacer. A piece of a 1-mm Gore-TexTM joint sealant (WL Gore & Associate, Inc., Elkton, MD) was placed at the inner edge of the hole of the spacer to serve as a gasket. Upon pressing during the cell assembly, the thickness of the joint sealant was negligible compared to the that of the spacer.

A schematic diagram of the coulometric flow-through cell is shown in Figure III-2. A two-way valve was placed in between a four-way valve and the thin-layer cell to direct any air bubble produced during the change of the solution injected. Each port of the four-way valve was connected to a disposable syringe filled with an appropriate solution. Initial start-up of the cell was performed by filling the cell with 0.1 M NaOH without the SCE inserted. The flow was maintained until the Plexiglas fitting was full and no air bubbles were trapped inside the cell. The two-way valve was then turned half-way to block the flow and the SCE was inserted in its place causing the excess 0.1 M NaOH to flow into the outlet of the thin-layer cell. After each use, the system was washed and rinsed with deionized water and the cell was always filled with deionized water upon storage.

Figure III-2. Coulometric flow system



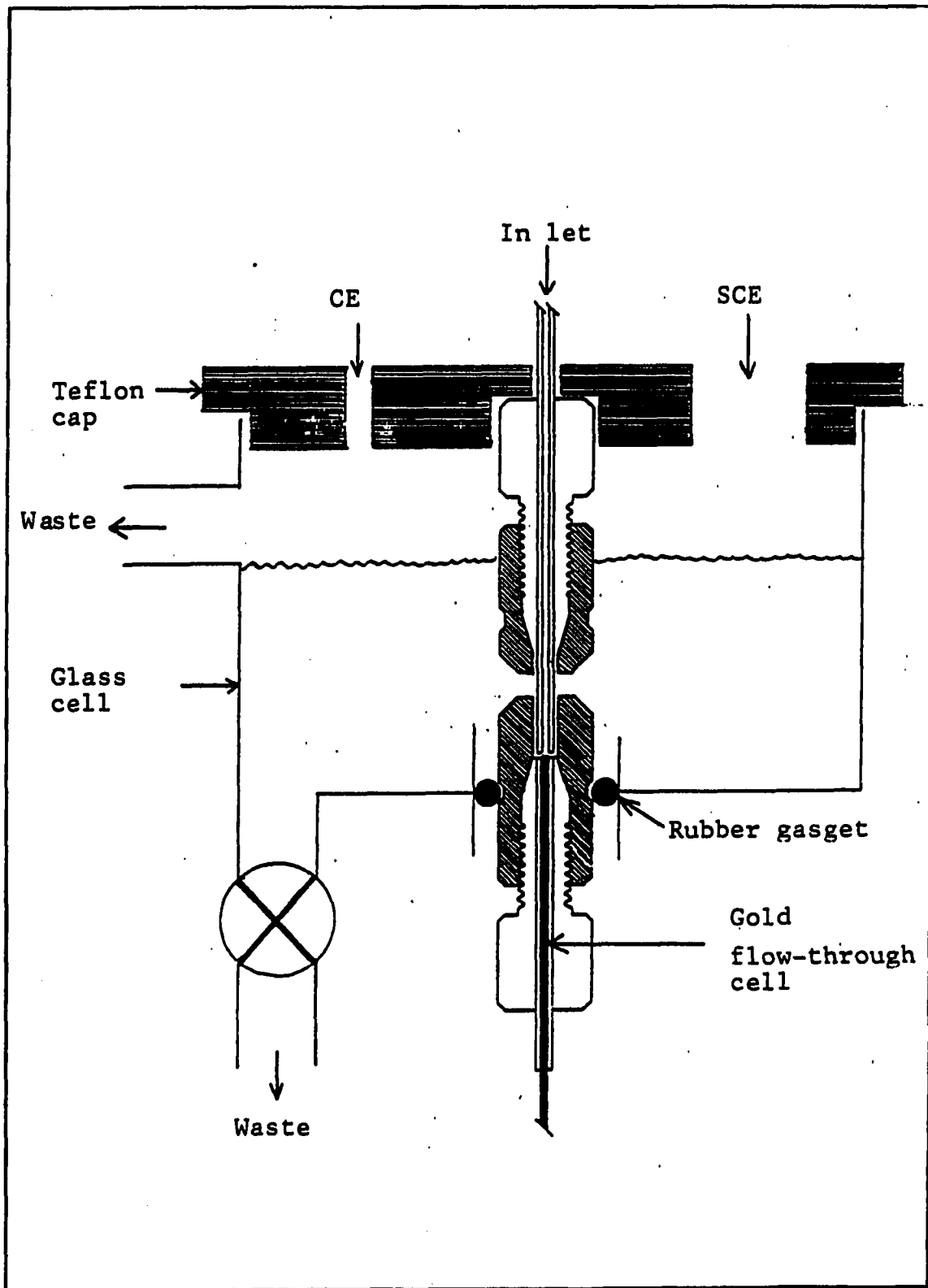
b. Potentiostat and recorder Potentiostatic control for constant potential coulometry in the thin-layer cell was achieved by a Model RDE-3 potentiostat (Pine Instrument Co.). Appropriate constant potentials were manually adjusted after desired potentials were read on a voltmeter. Current-time curves were monitored using a Model 125 strip-chart recorder (Curken, New Milford, CT).

3. Flow-injection studies

a. Flow-through cell Detection in flow injection studies was attained at a flow-through cell constructed with the help of the machine shop of the Department of Chemistry, Iowa State University after a design by D. C. Johnson cited in Polta (59). The detector rearrangement was modified, as shown in Figure III-3, for use with malodorous and toxic compounds. The cell body was unchanged, but the inlet fitting was turned upside down, and the electrode holder was constructed so that the distance between electrodes was kept constant.

b. Pump, injection system, potentiostat and recorder
The flow-injection system was assembled according to the conventional design. Flow of the electrolyte solution was maintained constant by a Milton-Roy dual-piston miniPumpTM (Laboratory Data Control, Riviera, FL) with a pulse dampener (Altech Associates, Inc.) and an MPICTM-NS1 column (Dionex Corp., Sunnyvale, CA) to eliminate pulsations in the flow

Figure III-3. Gold flow-through cell



rate. The sample solution was injected to the flow-through cell using a Model 70-10 injection Rheodyne valve with a 20 or 50- μ l sample loop, as specified later.

Potentiostatic control of the flow-through electrode was achieved by the Model UEM Pulsed Amperometric Detector (Dionex Corp.). The measurement of electrode current occurred during a 16.7 msec period in the last ca. 20 msec of the detection time period. Data were recorded using a Model 125 strip-chart recorder (Curken, Inc.). The dispersion factor in the flow system (i.e., $k = C_p/C_o$) was determined to be 0.6 using a 2-step pulsed-waveform detection of 0.5 mM dimethoate in 50% acetonitrile in acetate buffer at pH 5.0.

4. High Performance Liquid Chromatography (HPLC)

a. HPLC without preconcentration The liquid chromatographic system was assembled by modification of the flow-injection system. An RPIC-SG1 Ion PacTM guard column (P/N 037129, Dionex Corp.) in series with an RPIC-C18 10- μ m reversed phase column (P/N 037127, Dionex Corp.) was inserted between the injector and the flow-through cell detector of the FIA system. After each daily use, the analytical column was flushed with 50% aqueous acetonitrile for clean-up. On a monthly basis, the column was cleaned and regenerated by gradient passivation from water, methanol and methylene chloride, respectively.

b. HPLC with preconcentration The system was modified from the previous HPLC system. Preconcentration of pesticides was accomplished on an RPIC-SG1 Ion PacTM C-18 guard column (P/N 037129, Dionex Corp.) inserted in place of the sample loop of the injector. This guard column will be referred to later as the "Forecolumn". Schematic diagram of the flow is shown in Figure III-4. With the injector on the loading mode, a Milton Roy dual piston miniPumpTM (Laboratory Control, Riviera, FL) pumped the chromatographic eluent through the analytical column directly and the chromatographic baseline was maintained. Meanwhile, a Milton Roy miniPumpTM (Laboratory Control) pumped an aqueous solution of pesticide through the concentrator column. The sample volume was calculated as the product of the flow rate (ml/min) and the loading time (min). With the injector in the injection mode, accumulated pesticide on the concentrator column was back-flushed by the chromatographic eluent into the analytical column and detected by a 2-step PAD waveform in the flow-through cell.

c. Determination of the adsorption efficiency of the concentrator forecolumn A schematic diagram of the closed loop system used to determine the adsorption efficiency of the forecolumn is shown in Figure III-5. The rearrangement was simply modified from the previous preconcentration system by connecting the waste outlet to

Figure III-4. Preconcentration flow system

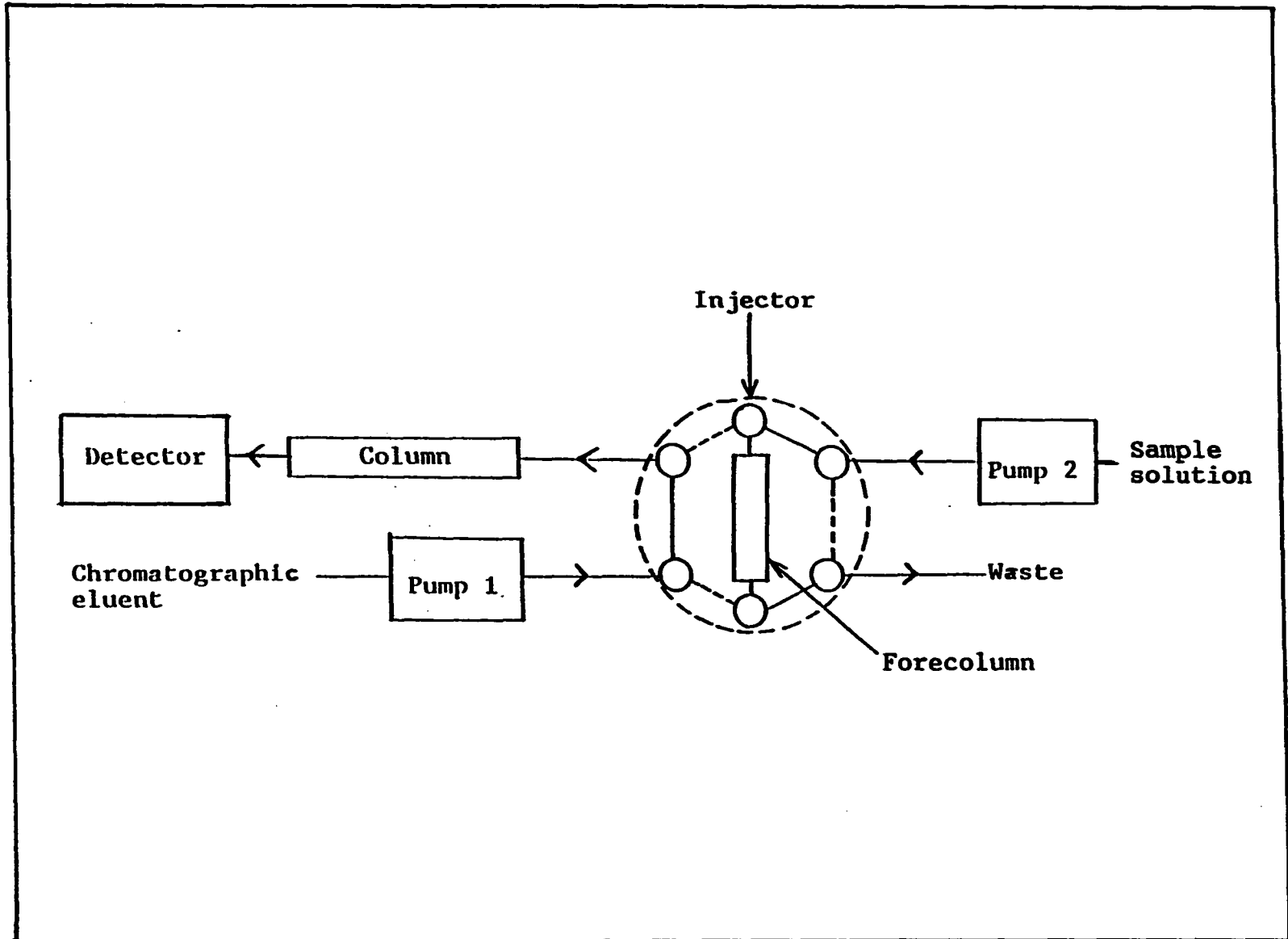
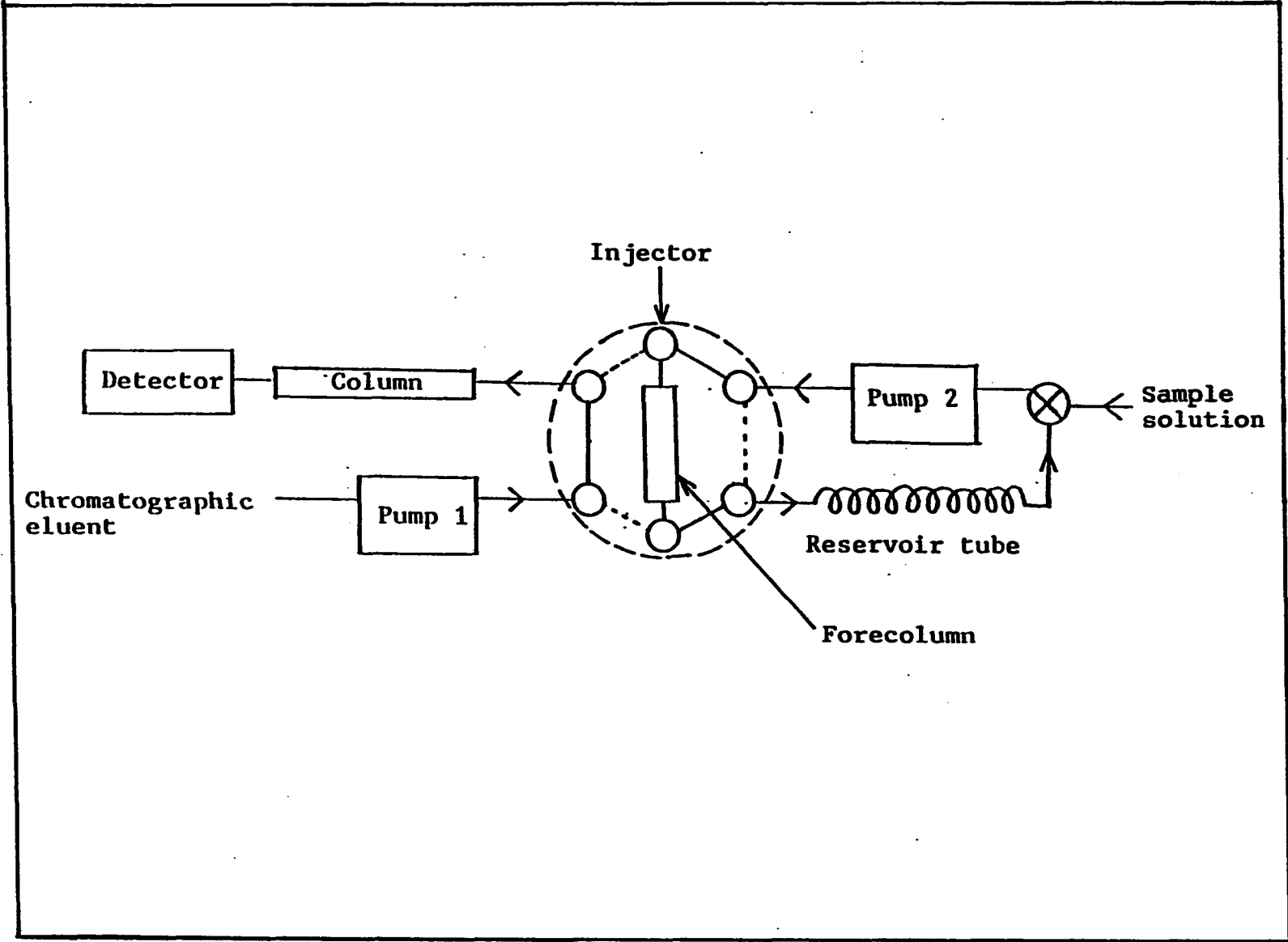


Figure III-5. Closed-loop system for determination of absolute efficiency of the forecolumn



the inlet of the sample loading pump by a two-way valve to form a closed loop containing the loading pump, the forecolumn and a coil of Teflon tubing (2 mm i.d. x 3.15 m).

To start the experiment, the loop was opened by disconnecting of the waste outlet from the two-way valve to drain the liquid being replaced during initial loading of the sample. After a specific amount of pesticide solution was pumped into the system, the loading pump was stopped and the system was turned into a closed loop. The pump was again turned on to pump the initial sample plug into the forecolumn. During the back-flushing of the first accumulation of pesticide to the detector, the loading pump was stopped and there was no flow in the closed loop. Before the forecolumn was inserted back into the closed loop, it was flushed with deionized water to avoid contamination of the chromatographic eluent to the aqueous solution in the closed loop. After the forecolumn was inserted, the loading pump was turned on to pump remaining pesticide not adsorbed during the first pass of the sample plug into the forecolumn. The same procedure was then performed to detect the adsorbed pesticide.

**IV. CYCLIC VOLTAMMETRY OF SULFUR COMPOUNDS
AT GOLD ELECTRODES IN ALKALINE
SOLUTIONS**

A. Introduction

Cyclic voltammetry permits the very rapid evaluation of a compound electrochemical reaction. The technique was performed at a gold rotating disc electrode and preliminary characterization of the anodic response of the analyte was achieved with linear scan, cyclic voltammetry. The effects of variation in analyte concentration, rotational speed of the electrode and potential scan rate were investigated.

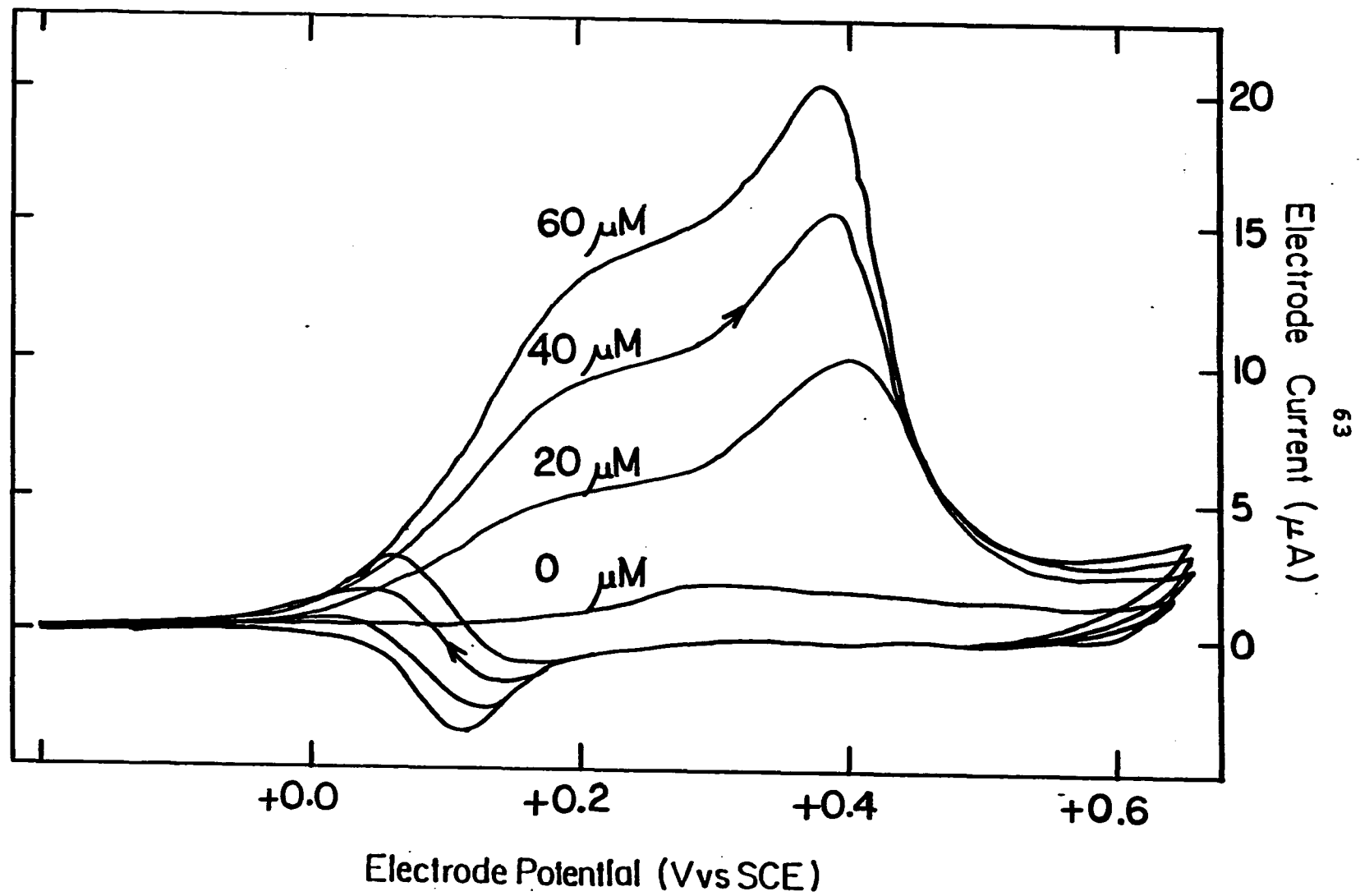
Sodium thiophosphate (Na_3SPO_3) was selected as the model compound for the initial work due to the similarity of the chemical structure of the compound to those of the organothiophosphorous pesticides - the largest class of sulfur-containing pesticides.

B. Concentration Dependence

The voltammetric response of sodium thiophosphate at a gold electrode in 0.1 M NaOH is illustrated by the current-potential curves shown in Figure IV-1. The residual response of the electrode obtained in the absence of sodium thiophosphate is characterized by an anodic wave during the positive scan for $E > 0.0$ V, which corresponds to the

Figure IV-1. Current-potential curves for sodium thiophosphate by cyclic voltammetry at a gold RDE in 0.1 M NaOH as a function of added sodium thiophosphate

Conditions: 1,600 rev/min rotation speed,
1.0 V/min potential scan



formation of the surface gold oxide layer (AuO). Rapid evolution of oxygen occurs for $E > +0.6$ V as a result of solvent decomposition. The oxide layer is reduced on the negative potential scan to produce the cathodic peak at ca. +0.11 V.

Upon the addition of sodium thiophosphate, oxidation of the analyte produces an anodic prewave at $E = +0.15$ V on the positive potential scan, as shown in Figure IV-1. The prewave current was found to increase as a linear function of the bulk concentration of the analyte with a zero intercept. Following the prewave, an anodic peak current was observed at $E = +0.38$ V. The peak current (i_p) at this potential was found also to increase as a linear function of the bulk concentration (C^b) of the analyte. However, the i_p-C^b plot exhibited a non-zero intercept. On the subsequent negative potential scan, oxidation of sodium thiophosphate was observed in the region $E = +0.15$ to 0.0 V. This anodic response occurred simultaneously and/or immediately following cathodic response of gold oxide reduction. Hence, the observed signal within this potential is the combination of the two signals originating from two different reactions.

C. Rotation Speed and Scan Rate Dependence

The anodic current peak for sodium thiophosphate obtained on the positive potential scan was determined to vary in height as a linear function of the square root of the rotational velocity ($w^{1/2}$) of the rotating disc electrode. This phenomenon was not observed for the residual response in the absence of sodium thiophosphate. Such behavior is consistent with the conclusion that oxidation of sodium thiophosphate on a gold electrode occurs by a mass-transport-controlled reaction under these conditions.

The height of the anodic peaks observed on the positive potential scan was found also to vary in proportion to the rate of potential scan (θ , V/min). This indicates that the quantity of charge, i.e. the integral of the current-time curve corresponding to these anodic processes, remains constant with increased θ . This property is indicative of surface-controlled reactions. Hence, the oxidation of sodium thiophosphate on a gold electrode is concluded to be surface-controlled processes as well as mass-transport-controlled processes.

D. Effect of Negative Potential Scan Limits

Current-potential curves for sodium thiophosphate as a function of negative potential limits by cyclic voltammetry

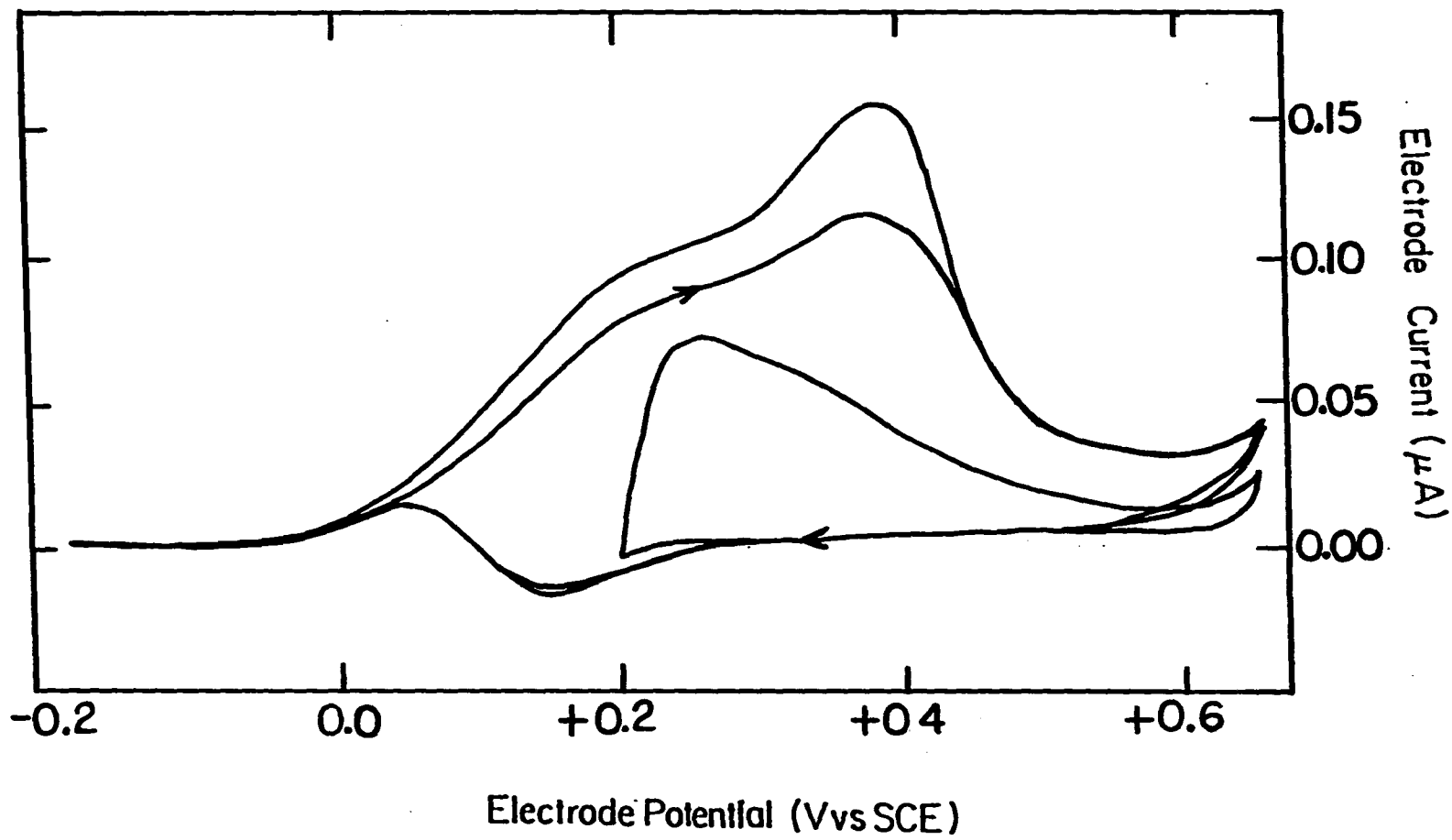
at a Au electrode in 0.1 M NaOH are shown in Figure IV-2. Upon the change of negative potential scan limits, it was observed that there was no anodic signal due to oxidation of sodium thiophosphate unless the limits were made more negative than +0.2 V, where reduction of gold oxide starts to occur. Two explanations are possible for this behavior. First, at the negative potential limit where the electrode potential is equal to or greater than +0.2 V, thiophosphate ions are not adsorbed at the electrode. Hence, the surface-controlled reactions could not occur on the subsequent positive potential scan. This explanation is reasonable since adsorption of sulfur compounds onto oxide-free gold surface has been observed for many of these compounds (59). Second, mass-transport-controlled processes are suppressed due to the loss of electrode activity because of coverage of the electrode surface by Au oxide.

E. Proof of Adsorption

Adsorption of sodium thiophosphate on an oxide-free gold surface was proved by the following experiment. Cyclic voltammetry was performed for sodium thiophosphate in 0.1 M NaOH as previously described. After several cyclic scans, the voltammogram was reproducible and the current response was recorded. The electrode potential was then held at the

Figure IV-2. Current-potential curves for sodium thiophosphate as a function of negative potential limits by cyclic voltammetry at a gold RDE in 0.1 M NaOH

Conditions: 2,500 rev/min rotation speed,
1.0 V/min potential scan rate,
20 μ M sodium thiophosphate



negative potential scan limit ($E = -0.1$ V) for a few minutes after which the electrode was removed from the solution. After rinsing with 0.1 M NaOH, the electrode was put into thiophosphate-free 0.1 M NaOH and cyclic voltammetry was continued by one positive potential scan followed by one negative potential scan.

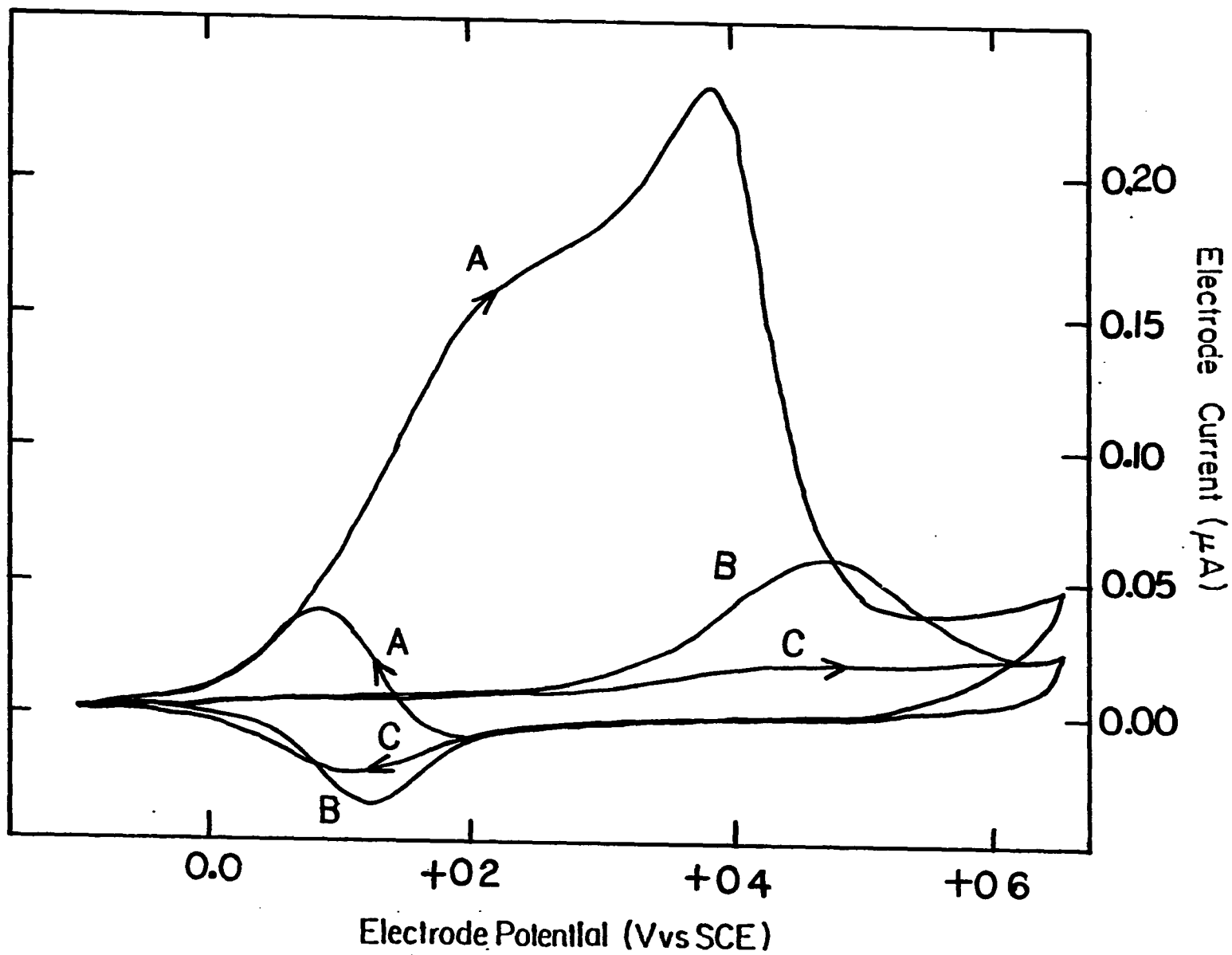
Figure IV-3 illustrates typical cyclic voltammetric response obtained according to this procedure. Curve B represents the cyclic voltammogram in 0.1 M NaOH when the electrode was removed from a 60- μ M sodium thiophosphate solution. The controlled response (Curve C) was obtained by performing cyclic voltammetry after the electrode was removed from a 0.1 M NaOH solution. For comparison, cyclic voltammogram for a 60- μ M sodium thiophosphate solution is shown also by Curve A. Substantial anodic current obtained even after the electrode was removed from the thiophosphate solution suggests that adsorption of thiophosphate occurred during the cathodic polarization of the electrode.

It was observed that under the range of bulk concentration studied (0.1 to 1.0 mM sodium thiophosphate), the same anodic charge due to adsorption was obtained regardless of the concentration of sodium thiophosphate. In other words, the gold surface was always at saturation with adsorbed sodium thiophosphate. Anodic charge per area of gold due to oxidation of adsorbed analyte at maximum surface

Figure IV-3. Current-potential curves for sodium thiophosphate demonstrating adsorption on a gold RDE by cyclic voltammetry in 0.1 M NaOH

Conditions: 2,500 rev/min rotation speed,
1.0 V/min potential scan rate,
60 μ M sodium thiophosphate

- Curves: (A) Cyclic voltammetry in 60 μ M sodium thiophosphate;
- (B) Cyclic voltammetry in 0.1 M NaOH after the electrode was held at a potential of -0.001 V in 60 μ M sodium thiophosphate and removed from the solution (see text for detail);
- (C) Same as (B) except the electrode was placed in 0.1 M NaOH prior to the removal (i.e., blank)



coverage was calculated to be $81.9 \mu\text{Coul}/\text{cm}^2$. Correction for the anodic charge corresponding to oxide formation was made by assuming that anodic charge for oxide formation on the positive scan was equal to the cathodic charge for oxide reduction during the consecutive negative potential scan.

F. Conclusion

The anodic response for sulfur-compounds on a gold rotating disc electrode has been illustrated using sodium thiophosphate as the model compound. Oxidation of sodium thiophosphate was concluded to be controlled by a mass-transport process as well as a surface process. Prior adsorption of the compound during the cathodic polarization of the electrode was proved to be necessary for oxidation of the compound through the surface-controlled process. Analyte molecules which are adsorbed at the electrode surface are oxidized in the potential region where the surface oxides are formed. The reactions were concluded to involve electrocatalytic oxygen-transfer mechanisms.

**V. CHRONOCOULOMETRIC STUDY OF SULFUR COMPOUNDS
AT A GOLD ELECTRODE IN A
THIN-LAYER CELL**

A. Introduction

All of the interesting action in electrochemistry take place at the interface between the conducting electrode and the electrolyte solution where the current is transformed into electronic current by electrochemical transformations. The electrode/electrolyte interface in any electrochemical cell often exhibits chemical properties that differ substantially from those observed in the bulk of the electrode and in the electrolyte solution far from the interface. One particularly interesting property of many electrode/electrolyte interfaces is the tendency to concentrate the reactants by their adsorption to the electrode.

Studies of the adsorption of ions and molecules at electrodes have occupied electrochemists for many years for reasons that are both important and obvious: all electrode processes involve an electronic interaction between reactants and the electrode surface which can be drastically altered by the presence of adsorbed ions and molecules. Adsorption can greatly enhance electrode reaction rates (e.g. the oxidation and reduction reactions of many cations

are accelerated by barely detectable quantities of adsorbed anions) or eliminate the electrode reaction altogether, e.g., certain organic amines prevent metal deposition reactions when they are adsorbed on electrode surfaces.

Considerable effort has been expended to devise methods for measuring the quantity of any reactant that may be adsorbed at the electrode/electrolyte interface. The problem is not trivial because the quantities adsorbed typically lie in the range between 10^{-12} to 10^{-9} mole/cm² of interface. The classical methods for studying adsorption on electrodes are based on the Gibbs adsorption equation which involves the determination of the interfacial tension at the electrode/electrolyte interface. The study can be performed directly by means of capillary electrometer measurements for adsorption at mercury, or indirectly from experimentally determined double-layer capacitances which can be doubly integrated to obtain the interfacial tension (106). Many highly precise measurements have been obtained by these methods, although they require much experimented labor and patience (107,108).

More recently, an alternate method for determining the quantities of adsorbed species has been developed which, while lacking the full thermodynamic rigor of the classical methods, offers much greater ease and speed in execution. This method, chronocoulometry, depends upon the measurement

of the charge consumed in the electrode reactions of adsorbed species and is therefore restricted to electroactive adsorbates. Although initial work utilized the area of voltammetric current-potential curves to measure the quantities of adsorbed reactants (109,110), later work utilized the area of the current-time curves by stepping rather than scanning the electrode potential (111). With this improvement, the same information could be obtained more simply, reliably and rapidly.

Exhaustive coulometric study is most satisfactory when the cell is constructed with a large electrode surface area and a small internal volume, such that the cell operates with an efficiency of 100%. An approach to obtain bulk electrolysis conditions with no convective mass transfer involves decreasing of the electrolysis volume so that a very small solution volume (a few μl) is confined within a thin-layer (2-100 μm) at the electrode surface. This so-called "thin-layer electrochemical cell" has a large ratio of electrode surface area to electrolysis volume and provides a short electrolysis time due to its small internal electrolysis volume.

Consider a thin-layer cell with the potential stepped from a value E_1 , where no current flows, to a value E_2 , where the reaction $R \rightarrow O + ne^-$ is virtually complete so that the concentration of R at the electrode surface is

essentially zero. The total charge passed by the electrolytic reaction is given by the following equations (112):

$$Q(t) = nFVC_0^* \left\{ 1 - \frac{8}{\pi^2} \sum_{m=1}^{\infty} \left(\frac{1}{2m-1} \right)^2 \exp \left[\frac{-(2m-1)^2 \pi^2 D_0 t}{l^2} \right] \right\} \quad [\text{V-1}]$$

$$Q(t) \approx nFVC_0^* \left(1 - \frac{8}{\pi^2} e^{-pt} \right) \quad (\text{later times}) \quad [\text{V-2}]$$

$$Q(t \rightarrow \infty) = nFVC_0^* = nFN_0 \quad [\text{V-3}]$$

In Equations V-1 to V-3, D_0 is the diffusion coefficient of the analyte; l is the thickness of the diffusion layer; $p = \pi^2 D_0 / l^2$, and other parameters are as conventionally defined. Notice that Equation V-3 is the same as the coulometry equation derived for conventional exhaustive coulometric experiments where the cell volume is large. Determination of total number of moles of analyte (N_0) and/or number of electrons transferred during coulometric process (n) are possible without the necessity of knowing D_0 . In actual experiments, the total measured charge (Q_{total}) will be larger than the net charge (Q_{net}) given by Equations V-1 to V-3 because of contributions from the double-layer charging and background faradaic reactions. These contributions can be determined with no difficulty if

the adsorption of a reactant produces little or no change in the interfacial capacitance so that the value of the charge measured in a blank experiment in the absence of reactant applies to measurements in the presence of the adsorbing reactant. However, adsorption of a reactant frequently produces significant changes in the interfacial capacitance so that values of the charge measured in the absence of the reactant do not apply exactly to the determination of the Q_{net} when the reactant is present.

This difficulty sometimes can be overcome by double-potential-step coulometry (113) in which the electrode potential is returned to its initial value once the experiment is terminated. The total charge obtained for the reverse step provides a direct measurement of the charge due to the double-layer charging and background reactions in the presence of adsorbed reactants (114,115), provided that there is no reverse reactions of the product occurring during the initial step.

This section is devoted to the coulometric study of sulfur compounds. The double-potential step coulometric technique was applied to determine the number of electrons transferred during the electrochemical oxidation of sodium thiophosphate at a gold electrode in 0.1 M NaOH. The adsorption isotherm of sodium thiophosphate on a gold surface was evaluated also using a newly developed method.

Experiments were conducted using a gold electrode in the thin-layer flow-through cell described in section III-2. Values of coulometric charge were calculated from recorded I-t and I-E data by the "cut-and-weigh method".

B. Determination of the Cell Volume

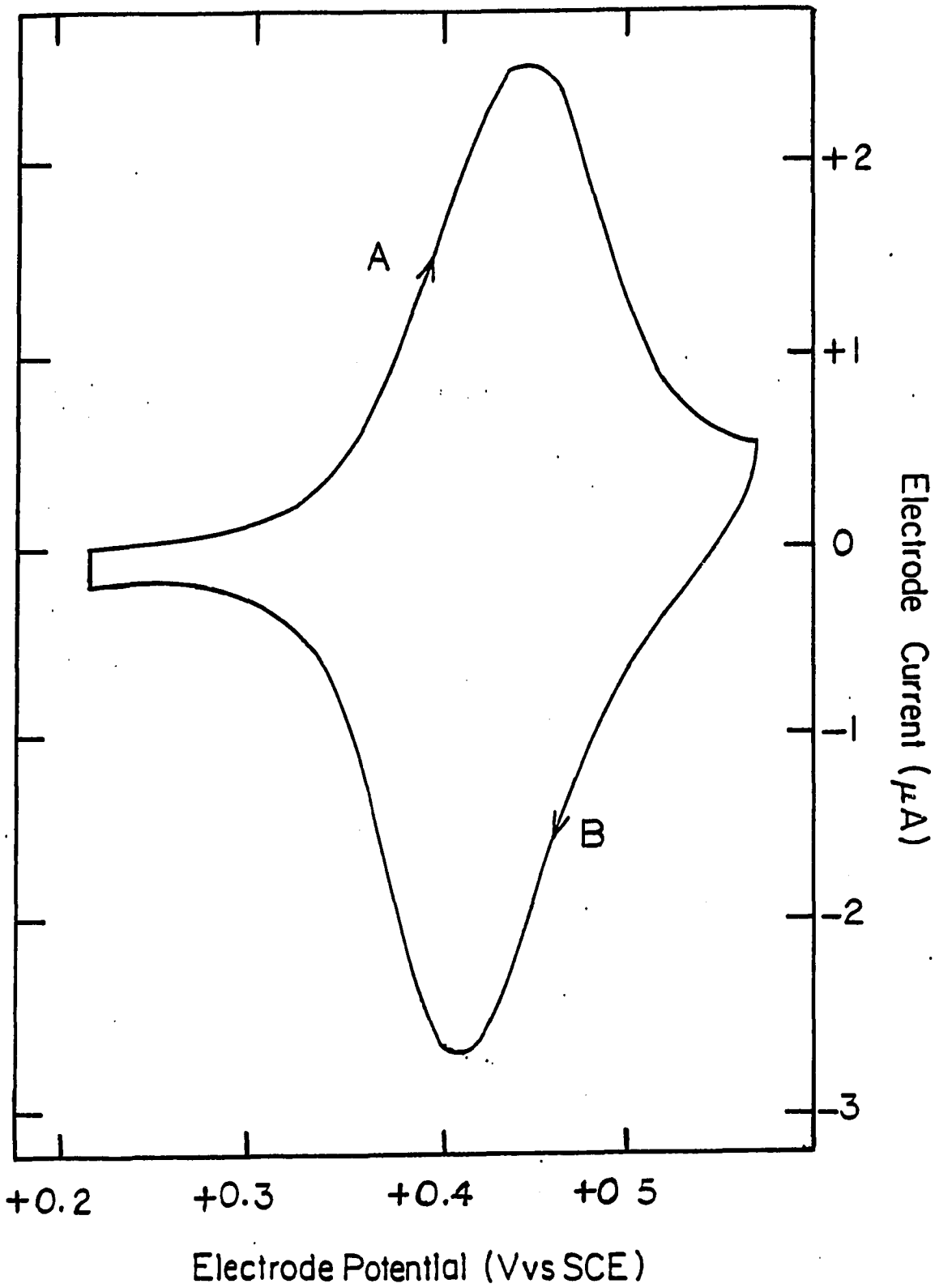
The internal cell volume was determined by a coulometric method using standard ferrocyanide solutions in 0.1 M NaOH ($n = 1$ eq/mol). Cyclic voltammetric current-potential curves for ferrocyanide solutions performed in this thin-layer cell are shown in Figure V-1. The anodic current peak for the oxidation of ferrocyanide on the positive scan is separated by about 50 mV from the cathodic current peak for the reduction of ferricyanide during the negative scan. This peak separation potential is expected even in practical cyclic voltammetry of this analyte system. An attempt to increase the cell conductivity by adding additional electrolyte (1.0 M NaNO₃) failed to bring these two peaks closer together. Hence, at this configuration, the thin-layer cell was at its optimum performance with regards to a minimal iR drop.

Prior to each coulometric measurement, the working electrode was electrochemically cleaned by potential cycling with a continuous flow (ca. 0.1 ml/min) of 0.1 M NaOH.

Figure V-1. Current-potential curve for $\text{Fe}(\text{CN})_6^{3-}/\text{Fe}(\text{CN})_6^{4-}$ system by cyclic voltammetry in 0.1 M NaOH at a gold electrode in a thin-layer cell

Conditions: 0.25 V/min potential scan rate,
11.4 μL thin-layer cell volume,
1.0 mM $\text{K}_4\text{Fe}(\text{CN})_6$

Curves: (A) Oxidation of $\text{Fe}(\text{CN})_6^{4-}$
(B) Reduction of $\text{Fe}(\text{CN})_6^{3-}$



Cyclic voltammetry was performed at a scan rate of 0.50 V/min between -0.2 V and +0.7 V for ca. 5 min or until the current-potential response observed was reproducible. Filling of the cell with the standard ferrocyanide solution was accomplished by manual injection of the solution into the cell while the electrode potential was held at a constant potential of -0.2 V at which no electrochemical reaction occurred for ferrocyanide. Current-time response was recorded once the electrode potential was stepped to +0.65 V where oxidation of ferrocyanide occurred. Recording of the current as a function of time was continued until the slope of the current-time plots became zero, as determined by visual examination, which corresponds to a cell current of zero.

Typical current-time curves are shown in Figure V-2 for chronocoulometric measurements of ferrocyanide in 0.1 M NaOH at concentrations of 0.0 mM to 2.5 mM. The plots of net coulometric charge (Q_{net}) after the correction for background were made vs. concentration (C^b) of ferrocyanide are shown in Figure V-3. The plots were found to be linear with a slope of $1,098.02 \pm 0.0079$ uCoul/mM¹, a virtually zero intercept of 2.62 ± 0.0009 uCoul and a correlation coefficient of 0.9998. The cell volume was calculated to be 11.38 ± 0.0079 ul using the equation; $V_{\text{cell}} = Q_{\text{net}}/nFVC^b$, where $n = 1$ and the slope of the $Q_{\text{net}} - C^b$ plots.

Figure V-2. Current-time curves for electrolysis of $\text{Fe}(\text{CN})_6^{4-}$ solutions at a gold electrode in a thin-layer cell

Conditions: 0.65 V coulometric oxidation potential,
0.1 M NaOH

Concentration $\text{Fe}(\text{CN})_6^{4-}$

A.	0.0 mM
B.	0.5 mM
C.	1.0 mM
D.	1.5 mM
E.	2.0 mM
F.	2.5 mM

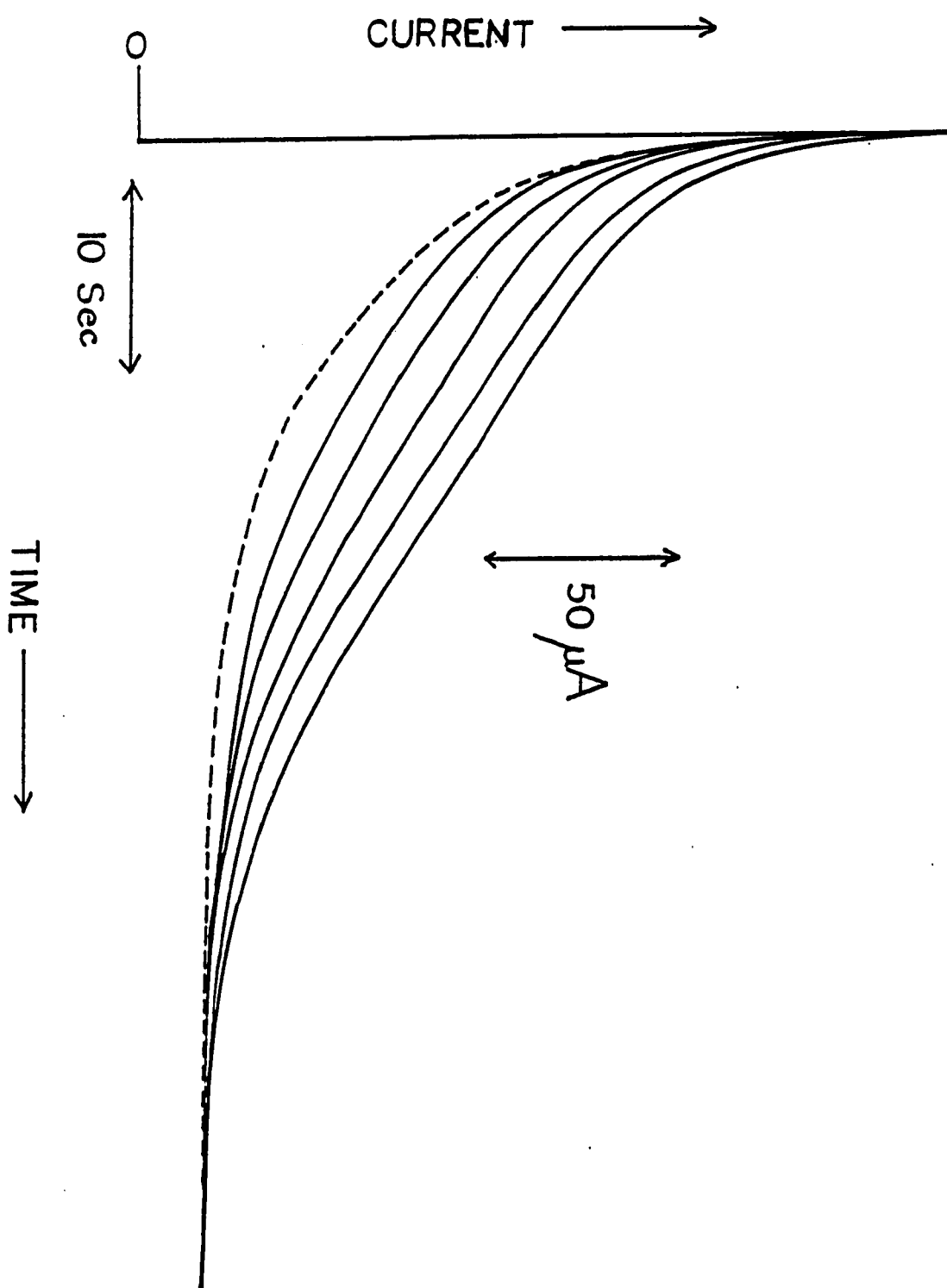
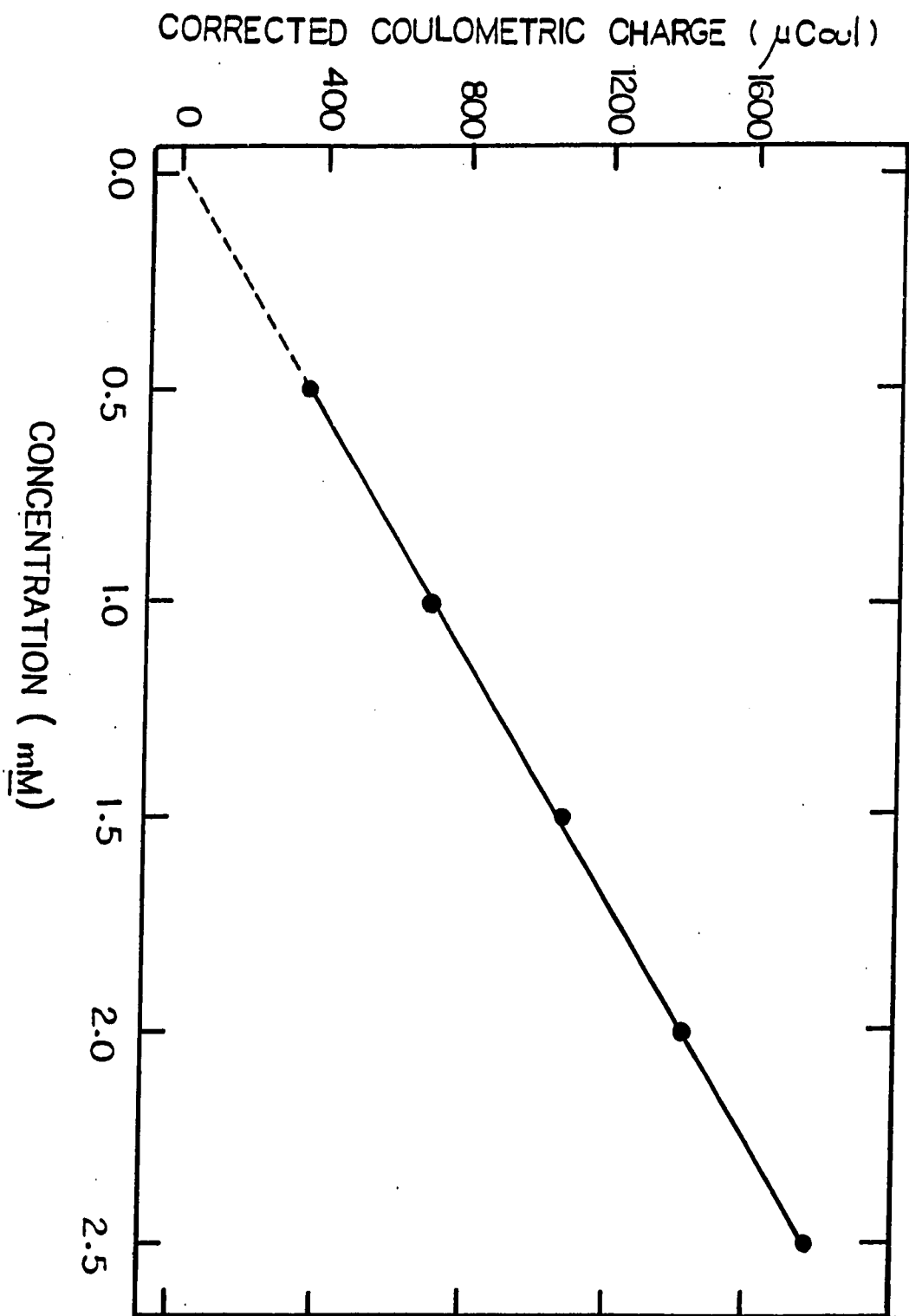


Figure V-3. Coulometric data for $\text{Fe}(\text{CN})_6^{4-}$ as a function of concentration at a gold electrode in a thin-layer cell

Conditions: as given by Figure V-2



From the cell volume obtained and the geometric area of the gold working electrode (2.56 cm^2), the thickness of the thin-layer solution in the cell was calculated to be ca. $44.5 \text{ }\mu\text{m}$. Hence the $50\text{-}\mu\text{m}$ TeflonTM sheet used as the spacer was compressed by ca. 11% during the cell assembling.

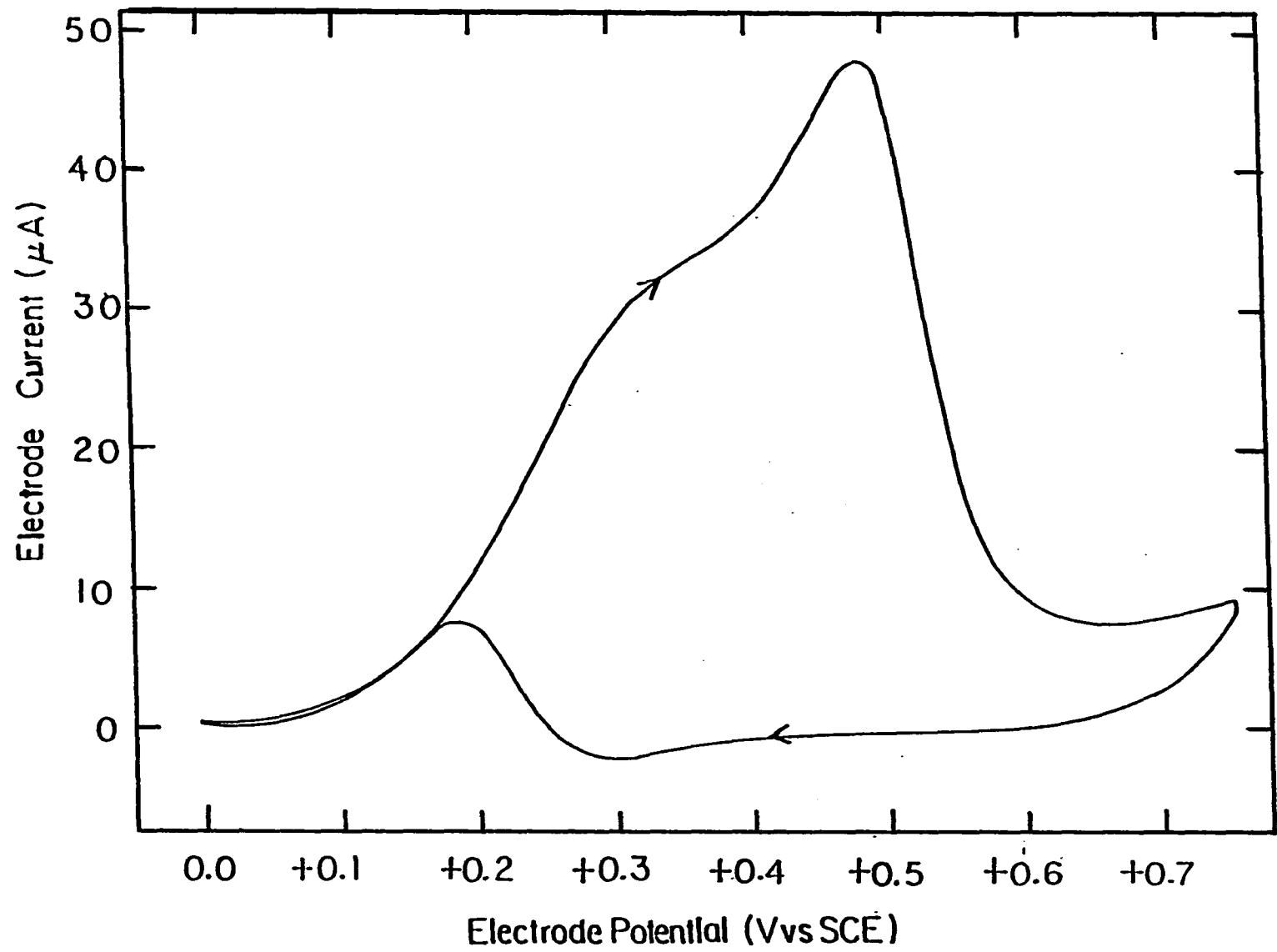
C. Determination of the Number of Electrons Transferred

Experiments were conducted to determine the number of electrons transferred during the electrochemical oxidation of sodium thiophosphate on a gold electrode in 0.1 M NaOH . Numbers of electrons were evaluated for both oxidation of the solution species (n_{soln}) and that of the adsorbed species (n_{ads}).

Cyclic voltammetric current-potential curves at a gold electrode in the thin-layer cell, obtained during the continuous flow of 0.1 mM sodium thiophosphate, are shown in Figure V-4. General features of the voltammogram are similar to those obtained from the cyclic voltammetry at a gold rotating disc electrode. Inspection of the cyclic voltammogram reveals that there are always some interactions between sodium thiophosphate and the gold electrode (either adsorption or electrochemical oxidations) occurring during the positive potential scan. Consequently, the value of the electrode potential applied during the filling of the cell with analyte solution must be considered carefully. If the

Figure V-4. Current-potential curves for sodium thiophosphate by cyclic voltammetry at a gold electrode in a thin-layer cell

Conditions: 0.25 V/min potential scan rate,
0.10 ml/min flow rate



electrode potential is held at the negative potential scan limit (-0.2 V), some of the analyte molecules in the solution stream are adsorbed on the gold surface causing the total number of moles of analyte in the cell to be higher than that calculated from the product of $C^b V_{\text{cell}}$. On the other hand, if the electrode potential is held at a more positive potential, oxidation of sodium thiophosphate occurs during the filling of the cell prior to the actual coulometric measurement. This causes the amount of analyte present to be less than that obtained from the product $C^b V_{\text{cell}}$.

This problem was overcome based on the fact that a gold electrode loses its activity to oxidation of sulfur compounds when the electrode is anodically polarized at a large positive potential such that the electrode surface is excessively covered with gold oxides. By looking at the cyclic voltammogram of sodium thiophosphate (Figure V-4), it can be seen that during the potential reversal at the positive potential scan limit, anodic current due to the oxidation of analyte gradually decays to zero when the electrode is covered with excessive oxides and is inactive.

A proper electrode potential applied during the filling of the thin-layer cell was determined experimentally. The electrode potential scan was interrupted during the negative potential scan and was held

constant at different values. The analyte solution was injected to the cell and the anodic current was observed. Upon the change of the holding potential, it was found that there was no anodic current due to oxidation of sodium thiophosphate when the electrode was held in the range ca. +0.4 V - +0.3 V. The value of +0.4 V was chosen for the holding potential.

Determination of the total coulometric charge due to mass-transport-controlled and surface-controlled processes was performed according to the following steps:

1. The electrode surface was cleaned electrochemically by potential cycling (0.50 V/min) at -0.2 V to +0.7 V with continuous flow (ca. 0.1 ml/min) of 0.1 M NaOH solution until the observed cyclic voltammograms were reproducible.

2. The electrode potential was held at +0.4 V on the negative potential scan to deactivate the electrode.

3. The analyte solution was filled into the cell with careful observation that there was no anodic current due to oxidation of sodium thiophosphate occurs.

4. The electrode potential was stepped to -0.2 V and held for about 2 minutes to reactivate the electrode by oxide reduction and to allow the adsorption of the analyte to occur.

5. The electrode potential was stepped to +0.5 V to oxidize sodium thiophosphate adsorbed on the electrode

surface and that remaining in the solution. The current-time curves were recorded until the slope of the curve was zero. The time used for complete electrolysis was observed.

6. The electrode potential was stepped back to -0.2 V and held for the same amount of time as that used for complete electrolysis performed in step 5 to correct for the background and charging currents.

7. Steps 5 and 6 were repeated until consecutive anodic and cathodic charges were equal ($\pm 1\%$) to assure that all analyte was completely electrolyzed.

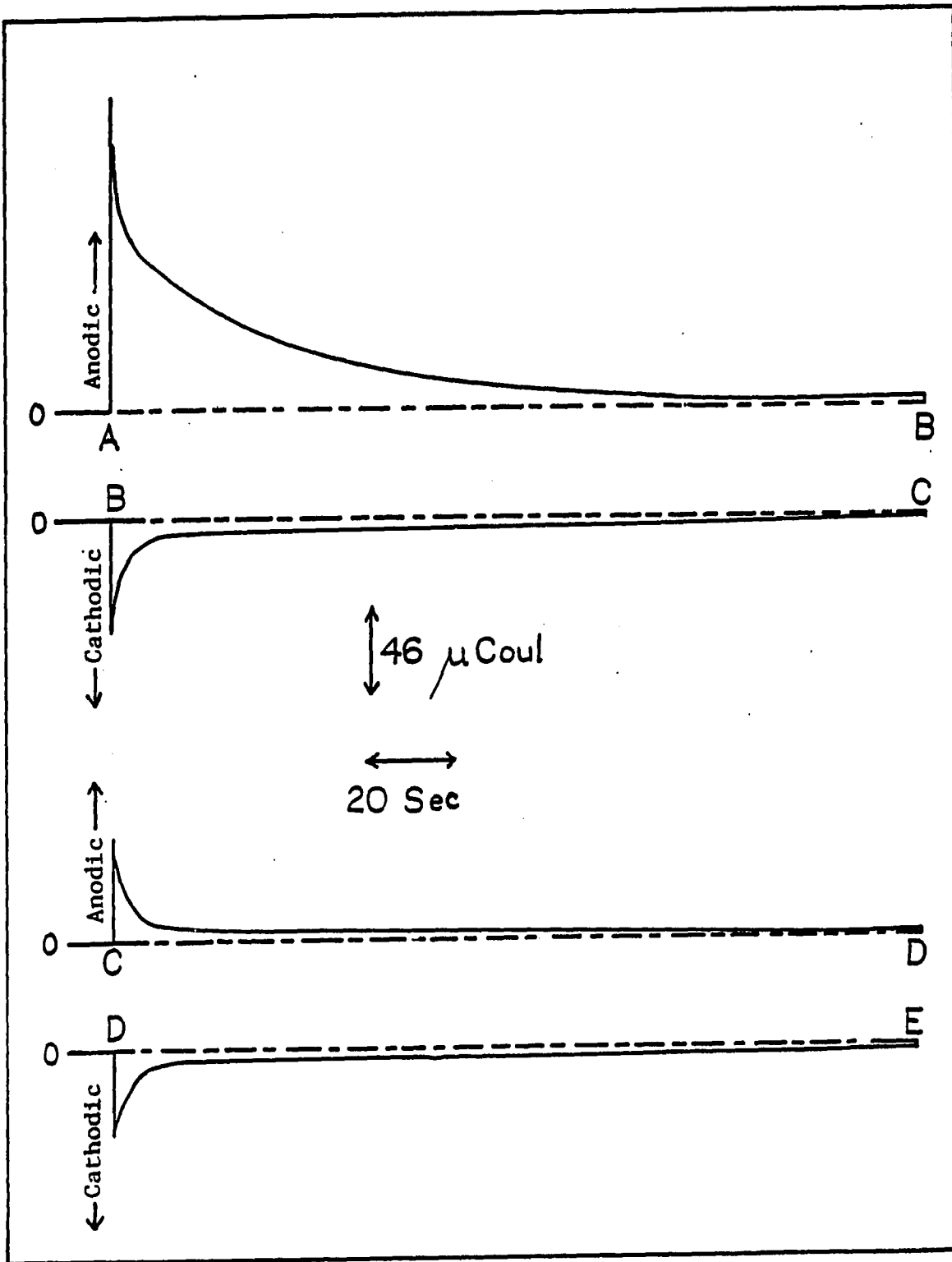
8. The net coulometric charge due to the electrochemical oxidation of sodium thiophosphate was evaluated by subtracting the integral of the cathodic charge from that of the anodic charge.

Typical current-time plots for sodium thiophosphate are shown in Figure V-5 for the bulk concentration of 0.4 mM. The exhaustive electrolysis of sodium thiophosphate was complete in a single potential cycle. Hence the electrode fouling phenomenon was not observed for oxidation of sodium thiophosphate on a gold electrode utilizing this coulometric technique.

Coulometric charge due to oxidation of adsorbed sodium thiophosphate was determined by a similar procedure. Prior to the step of the electrode potential to $+0.5$ V for actual coulometric measurement, the thin-layer cell was rinsed with

Figure V-5. Current-time curves for sodium thiophosphate by double-potential step coulometry at a gold electrode in a thin-layer cell

Conditions: 11.30 μL cell volume,
+0.50 V coulometric oxidation
potential.



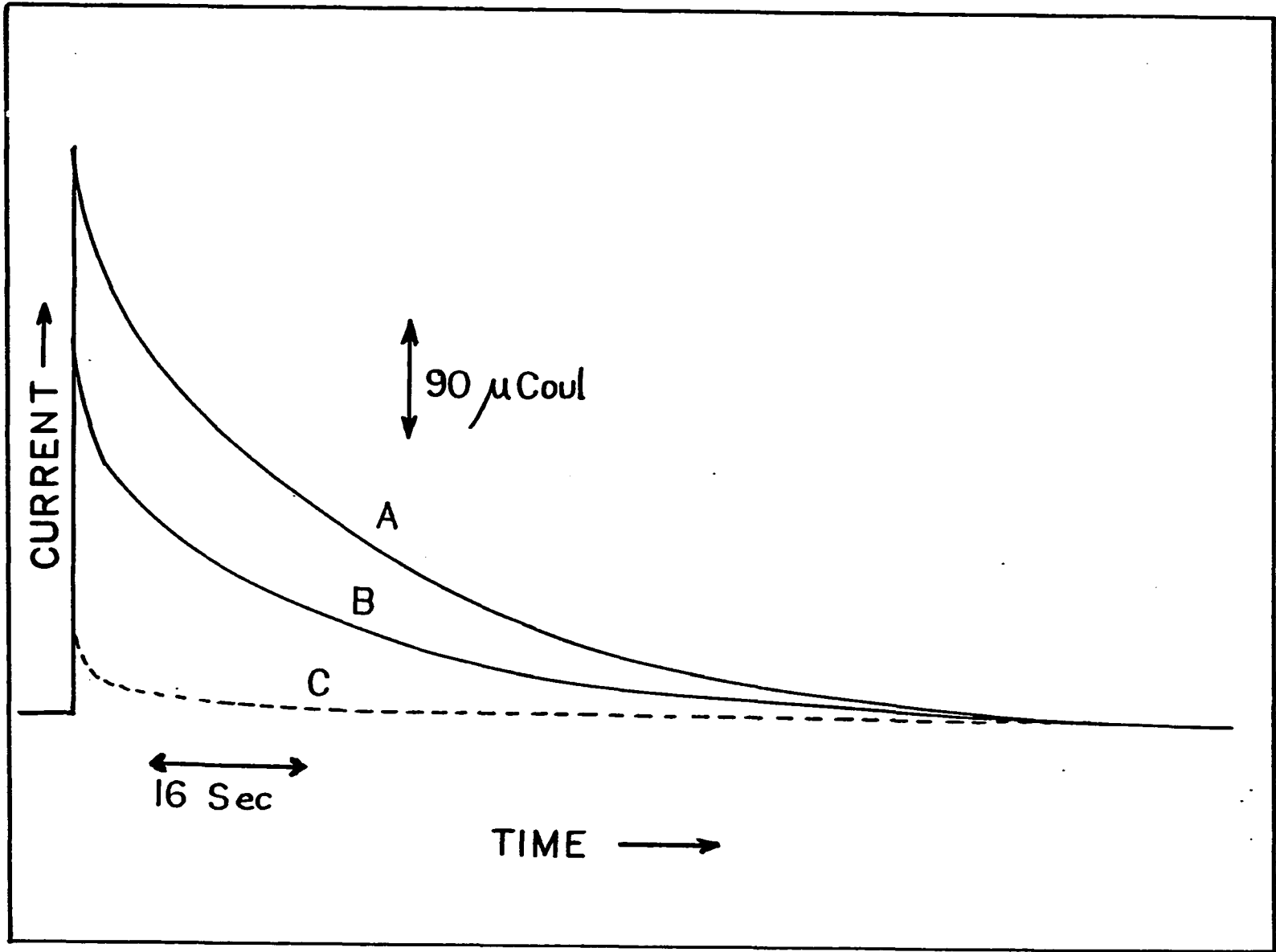
a small volume (< 1 ml) of 0.1 M NaOH to flush the sodium thiophosphate remaining in the solution. Coulometry was continued then to determine the charge due to oxidation of sodium thiophosphate which was adsorbed on the electrode surface and was not flushed with 0.1 M NaOH.

Current-time plots are shown in Figure V-6 for coulometric measurements of 0.5 mM sodium thiophosphate obtained with and without washing with 0.1 M NaOH. The subsequent cathodic backgrounds which were inverted and superimposed upon the anodic traces for convenient inspection of the data are shown also. In both cases (i.e., coulometry with and without washing with 0.1 M NaOH), the backgrounds were found to be identical. Substantial net charge observed even after the cell was flushed with 0.1 M NaOH (Q_{ads} , curve B in Figure V-6) was evidence of adsorption of sodium thiophosphate onto the gold surface during the cathodic polarization of the electrode. The fact that this net charge (Q_{ads}) was less than that obtained when the cell was not flushed with 0.1 M NaOH (Q_{total} , curve A in Figure V-6) implies that at this concentration (0.5 mM), not all sodium thiophosphate in the cell was adsorbed onto the gold surface. Subtraction of the charge under curve B (Q_{ads}) from that under curve A (Q_{total}) provides a direct measurement of the charge due to oxidation of sodium thiophosphate remaining in the solution (Q_{soln}). If it is

Figure V-6. Current-time curves for sodium thiophosphate demonstrating determination of Q_{total} and Q_{ads} by coulometry at a gold electrode in a thin-layer cell

Conditions: 0.5 mM sodium thiophosphate,
+0.5 V coulometric oxidation potential,
11.3 μ L cell volume

Curves: (A) Total anodic current by coulometry without washing with 0.1 M NaOH prior to oxidation
(B) Total anodic current by coulometry after washing with 0.1 M NaOH prior to oxidation
(C) Cathodic currents after the steps from +0.5 V to -0.2 V at the end of coulometric processes in (A) and (B)



assumed that there was no loss of the adsorbed sodium thiophosphate during the washing with 0.1 M NaOH, this Q_{soln} would reflect the amount of sodium thiophosphate that was in equilibrium with that adsorbed on the electrode surface.

For coulometry without washing with 0.1 M NaOH, the net total charge (Q_{total}) is equal to the addition of the net charge due to oxidation of the analyte in the solution and the net charge due to oxidation of the analyte adsorbed on the electrode surface.

$$Q_{\text{total}} = Q_{\text{soln}} + Q_{\text{ads}} \quad [\text{V-4}]$$

$$= [n_{\text{soln}} F N_{\text{soln}}] + [n_{\text{ads}} F N_{\text{ads}}] \quad [\text{V-5}]$$

$$= [n_{\text{soln}} F (N_{\text{total}} - N_{\text{ads}})] + [n_{\text{ads}} F N_{\text{ads}}] \quad [\text{V-6}]$$

$$= [n_{\text{soln}} F N_{\text{total}}] - [n_{\text{soln}} - n_{\text{ads}}] F N_{\text{ads}} \quad [\text{V-7}]$$

At high concentrations (i.e., high N_{total}), the second term in Equation V-7 approaches a constant value since the electrode surface is saturated with sodium thiophosphate causing N_{ads} to be approximately constant. Consequently,

$$\frac{d Q_{\text{total}}}{d N_{\text{total}}} = n_{\text{soln}} F \quad [\text{V-8}]$$

Hence n_{soln} can be determined from the slope of the plots of Q_{total} vs. N_{total} at high N_{total} .

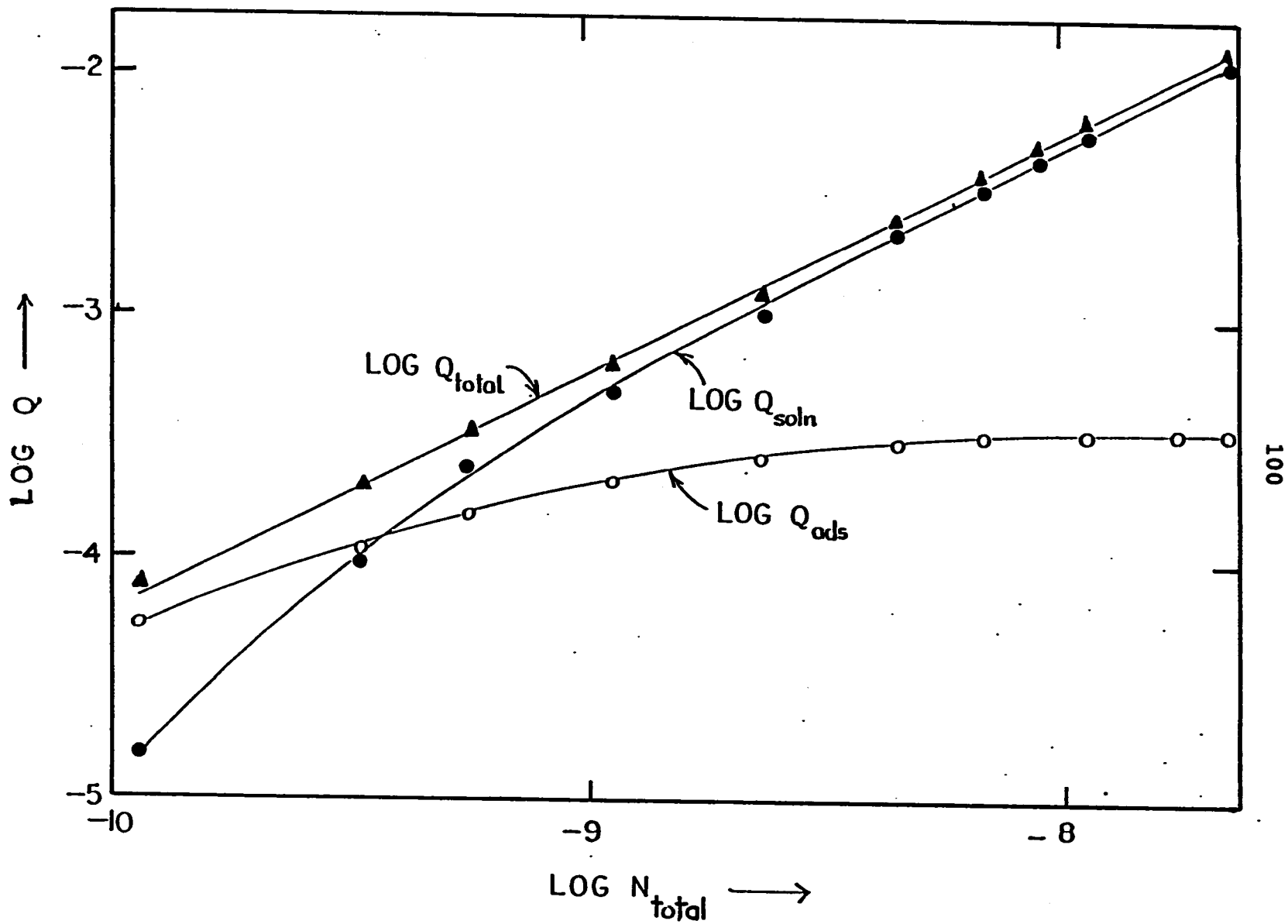
Since the value of the second term in Equation V-5 can be obtained experimentally by performing coulometry after the thin-layer cell is washed with 0.1 M NaOH, n_{ads} can be determined also.

To evaluate n_{ads} and n_{soln} for the oxidation of sodium thiophosphate using the method previously described, coulometric measurements were performed for the concentration range of 0.01-2.0 mM. At each concentration, both net total charge (Q_{total}) and net charge due to oxidation of adsorbed analyte (Q_{ads}) were obtained experimentally. The net charge due to oxidation of the analyte in the solution (Q_{soln}) was obtained by subtraction ($Q_{\text{soln}} = Q_{\text{total}} - Q_{\text{ads}}$).

Results are shown in Figure V-7 as the plots of $\log Q$ vs. $\log N_{\text{total}}$ instead of Q vs. N_{total} to allow a presentation of an even distribution of the data. Plots of $\log Q_{\text{ads}}$ vs. $\log N_{\text{total}}$ (Curve C) exhibit curvature as expected since the amount of sodium thiophosphate adsorbed is influenced by the adsorption isotherm of the compound. Plots of $\log Q_{\text{soln}}$ vs. $\log N_{\text{total}}$ are linear only at high values of $\log N_{\text{total}}$ where the amounts of the adsorbed analyte become constant and the charge increases linearly as a function of the analyte concentration. A plot of $\log Q_{\text{total}}$ vs. $\log N_{\text{total}}$ is linear ($r = 0.9984$), which implies the interesting conclusion that $n_{\text{ads}} = n_{\text{soln}}$.

Figure V-7. Plots of $\log Q$ vs. $\log N_{\text{total}}$ for sodium thiophosphate in 0.1 M NaOH

Conditions: as given by Figure V-6, concentration of sodium thiophosphate = $0.01 - 2.0 \text{ mM}$



Plot of Q vs. N_{total} (not shown) is linear with similar features to those of $\log Q$ vs. $\log N_{\text{total}}$. The slope of the plot of Q_{soln} vs. N_{total} at high values of N_{total} is $570,000 \pm 546$ Coul/mol. The value of n_{soln} was calculated to be 5.91 ± 0.11 according to Equation V-8.

Substitution of the value of n_{soln} into each experimental data performed at different concentrations of sodium thiophosphate (according to equation V-5) gave values of n_{ads} as shown in Table V-1. The average value of n_{ads} was calculated to be 5.85 ± 0.66 .

The fact that the values of n_{soln} (5.9) and n_{ads} (5.8) did not come up to be integral numbers could be attributed to many experimental errors, such as impurities in the analyte, decomposition of sodium thiophosphate upon standing, and errors due to the current-time recording on the strip-chart recorder especially during the very first moment when the potential was stepped to the oxidation potential where the current jumped abruptly to a very high value such that the inertia of the recorder was suspected. Theoretically, there might be also some minor oxidation mechanisms of sodium thiophosphate that give number of electrons less than 6 occurring simultaneously with the one where n is equal to 6.

It is concluded from these experimental results that both sodium thiophosphate molecules that are adsorbed and

Table V-1. Numerical experimental data for coulometry of sodium thiophosphate

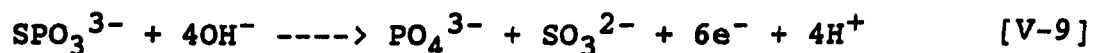
C^b (mM)	N_{total} (nmol)	Q_{total} (μ Coul)	Q_{ads} (μ Coul)	Q_{soln} (μ Coul)	n_{ads}	N_{ads} (pmol)	θ
0.01	0.11	65	50	50	5.90	9	0.015
0.03	0.34	193	102	91	5.89	181	0.290
0.05	0.57	348	146	238	7.05	258	0.430
0.10	1.14	636	210	426	5.57	372	0.600
0.20	2.28	1223	262	961	4.61	464	0.750
0.40	4.55	2603	310	2292	6.21	549	0.890
0.60	6.89	3892	344	3548	5.51	609	0.990
0.80	9.10	5181	352	4829	6.05	624	1.020
1.00	11.38	6497	350	6147	6.44	620	1.000
2.00	22.76	12897	348	12549	5.31	616	1.000

those that are not adsorbed undergo electrochemical oxidation on a gold electrode by the same reaction order where $n = 6$.

The value of $n = 6$ was found to be consistent with that obtained from volumetric titration method carried out under the following procedure: The sample of sodium thiophosphate (ca. 0.05 g) was dissolved completely in a 50-ml solution of warm 2 N H_2SO_4 and titrated immediately with a standard 0.1 N KMnO_4 (previously standardized with primary standard $\text{Na}_2\text{C}_2\text{O}_4$) until a permanent pink endpoint was obtained. The average number of electrons obtained for four titrations was found to be 6 ± 0.10 eq/mole.

D. Identification of the Oxidation Products

At least two possible redox reactions can be written to satisfy the conditions $n = 6$ eq/mol during the electrochemical oxidation of sodium thiophosphate in 0.1 M NaOH .



Identification of the oxidation products was necessary to confirm the right mechanism.

Although the solution obtained after a prolong exhaustive electrolysis of sodium thiophosphate in 0.1 M NaOH (at +0.6 V) on a gold wire gauge electrode gave a positive test for SO_4^{2-} when BaCl_2 was used as a test solution, identification of other components by wet chemical analysis using specific test solutions was not possible due to chemical interferences among the ions in the sample matrix.

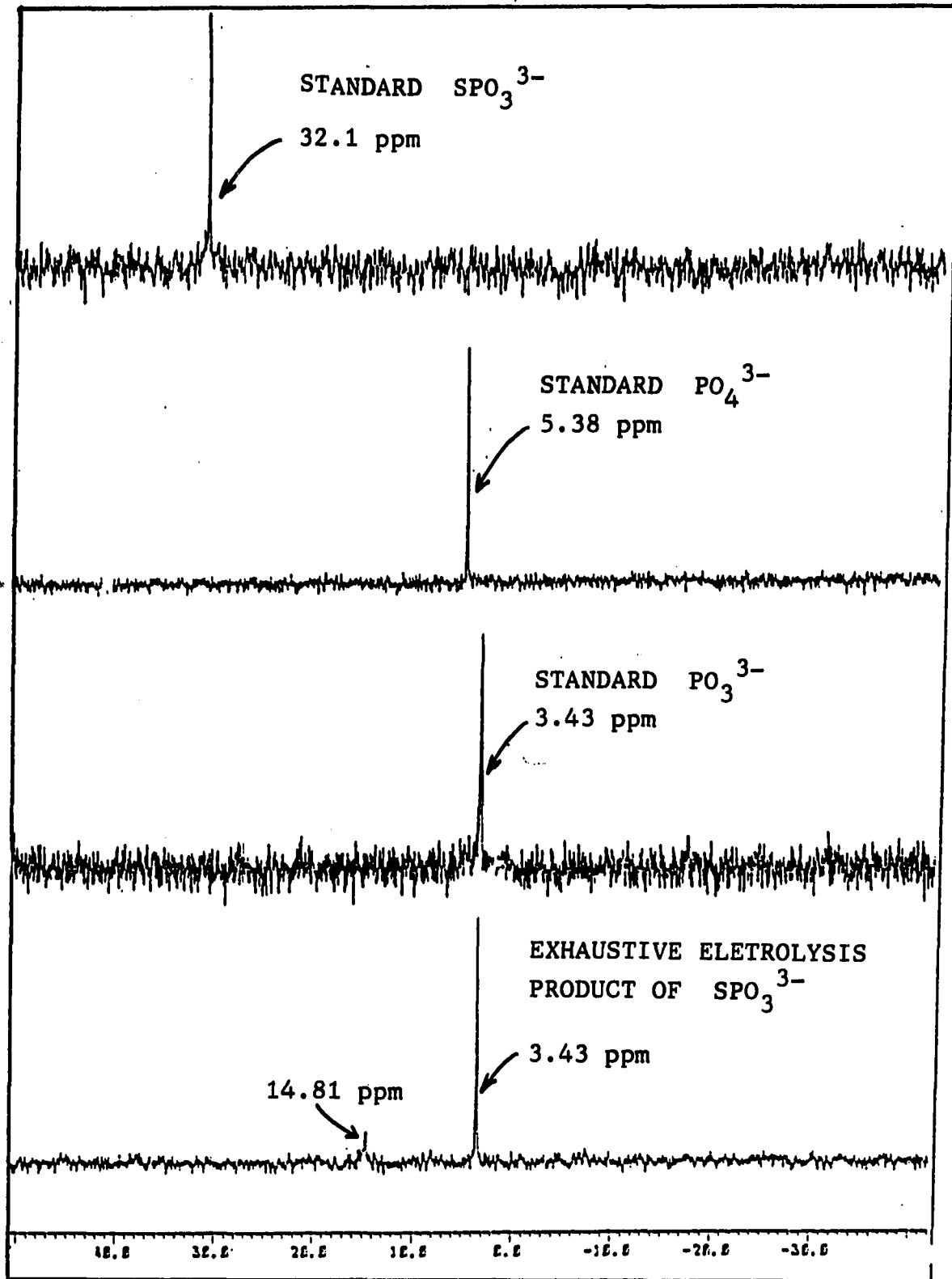
An alternate instrumental method utilizing P-31 NMR technique was used successfully to identify the correct oxidation state of phosphorus. The solution which had shown the positive test for SO_4^{2-} was diluted with deuterated water (D_2O) to give a final composition of 30% in D_2O . A P-31 NMR model WM-200 (Bruker Instrument Inc., Billerica, MA) was used to obtain the chemical shifts of the phosphorous products in the mixture and the results are shown in Figure V-8. Chemical shifts of the product after the exhaustive electrolysis of 5.0 mM of sodium thiophosphate in 0.1 M NaOH are shown along with the chemical shifts of sodium thiophosphate (the starting material), phosphate (as H_3PO_4) and phosphite (as H_3PO_3).

Standard 5.0 mM sodium thiophosphate in 30% D_2O / 0.1 M NaOH gave one chemical shift at $\delta = 32.1$ ppm for SPO_3^{3-} ion (Figure V-8A), while the standard acids gave chemical shifts at $\delta = 5.38$ ppm for PO_4^{3-} ion (Figure V-8B) and $\delta = 3.43$ ppm

Figure V-8. P-31 NMR chemical shifts for standard SPO_3^{3-} , PO_4^{3-} and PO_3^{3-} , and the product solution after exhaustive electrolysis of 0.5 mM sodium thiophosphate at a gold electrode

Conditions: 5.0 mM each standard in 0.1 M NaOH diluted to 70% with D_2O .

Scaling: $\delta = 0$ ppm adjusted by standard H_3PO_4 in a capillary tube inserted in each sample tube during the scan.



for PO_3^{3-} ion (Figure V-8C) respectively. The solution obtained after an exhaustive electrolysis of 5.0 mM sodium thiophosphate gave two distinguishable chemical shifts (Figure V-8D). The minor peak at $\delta = 14.81$ ppm was an unidentified phosphorous-containing species. The major peak at $\delta = 3.43$ ppm confirms the presence of PO_3^{3-} as the major component in the mixture. The relative peak intensity of the minor peak was calculated to be ca. 12% of that of the major peak. The fact that there were two chemical shifts obtained for the solution after the exhaustive electrolysis of sodium thiophosphate, implies that oxidation of this compound involves at least two oxidation mechanisms. The major mechanism (ca. 88%) gives SO_4^{2-} and PO_3^{3-} as the oxidation products, corresponding to the value of $n = 6$ as described by Equation V-10. The minor mechanism (ca. 12%) gives a phosphorous-containing product whose chemical structure is presently unidentified. Nevertheless, based on the ratio of the peak intensity of the minor peak and the major peak, and the number of electron $n = 6$ for the major reaction, this phosphorous-containing product was suspected to be dissipated as a result of oxidation of sodium thiophosphate where $n = 5$.

E. Determination of the Adsorption Isotherm

The fractional surface coverage, Θ , for sodium thiophosphate on a gold surface is related to the molar coverage of the electrode surface by

$$\Theta = \Gamma / \Gamma_{\max} \quad [\text{V-11}]$$

where Γ and Γ_{\max} are equilibrium coverage of sodium thiophosphate (mol/cm^2) on a gold surface at any value of C^b and that at an infinitive value of C^b , respectively. Under the conditions where the electrode surface area is constant, surface coverage can be alternatively written as

$$\Theta = N / N_{\max} \quad [\text{V-12}]$$

where N and N_{\max} are the total numbers of moles of analyte covering the electrode surface at any value of C^b and that at an infinite value of C^b respectively.

In this coulometric study, the value of N_{ads} was obtained for all values of C^b according to the equation

$$Q_{\text{ads}} = n_{\text{ads}} F N_{\text{ads}} \quad [\text{V-13}]$$

where Q_{ads} was obtained experimentally by coulometric measurement after the cell was rinsed with 0.1 M NaOH. Calculated values of N_{ads} at all values of C^b studied (0.1-2.00 mM) are shown in Table V-1. N_{ads} approaches a constant value at ca. 620 pmol for $C^b > 0.8$ mM. By using

this N_{ads} value as the N_{max} , Θ at each value of C^b was calculated and the results are shown in Table V-1.

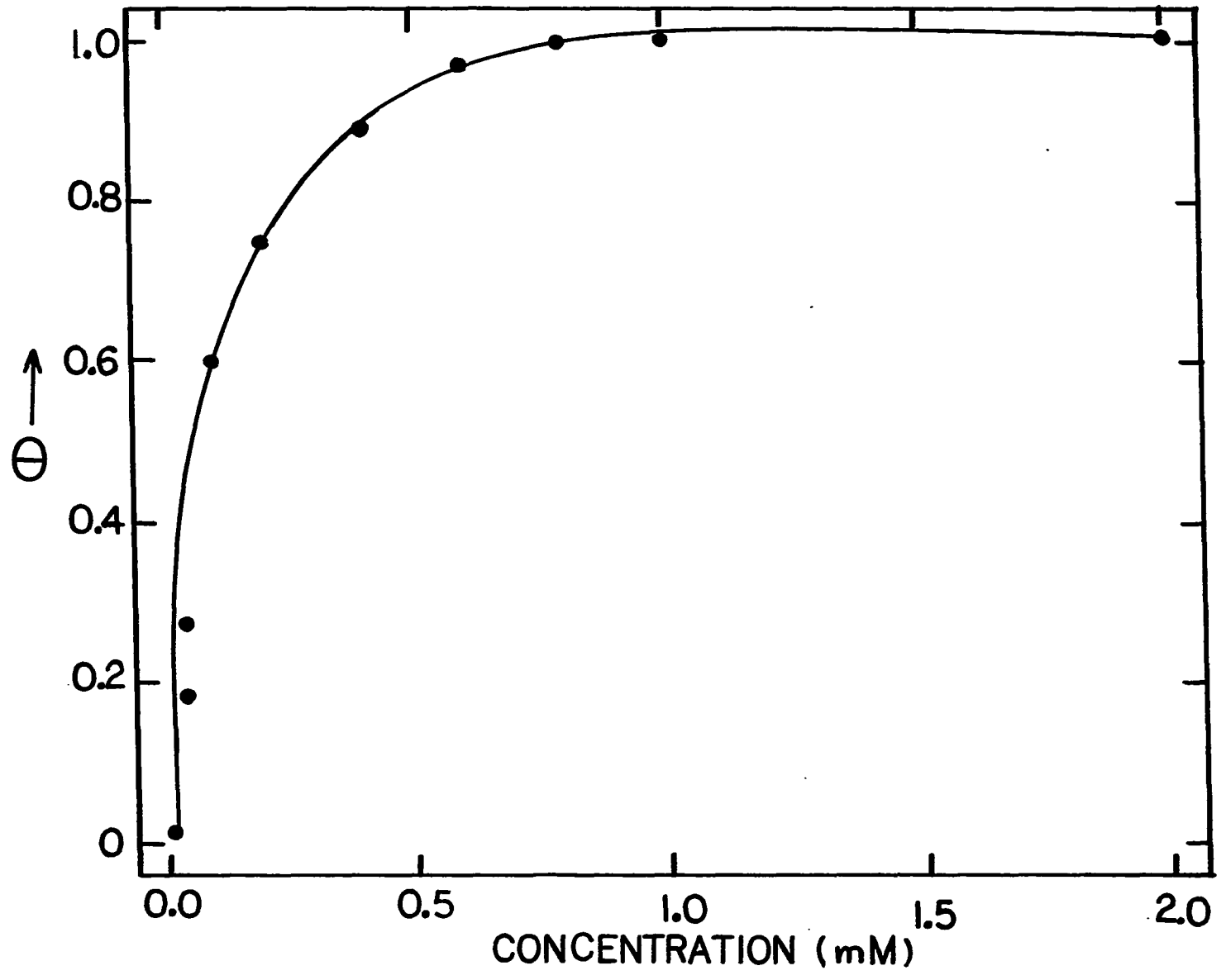
Plots of Θ vs. C^b , i.e., the adsorption isotherm (Figure V-9), exhibits Langmuirian behaviors. The surface becomes saturated with the analyte at the values of $C^b > 0.8$ mM. The maximum surface coverage (Γ_{max}) was calculated to be 337 pmol/cm² which is equivalent to 0.20×10^{15} atom of sodium thiophosphate per cm² of the gold surface. Kostelitz et al. (116) found the average maximum surface coverage of sulfur (S^0) on a single crystal surfaces to be 0.72×10^{15} atom/cm². The approximate gold surface-atom density on a polycrystalline surface is 1.5×10^{15} atom/cm². Thus, the thiophosphate ion monolayer is determined by the size of the ion and not by the number of gold surface sites.

F. Coulometric Study of some other Sulfur Compounds

An effort was made to extend double potential-step coulometry at the gold electrode in the thin-layer cell to coulometric study for some other sulfur compounds. The compounds tested were sodium sulfite (Na_2SO_3), thiourea ($(\text{NH}_2)_2\text{CS}$), sodium thiocyanate (NaSCN) and two sulfur-containing pesticides: Guthion and dimethoate (see structures in Table VII-1). All coulometry was performed using 0.1 M NaOH as the electrolyte except for those of the

Figure V-9. Adsorption isotherm for sodium thiophosphate on gold in
0.1 M NaOH

Conditions: as given by Figure V-7



pesticides where acetonitrile was added (50% by volume) to enhance the solubilities of these compounds. Anodic current was recorded as a function of time during the coulometric oxidation at +0.6 V until the current became constant. The cathodic background (not zero) was recorded once the potential was stepped to the cathodic potential at -0.2 V for the same amount of time as that used for the anodic current measurement. The process was repeated until the consecutive anodic charge (Q_A) and the cathodic charge (Q_C) were equal, i.e. $Q_A/Q_C = 1 \pm 0.01$. In all cases, more than one potential cycle was needed to achieve a unity value for this coulometric charge ratio. Net anodic coulometric charge (Q_{net}) was evaluated by Equation V-13.

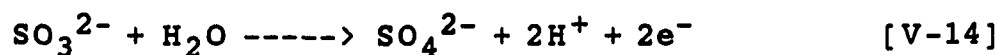
$$\sum Q_{net} = \sum Q_A - \sum Q_C \quad [V-13]$$

Results are shown in Table V-2 for the numbers of electrons obtained for oxidation of compounds tested. In most cases it was not trivial to continue the coulometric measurement to obtain the ratio of Q_A and Q_C of unity and the experiments were terminated at some value of i . Calculated values of n and Q_A/Q_C were reported for the last value of i .

Table V-2. Coulometric results for selected sulfur compounds

Compounds	$n_{i=1}$	$n_{\text{last } i}$	Q_A/Q_C at last i
SO_3^{2-}	1.98	2.08 ₂	1.01
Thiourea	5.40	5.64 ₄	1.06
Guthion	0.17	2.80 ₁₁	3.38
Dimethoate	0.24	2.05 ₈	3.19
SCN^-	0.38	2.34 ₁₉	1.04

Exhaustive coulometry of SO_3^{2-} was complete with $i = 2$ and n was calculated to be 2.0 ± 0.14 . The oxidation process was proposed to involve sulfate as the product according to Equation V-14.



It was not trivial to complete the exhaustive electrolysis of other compounds tested. Oxidation of these compounds on a gold electrode was concluded to be far more complicated than that of sodium thiophosphate. It was concluded from these double-potential-step coulometric results that electrode fouling occurred during the

electrochemical oxidation of these compounds on the gold surface. Stepping the electrode potential to a negative potential prior to each anodic exhaustive electrolysis was not effective enough to recondition the electrode surface. Consequently, the method is not applicable for the determination of n for these sulfur compounds.

G. Conclusion

It has been demonstrated that double potential step chronocoulometric method was useful for the study of reactant adsorption when sodium thiophosphate was the analyte. The technique relies on assumptions that the adsorbed material reacts immediately when the potential is stepped to a value at which oxidation occurs and that there is no coupling between the reaction of the adsorbed and the diffusing material. Results obtained for the evaluation of n and the adsorption isotherm for sodium thiophosphate were satisfactory. The number of electrons transferred during the electrochemical oxidation of sodium thiophosphate on a gold surface was calculated to be 6 eq/mol. Adsorption of this compound on a gold electrode was concluded to behave according to the Langmuir isotherm.

The technique was not applicable for other sulfur compounds tested due to electrode fouling. Recondition of the electrode surface was not accomplished with simple

anodic detection and cathodic polarization. Since oxidation of these sulfur compounds is speculated to be more complicated than that of sodium thiophosphate, better understanding of their oxidation mechanisms as well as the nature of the oxidation products are necessary for proper modification of the method.

VI. FLOW-INJECTION ELECTROCHEMICAL DETECTION OF SULFUR COMPOUNDS IN ALKALINE SOLUTIONS

A. Introduction

The value of peak current for injection of a small volume of analyte concentration (C^b) in a flow-injection system is less than that which would be observed for a continual flow of a solution containing the analyte at a concentration of C^b . The peak concentration in the flow stream (C_p) is less than the analyte concentration in the injected sample because of dispersion within the stream. However, since dispersion is constant in a well-managed flow system, the ratio C_p/C^b is constant for a given compound (117).

Inspection of the voltammetric response of sodium thiophosphate at a gold electrode in 0.1 M NaOH (Figure IV-1) reveals that at least two anodic electrochemical methods are possible for anodic detection of this compound. The simplest method would be detection at a constant potential (DC) at the potential ca. $> +0.2$ V where it appears that mass transport controlled reaction of sodium thiophosphate occurs on the gold electrode surface. Secondly, two-step pulsed amperometric detection (PAD) could be used also to detect the surface-controlled reaction and mass-transport-controlled reaction simultaneously. In this case, the

electrode reactivity is maintained by applying a potential ($E_{\text{ads}} < 0.0 \text{ V}$) for oxide reduction and analyte adsorption followed by the step to a more positive potential ($E_{\text{det}} > +0.4 \text{ V}$) where the adsorbed analyte and the mass-transported analyte are detected anodically.

In this section the electrochemical detection at the gold flow-through detector will be evaluated for application to flow-injection detection, e.g., using the system described in Section IIIB-3. A sample plug was introduced into a flowing stream of 0.1 M NaOH and the peak current (i_p) was measured. The dependence of the peak current on the analyte concentration was investigated for sodium thiophosphate.

B. Flow-Injection Electrochemical Detection of Sodium Thiophosphate

Although the cyclic voltammetric behavior of sodium thiophosphate (Figure IV-1) suggested that any potential greater than +0.15 V can be used as a working potential for anodic detection of the compound under these conditions, it was found by actual investigation of the electrochemical detection in a flow-injection mode that in order to obtain stable and reproducible signals, the anodic detection potential must be in the range of ca. +0.500 to +0.800 V. More positive detection potentials cause the peak currents to be irreproducible due to sharp current spikes concluded

to be caused by oxygen bubbles evolved at the more positive value of the potential.

At any detection potentials less positive than +0.500 V, the anodic peak currents decay as a function of time with subsequent injections of the analyte. This phenomenon is evidence of electrode fouling due to insufficient catalytic reaction from the gold oxide surface formed at potentials less than +0.500 V.

The advantage of pulsed amperometric detection in comparison to DC detection is illustrated in Figure VI-1 for detection of 3.0 mM sodium thiophosphate. Parameters of these waveforms are given below. In all cases, sampling of

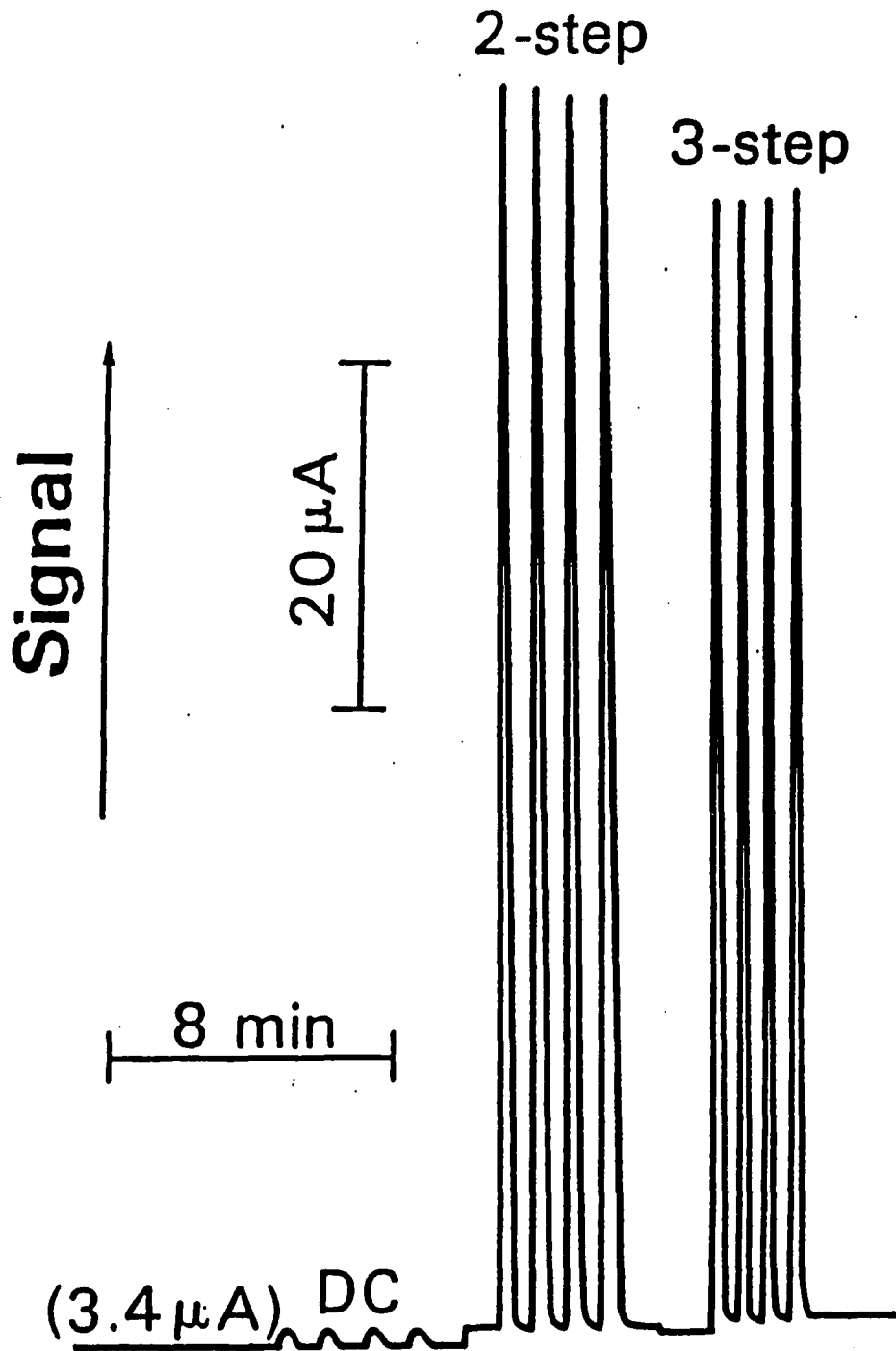
waveform parameter	waveform A (DC)	waveform B (2-step PAD)	waveform C (3-step PAD)
E_d	+0.600 V	+0.600 V	+0.600 V
t_d	500 msec	500 msec	500 msec
E_{clean}	-	-	+1.200 V
t_{clean}	-	-	100 msec
E_{ads}	-	-0.500 V	-0.500 V
t_{ads}	-	500 msec	500 msec

the electrode current occurs near the end of the detection period, t_{det} (500 msec), at the detection potential, E_{det} (600 mV). DC detection, as obtained by execution of

Figure VI-1. Comparison of DC, 2-step and 3-step PAD for sodium thiophosphate

Conditions: 3.0 mM sodium thiophosphate,
50 μ L injections, 0.80 ml/min
flow rate.

Waveform: see text.



waveform A, results in anodic detection of the analyte due to oxidation through the mass-transport-controlled process. In waveform B, a step to a negative potential E_{ads} (-500 mV) is made prior to anodic detection. This potential is negative enough to quickly reduce the oxidized electrode surface to the clean gold metal. Analyte is adsorbed also during period t_{ads} (500 msec) to be detected following the subsequent application of E_{det} +600 mV. Waveform C is included for complete comparison. A step to a more positive potential E_{clean} (1,000 mV) is made prior to a step to a negative potential following by the detection potential.

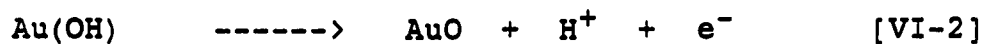
By looking at the peak signal obtained from executions of these waveforms (Figure VI-1), it is obvious that DC detection gives the smallest anodic peak currents as compared to those obtained by pulsed amperometric detections. Therefore, it is concluded that under these experimental conditions the majority of the anodic signal comes from the oxidation of the analyte molecules adsorbed onto the electrode surface during the cathodic polarization at negative potentials prior to the anodic detection. Despite this conclusion, however, it should not be said that dc detection is less sensitive than pulsed amperometric detections without investigation of the values of signal to noise ratio for these methods.

Two-step and three-step pulsed amperometric detections of sodium thiophosphate at a concentration of 3.0 mM give comparable anodic signals and backgrounds as shown in Figure VI-1. Hence, these two detection modes can be interchanged, although the two-step mode is preferred since the detection can be achieved using a simple potentiostat capable of performing normal pulsed amperometric analysis, e.g., EG&G Princeton Applied Research 174A (95). The need for a three-step pulsed potential waveform will become obvious for detections of high molecular weight sulfur compounds at high concentrations as will be discussed later.

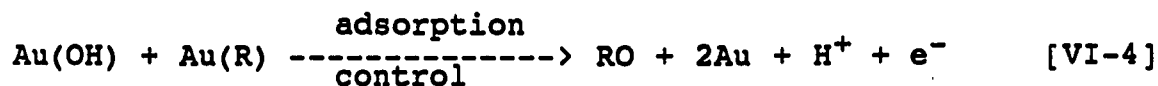
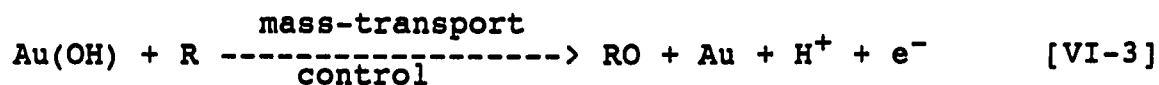
The literature of the anodic formation of surface oxide at gold electrodes has been reviewed by Hoare (118). It is commonly concluded that the first step corresponds to the reversible generation of hydrated gold oxide, Au(OH), by Reaction VI-1. A further oxidation step generates a fully



developed surface gold oxide, AuO, according to Reaction VI-2. Oxidation of sodium thiophosphate on a gold



electrode is believed to involve electrocatalytic oxygen-transfer mechanism. Analyte molecules are oxidatively detected in the region where the surface oxide is formed as described by Equations VI-3 and VI-4.



R = analyte

The greatest detriment to this electrochemical detection is the fouling of the electrode surface by the presence of a fully developed surface oxide (AuO). This conclusion is consistent with the observation of the dramatic decrease in anodic current upon the reversal of the positive potential scan as shown by the cyclic voltammogram of sodium thiophosphate (Figure IV-1).

C. Calibrations

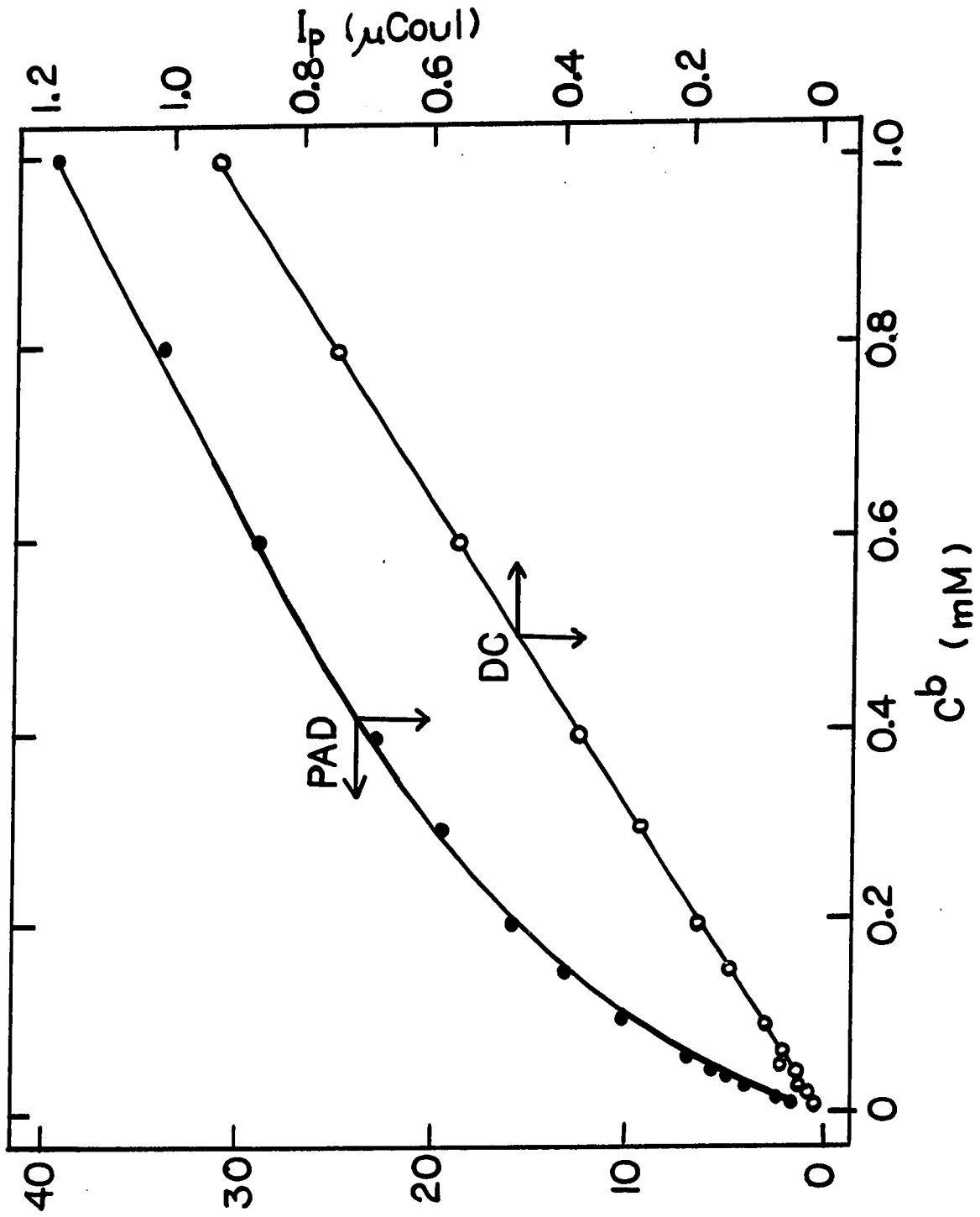
Calibration studies were made for sodium thiophosphate by the flow injection method. Concentrations were in the range 0.01-1.0 mM (0.08-0.80 μg per 20 μl sample). Results are shown in Figure VI-2 for DC detection and pulsed

Figure VI-2. Calibration plots (i_p vs. C^b) for sodium thiophosphate by PAD and DC

Conditions: 20.0 μ L injections, 0.8 ml/min flow rate

Waveforms: PAD, $E_{det} = +800$ mV, $t_{det} = 500$ msec;
 $E_{ads} = -500$ mV, $t_{ads} = 500$ msec

DC, $E_{det} = +800$ mV, $t_{det} = 500$ msec



amperometric detection.

The calibration plot of anodic peak height vs. concentration of sodium thiophosphate (i_p vs. C^b) obtained by DC detection is linear with a slope = 0.9431 ± 0.0019 $\mu\text{A}/\text{mM}$, intercept = 0.0061 ± 0.0007 μA and $r = 0.9993$. The uncertainties in slope and intercept represent the 90% confidence intervals. This linear response behavior under the concentration range studied (0.01-1.0 mM) is consistent with the conclusion that the anodic signal obtained by of dc detection is due to anodic oxidation of sodium thiophosphate carried to the electrode by convective mass transport processes.

The plot of i_p vs. C^b obtained by a two-step pulsed amperometric detection for sodium thiophosphate is shown also in Figure VI-2. Non-linearity of the plots was observed since application of the two-step pulsed potential waveform resulted in anodic detection of sodium thiophosphate molecules that were transported to the electrode surface by mass transport processes as well as those that are adsorbed onto the electrode surface during the cathodic polarization potential. Hence, the shape of the calibration curve is expected to be partially influenced by the adsorption isotherm of the analyte and, therefore, is expected to deviate from linearity at high concentrations.

**D. Dependence of the Peak Shape on Waveform
and Analyte Concentration**

For flow-injection detection in a well-managed system, the system dispersion coefficient (i.e. C_p/C^b) is constant for a given compound regardless of the analyte bulk concentrations (117). Subsequent injection of small volumes analyte into the flow stream should give peak signals with same peakwidths for analyte at all bulk concentrations. Observation of the variation of the peakwidths in flow-injection electrochemical detection of a particular compound reflects the change of the electrode surface mainly caused by electrode fouling.

Dependence of the peak width on electrochemical waveform was investigated by flow-injection detection of sodium thiophosphate using DC, two-step and three-step pulsed potential waveforms under the same system conditions. Anodic peak signals are shown in Figure VI-3A for detection of 3.0 mM sodium thiophosphate. Lowest signal is obtained for DC detection, and comparable signals are obtained for two-step and three-step pulsed amperometric detections. For easy comparison of the peakwidths, all anodic peak signals were made approximately equal by adjustments of detector sensitivity and recorder output, and the time scale was expanded. These, as will be called, "normalized signals"

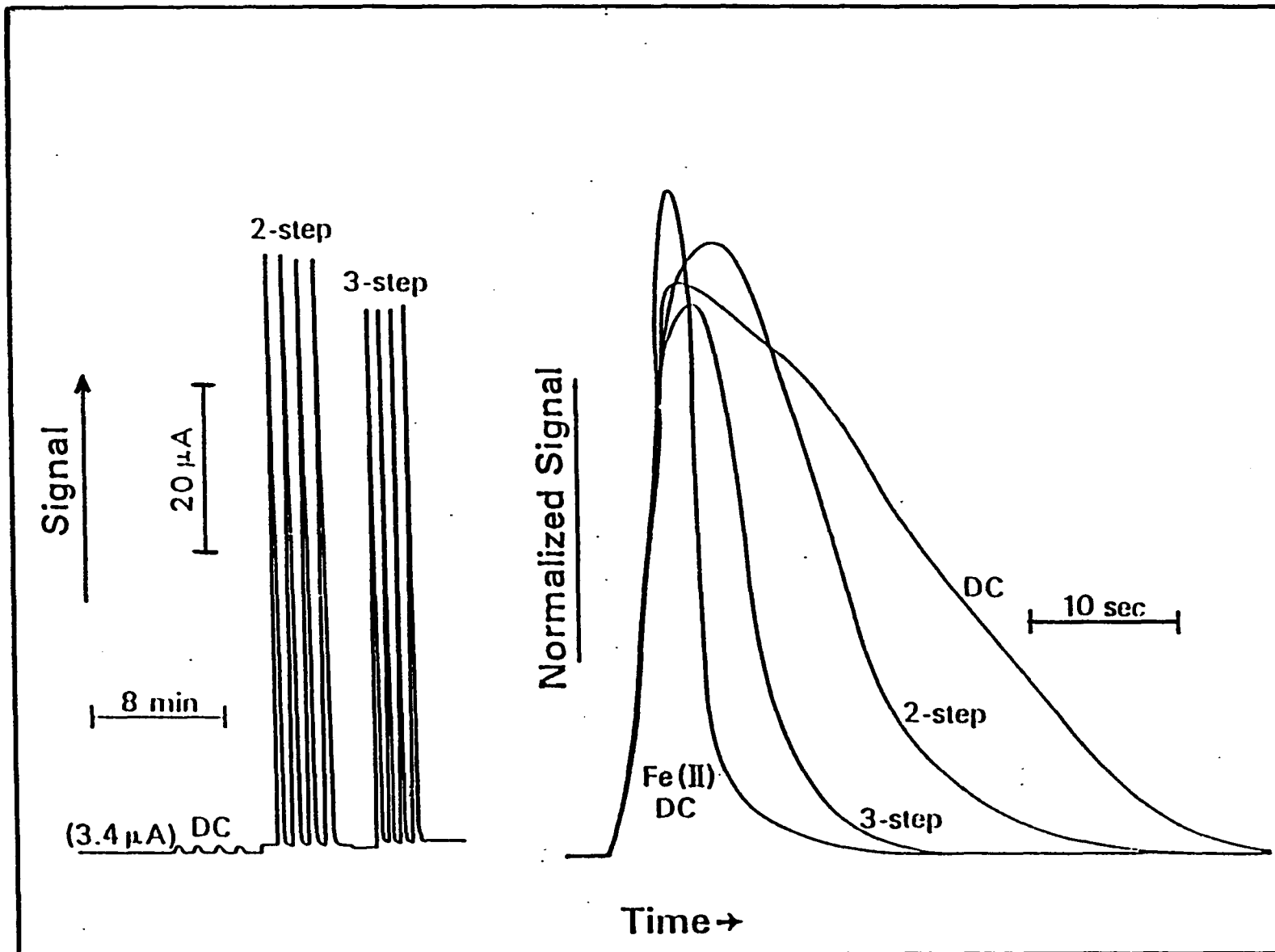
Figure VI-3. Dependence of the peak width on waveform for detection of 3.0 mM sodium thiophosphate in 0.1 M NaOH

Conditions: 50 μ L injections, 0.61 ml/min flow rate

Waveform: dc $E_{det} = 600$ mV, $t_{det} = 500$ msec

2-step $E_{det} = 600$ mV, $t_{det} = 500$ msec;
 $E_{ads} = -500$ mV, $t_{ads} = 500$ msec

3-step $E_{det} = 600$ mV, $t_{det} = 500$ msec;
 $E_{ads} = -500$ mV, $t_{ads} = 500$ msec;
 $E_{clean} = 1,200$ mV, $t_{clean} = 200$ msec



are superimposed as shown in Figure VI-3B. Narrowing of the peakwidths upon the change of the electrochemical waveforms from DC -> two-step -> three-step pulsed potential detections implies the improvement of the efficiency of electrode reconditioning by the same order. Constant potential anodic detection of Fe^{2+} is shown in Figure VI-3B as a controlled signal where no electrode fouling occurred. Notice that under these experimental conditions, three-step pulsed amperometric detection still showed a little electrode fouling effect as the peak width obtained by this detection mode is broader than that of the controlled peak of Fe^{2+} .

Dependence of the peak shape on the analyte concentration is shown in Figure VI-4 for two-step pulsed amperometric detection of sodium thiophosphate at concentrations of 1.0 and 3.0 mM. Actual anodic peak signals for each concentration are shown in Figure VI-5A and the superimposed "normalized signals" are shown in Figure VI-4B along with the controlled peak of Fe^{2+} . Broader peakwidth at 3.0 mM as compared to that at 1.0 mM concentration suggests that electrode cleaning is made more difficult at higher analyte concentrations.

Investigation of the dependences of peakwidth on analyte concentration and potential waveform is significant for evaluation of the optimum conditions for detection of

Figure VI-4. Dependence of the peak width on concentration for 3-step PAD of sodium thiophosphate in 0.1 M NaOH

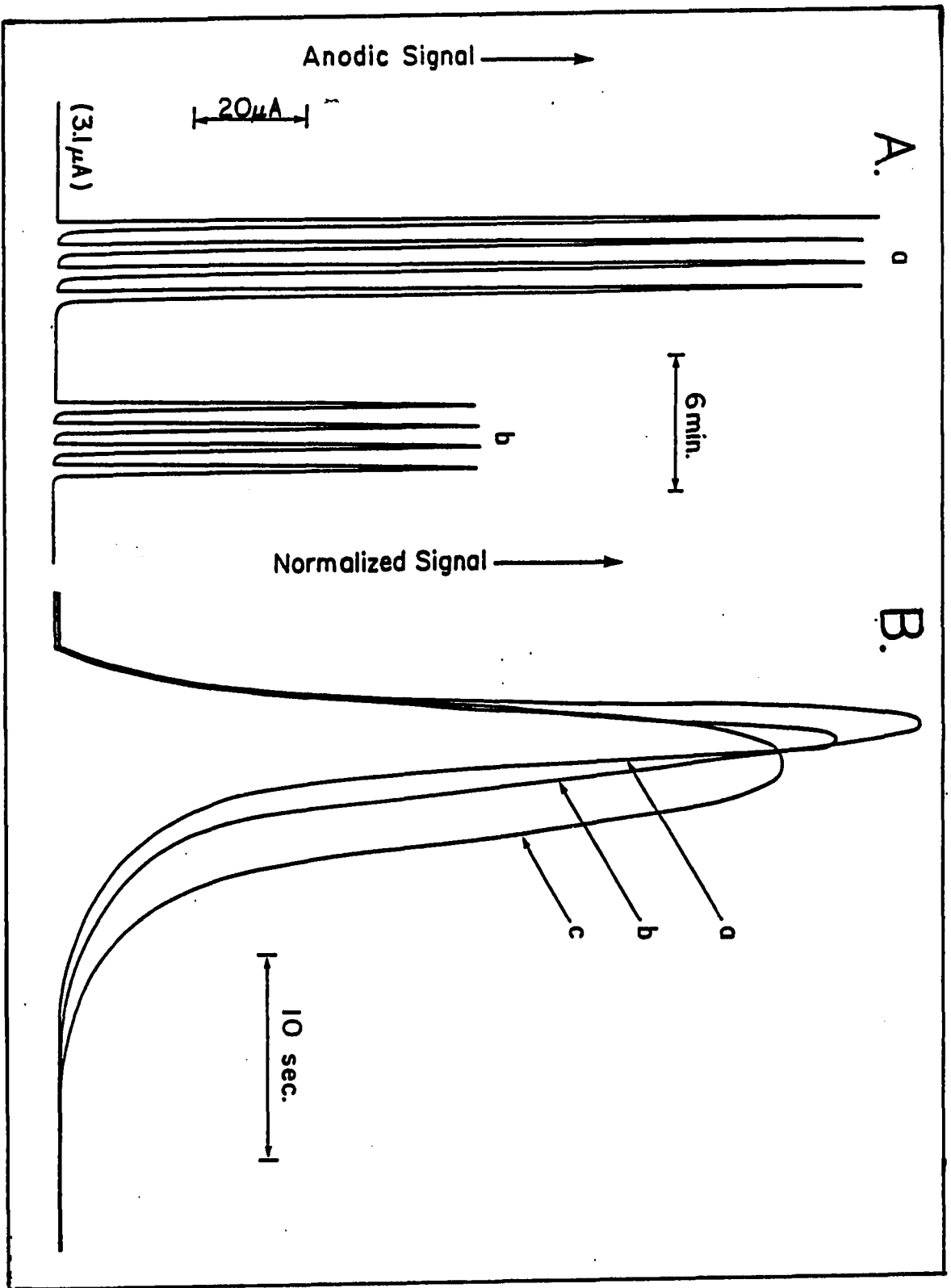
Waveform: $E_{\text{det}} = 600 \text{ mV}$, $t_{\text{det}} = 500 \text{ msec}$;
 $E_{\text{ads}} = -500 \text{ mV}$, $t_{\text{ads}} = 500 \text{ msec}$;
 $E_{\text{clean}} = 1,200 \text{ mV}$, $t_{\text{clean}} = 200 \text{ msec}$

Concentration: A. Actual peak signals

- a) 3.0 mM Na_3SPO_3
- b) 1.0 mM Na_3SPO_3

B. Normalized peak signals

- a) 0.5 mM Fe^{2+}
- b) 1.0 mM Na_3SPO_3
- c) 3.0 mM Na_3SPO_3



the analyte. In cases where broadening of peak currents becomes severe, the injection volume should be made smaller, the concentration should be made more dilute, and/or the waveform should be made of steps with more efficient cleaning of the electrode surface.

E. Conclusion

Anodic electrochemical detection in flow-injection detection of sodium thiophosphate is possible by DC, two-step and three-step pulsed amperometric detections. For pulsed amperometric detection, neither $i_p - C^b$ nor $1/i_p - 1/C^b$ plots was linear. This behavior is expected since the anodic detection is concluded to involve a reaction with mixed transport-adsorption control. Peak width is influenced by mode of electrochemical detection and analyte concentration. The best peak width, i.e., the narrowest peak, is obtained using a three-step pulsed amperometric detection at a low concentration of sodium thiophosphate.

**VII. CYCLIC VOLTAMMETRY OF SULFUR-CONTAINING PESTICIDES
IN 50% ACETONITRILE/ACETATE BUFFER
AT GOLD ELECTRODES**

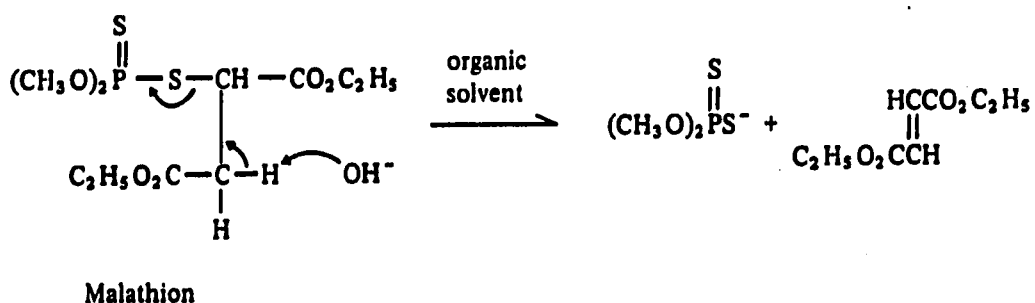
A. Introduction

Pesticides are known to have limited solubility in aqueous solutions. Therefore, an organic modifier is needed to enhance the solubility of the desired analytes. Experiments were conducted to find the most appropriate solvent system to serve the need for adequate pesticide solubility, chromatographic separation and electrochemical detection.

Cyclic voltammetric studies of pesticides in various solvent systems were performed on MeOH-H₂O, EtOH-H₂O, Bu₄NOH-H₂O, DMSO-H₂O and acetonitrile-water (ACN-H₂O). Acetonitrile-water was found to be the most appropriate mixture due to low background and wider overpotential range in which interesting anodic oxidations of pesticides could occur on a gold surface.

Sodium hydroxide, previously used as an electrolyte in the aqueous system, can no longer be used since it was observed that the anodic peak currents obtained for pesticides by cyclic voltammetry in 50% ACN/0.1 M NaOH increased with time and reproducible signals could not be obtained. This phenomenon is consistent with the fact that

all organothiophosphates undergo alkaline hydrolysis in organic solvents (119). An example is given below for alkaline hydrolysis of malathion. The fact that the peak currents increased with time in cyclic voltammetry implies that the hydrolyzed analytes are more electroactive at gold electrode than the unhydrolyzed analytes.



In this study, mixtures of acetonitrile in acetate buffer at pH 5.0 were chosen since successful separation of similar pesticides by reversed phase high performance liquid chromatography had been reported recently using this solvent mixture system (120).

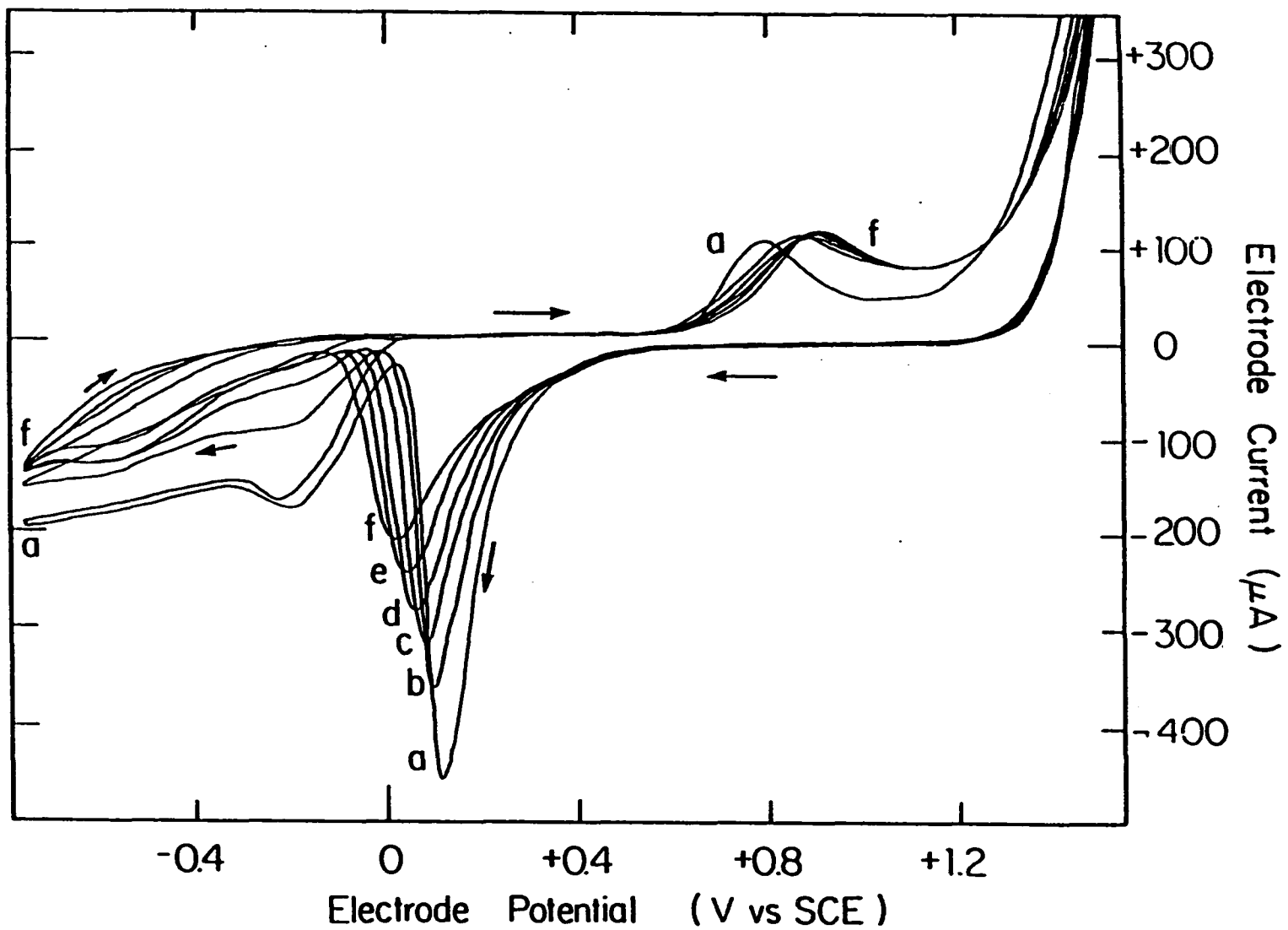
B. Acetate Buffer with Acetonitrile Added

The residual current-potential response of the gold rotating disc electrode in acetate buffer at pH 5.0 is shown in Figure VII-1 as a function of added acetonitrile.

Figure VII-1. Current-potential curves at RDE for acetate buffer at pH 5.0 as a function of added acetonitrile

Conditions: 1,000 rev/min rotation speed,
6.0 V/min scan rate

Concentration acetonitrile (% v/v): (a) 0
(b) 10
(c) 20
(d) 30
(e) 40
(f) 50



For the positive potential scan, formation of gold oxide occurred at $E > \text{ca. } 0.7 \text{ V}$ followed by the evolution of oxygen at $E > \text{ca. } 1.3 \text{ V}$. Upon reversal of the potential scan, the anodic response from oxygen evolution and oxide formation decayed quickly such that current was virtually zero obtained for $E = 1.2 - 0.6 \text{ V}$. At $E < 0.6 \text{ V}$ on the negative scan, reduction of gold oxide was observed with the peak current at $\text{ca. } 0.1 \text{ V}$ followed by reduction of the dissolved oxygen at $E < \text{ca. } 0.0 \text{ V}$.

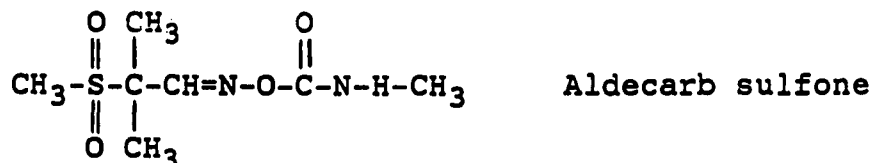
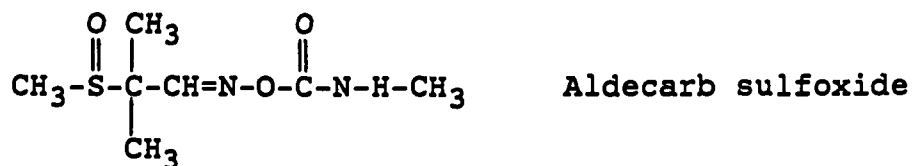
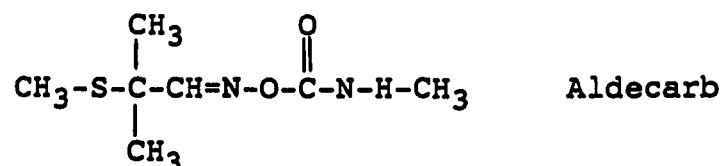
With the addition of acetonitrile, formation of gold oxide on the positive scan was suppressed slightly to more positive potentials ($E > 0.7 \text{ V}$). By looking at the peak area for the reduction of gold oxide as a function of added acetonitrile during the negative scan, it is concluded that acetonitrile suppressed the gold oxide formation reaction. The presence of acetonitrile also caused oxidation of the solvent at slightly more positive potentials.

Reactions of acetonitrile on gold electrode in acetate buffer were concluded to be surface-controlled processes since the current-potential response in cyclic voltammetric study showed a sweep rate dependence and no rotational speed dependence.

Composition of 50% acetonitrile was chosen as the residual for pesticides in later study.

C. 50% Acetonitrile/Acetate Buffer with Pesticides Added

The voltammetric response of sulfur-containing pesticides was obtained for preliminary characterization using cyclic voltammetry at gold electrodes in 50% acetonitrile/acetate buffer pH 5.0. Anodic response was observed for numerous sulfur-compounds as shown in Table VII-1. It should be mentioned that, although anodic signal was observed for aldecarb, there was no or very small anodic response for aldecarb sulfone and aldecarb sulfoxide.



This can be understood easily by looking at the chemical structures of this compounds. Aldecarb sulfoxide and

Table VII-1. Representative sulfur-containing pesticides showing anodic responses by cyclic voltammetry at a gold RDE in 50% acetonitrile in acetate buffer pH 5.0


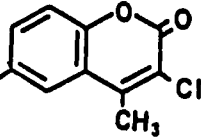
Common Name	Structure
Aldicarb (Temik)	$\begin{array}{c} \text{CH}_3 \\ \\ \text{CH}_3\text{S}-\text{C}-\text{CH}=\text{N}-\text{O}-\overset{\text{O}}{\parallel}{\text{C}}-\text{N}-\text{CH}_3 \\ \\ \text{CH}_3 \\ \\ \text{H} \end{array}$
Aspon (NPD)	$(\text{C}_2\text{H}_5\text{O})_2\overset{\text{S}}{\parallel}\text{P}-\text{O}-\overset{\text{S}}{\parallel}\text{P}(\text{OC}_2\text{H}_5)_2$
Azinphos methyl (Guthion)	$(\text{CH}_3\text{O})_2\overset{\text{S}}{\parallel}\text{P}-\text{S}-\text{CH}_2-\text{N} \begin{array}{l} \diagup \text{O} \\ \diagdown \text{N} \end{array} \text{C}_6\text{H}_4$
Bensulide (Prefar)	$\text{O} \quad \text{H} \quad \text{S} \\ \parallel \quad \quad \parallel \\ \text{O}=\text{S}-\text{N}(\text{CH}_2)_2\text{S}-\text{P}[\text{OCH}(\text{CH}_3)_2]_2$ 
Bromophos (Nexion)	$(\text{CH}_3\text{O})_2\overset{\text{S}}{\parallel}\text{P}-\text{O}-\text{C}_6\text{H}_2(\text{Cl})_2(\text{Br})$
Chlorpyrifos (Dursban)	$(\text{C}_2\text{H}_5\text{O})_2\overset{\text{S}}{\parallel}\text{P}-\text{O}-\text{C}_6\text{H}_3(\text{Cl})_2(\text{CH}_3)$ 

Table VII-1. (continued)

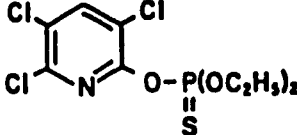
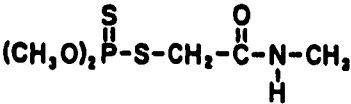
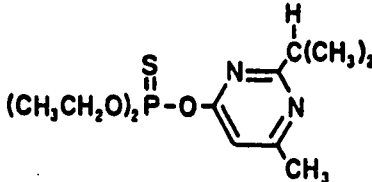
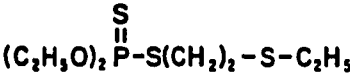
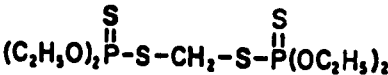
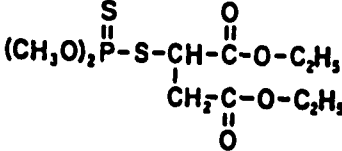
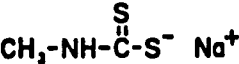
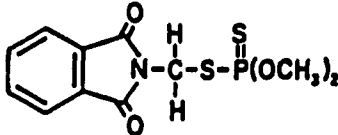
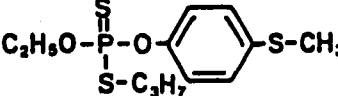
Common Name	Structure
Coumaphos (Co-Ral)	
Dimethoate (Cygon)	
Diazinon (Spectracide)	
Disulfoton (Di-Syston)	
Ethion (Bladan)	
Malathion (Sumitox)	
Metham sodium (Vapam)	

Table VII-1. (continued)

Common Name	Structure
Methomyl (Lannate)	$\begin{array}{c} \text{O} \\ \parallel \\ \text{CH}_3-\text{C}=\text{N}-\text{O}-\text{C}-\text{N}-\text{CH}_3 \\ \quad \\ \text{S}-\text{CH}_3 \quad \text{H} \end{array}$
Phorate (Thimet)	$(\text{C}_2\text{H}_5\text{O})_2\text{P}(=\text{S})-\text{S}-\text{CH}_2-\text{S}-\text{C}_2\text{H}_5$
Phosmet (Imidan)	
Sulprofos (Bolstar)	
Terbufos (Counter)	$(\text{C}_2\text{H}_5\text{O})_2\text{P}(=\text{S})-\text{S}-\text{CH}_2-\text{S}-\text{C}(\text{CH}_3)_3$
Thiometon (Ekatin)	$(\text{CH}_3\text{O})_2\text{P}(=\text{S})-\text{S}-(\text{CH}_2)_2-\text{S}-\text{C}_2\text{H}_5$
Thiram (Arasan)	$(\text{CH}_3)_2\text{N}-\overset{\text{S}}{\parallel}{\text{C}}-\text{S}-\text{S}-\overset{\text{S}}{\parallel}{\text{C}}-\text{N}(\text{CH}_3)_2$

aldecarb sulfone constitute of sulfurs at higher oxidation state hence oxidation could occur with difficulty or not at all.

Initial inspection revealed that the voltammetric behavior of all sulfur-containing pesticides are surprisingly similar. Dimethoate was chosen as a representative compound for further study due to its relatively low toxicity. Current-potential curves are shown in Figure VII-2 for dimethoate in 50% acetonitrile/acetate buffer at pH 5.0. Unlike the effect of addition of acetonitrile, the addition of dimethoate had only a slight effect on the total amount of gold oxide formed during the positive scan to 1.5 V, as determined by the area of the cathodic peak for the oxide reduction on the negative scan. Oxidation of dimethoate on the positive potential sweep occurred simultaneously with gold oxide formation to produce a current peak at ca. 0.95 V. The total anodic response increased as the concentration of dimethoate increased.

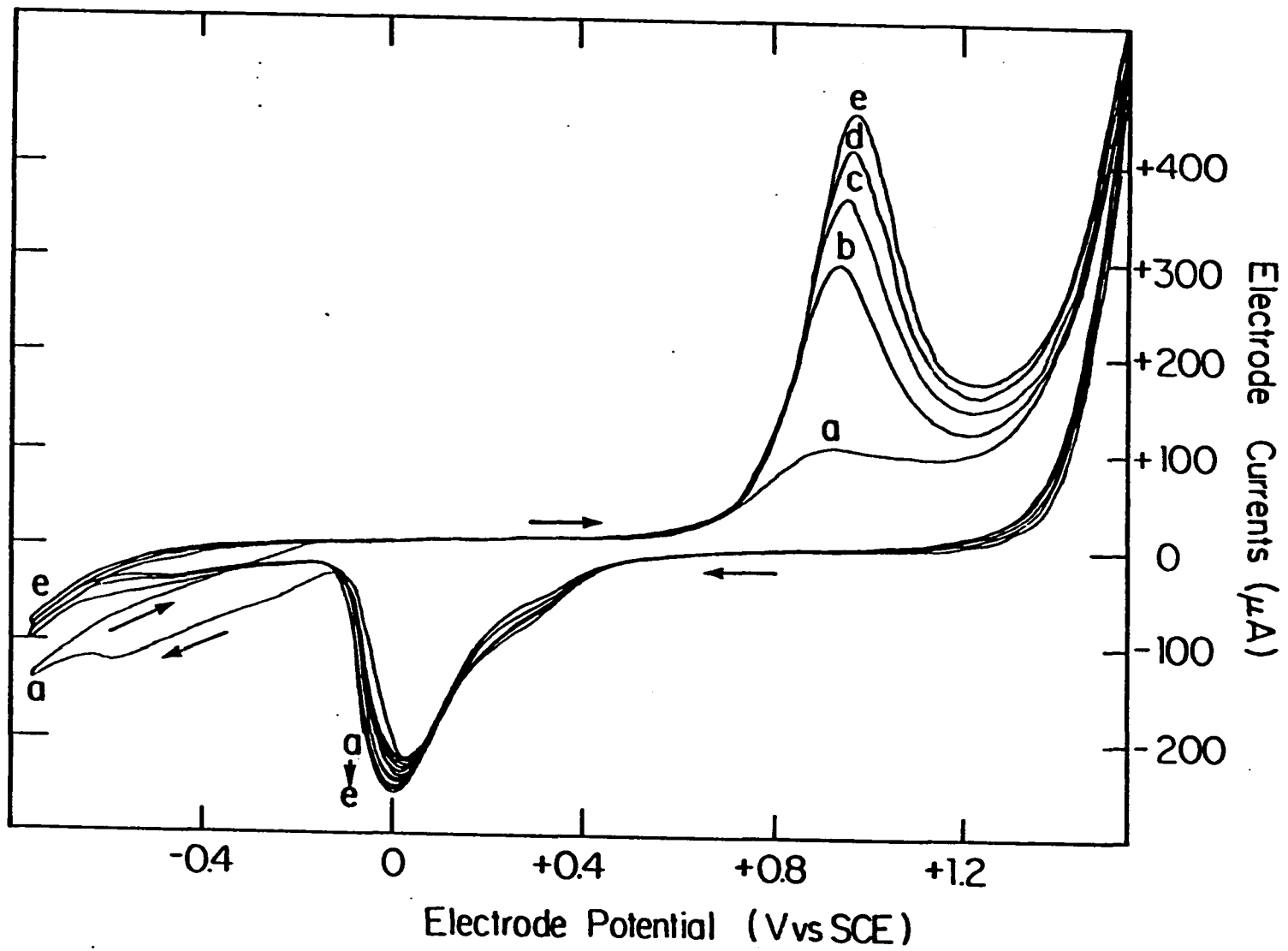
D. Dependence on Rotational Speed and Potential Scan Rate

For the conditions of concentration (0.5-2.0 mM) and potential scan rate (6 V/min), the variation of rotational speed of rotating disc electrode (400-3,600 rev/min) produced a negligible change in the anodic signal (< ca. 10%), i.e., rotational speed independent. On the

Figure VII-2. Current-potential curves at RDE for 50% acetonitrile in acetate buffer at pH 5.0 as a function dimethoate added

Conditions: 1,000 rev/min rotation speed,
6.0 V/min scan rate

Concentration dimethoate (mM): (a) 0.0
(b) 0.5
(c) 1.0
(d) 1.5
(e) 2.0



other hand, the peak anodic signal for dimethoate was strongly dependent on scan rate as shown in Figure VII-3. This behavior is characteristic of surface-controlled detection mechanism. The fact that the anodic signal is not rotational speed dependent implies that the surface coverage was apparently at its equilibrium value as controlled by the adsorption isotherm and the analytical signal is concluded to result from the oxidation of adsorbed analyte simultaneously with anodic formation of surface oxide.

E. Proof of Adsorption of Dimethoate on Gold

Effects of negative potential scan limits on anodic response of dimethoate on a gold electrode in 50% acetonitrile/acetate buffer at pH 5.0 is shown in Figure VII-4. Upon the change of the negative potential scan limit, it was found that there was no anodic response from dimethoate unless the negative scan limit was made more negative than 0.0 V where adsorption of this compound on the oxide-free electrode surface could occur. The limits of the negative potential scan that allow the adsorption of the compounds were found to be slightly variable. For example, ethion was adsorbed for $E < -0.2$ V. Anodic response was found for all compounds studied when the negative potential scan limit was < -0.4 V. In addition to this observation, the fact that reduction of dissolved oxygen was shifted to

Figure VII-3. Current-potential curves at RDE for dimethoate in 50% acetonitrile in acetate buffer at pH 5.0 as a function of potential scan rate

Conditions: 2.0 mM dimethoate,
1,000 rev/min rotation speed

Scan rates (V/min): (a) 2.0
(b) 4.0
(c) 6.0
(d) 8.0
(e) 10.0

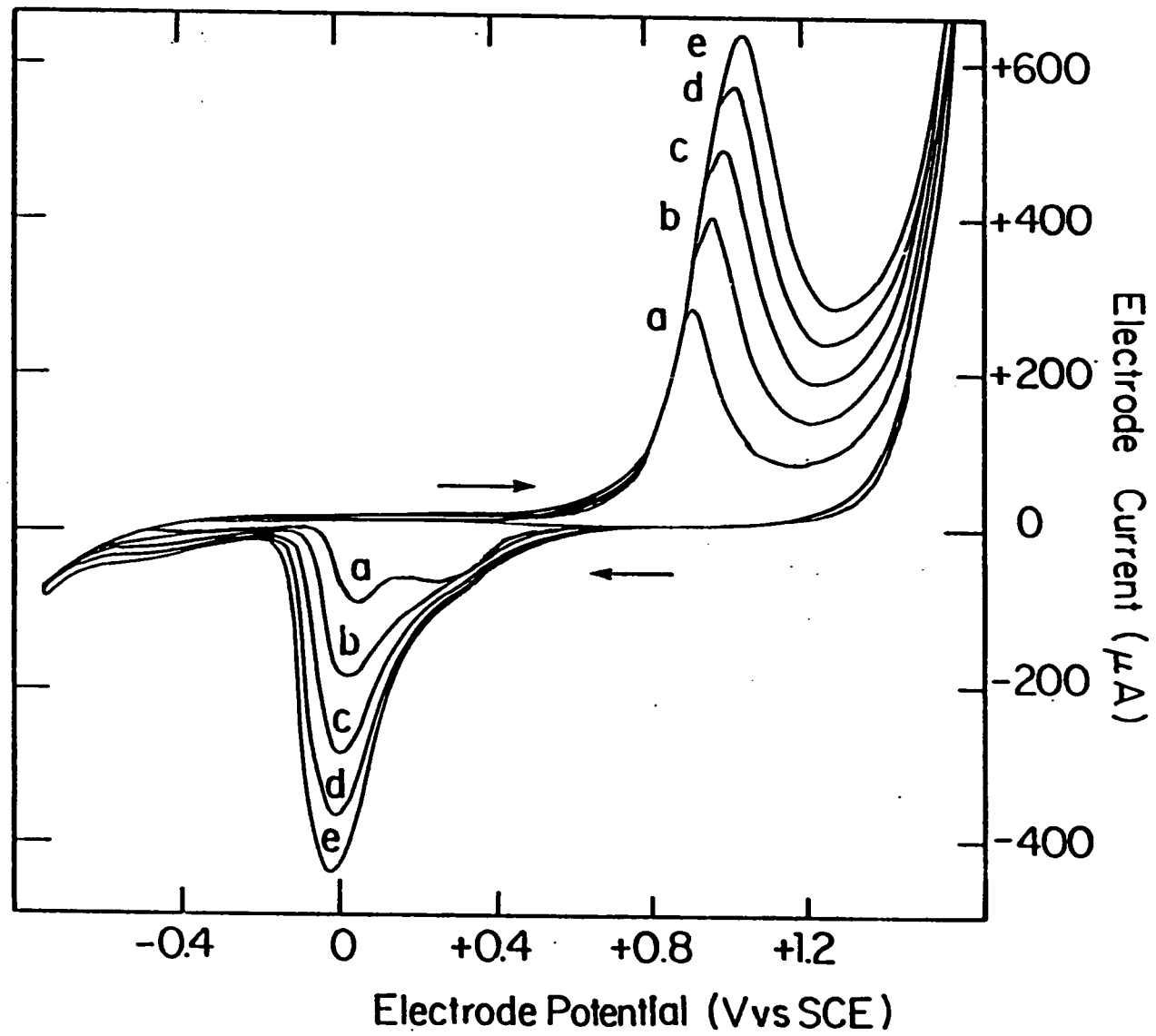
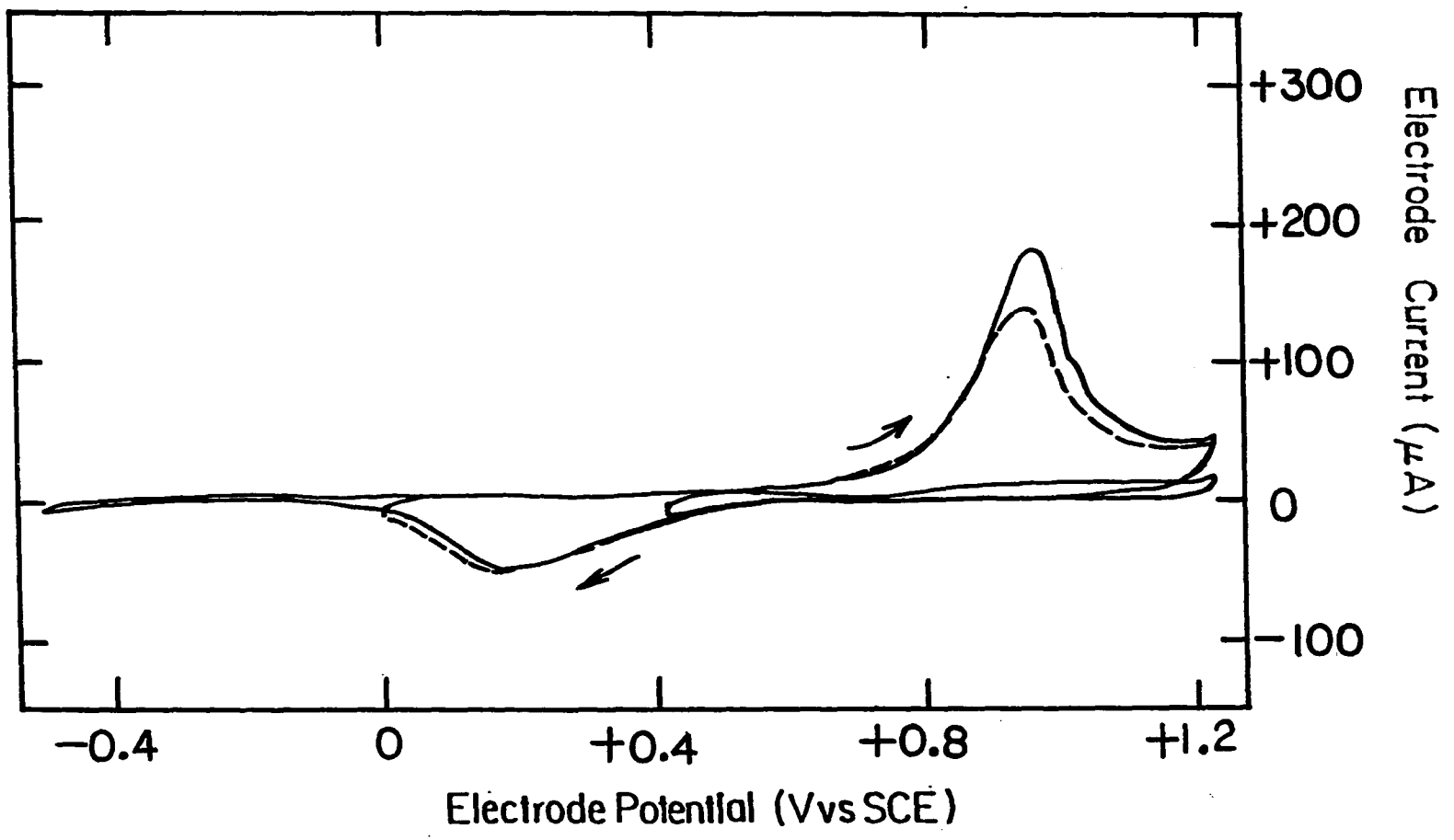


Figure VII-4. Current-potential curves at RDE for dimethoate in 50% acetonitrile in acetate buffer at pH 5.0 as a function of the negative potential scan limit

Conditions: 1.0 mM dimethoate,
6.0 V/min scan rate,
1,000 rev/min rotation speed



significantly more negative potentials in the presence of dimethoate is evidence for adsorption on the reduced electrode surface.

The conclusion that the sulfur compounds are adsorbed on the oxide-free gold surface was proved by performing cyclic voltammetry at the gold electrode in a flow-through cell in the flow-injection mode. The value of the electrode potential was maintained at -0.8 V during the sample injection. The current-potential curves for dimethoate are shown in Figure VII-5 as a function of delay time after the sample plug had passed completely by the electrode prior to start of the positive scan to $+1.6$ V. The current-potential curve is shown also for the background process obtained under the same conditions. Substantial peaks were obtained even after 35 sec of delay time proving that dimethoate is strongly adsorbed on the gold surface and is slowly desorbed into the pure solvent.

F. Conclusion

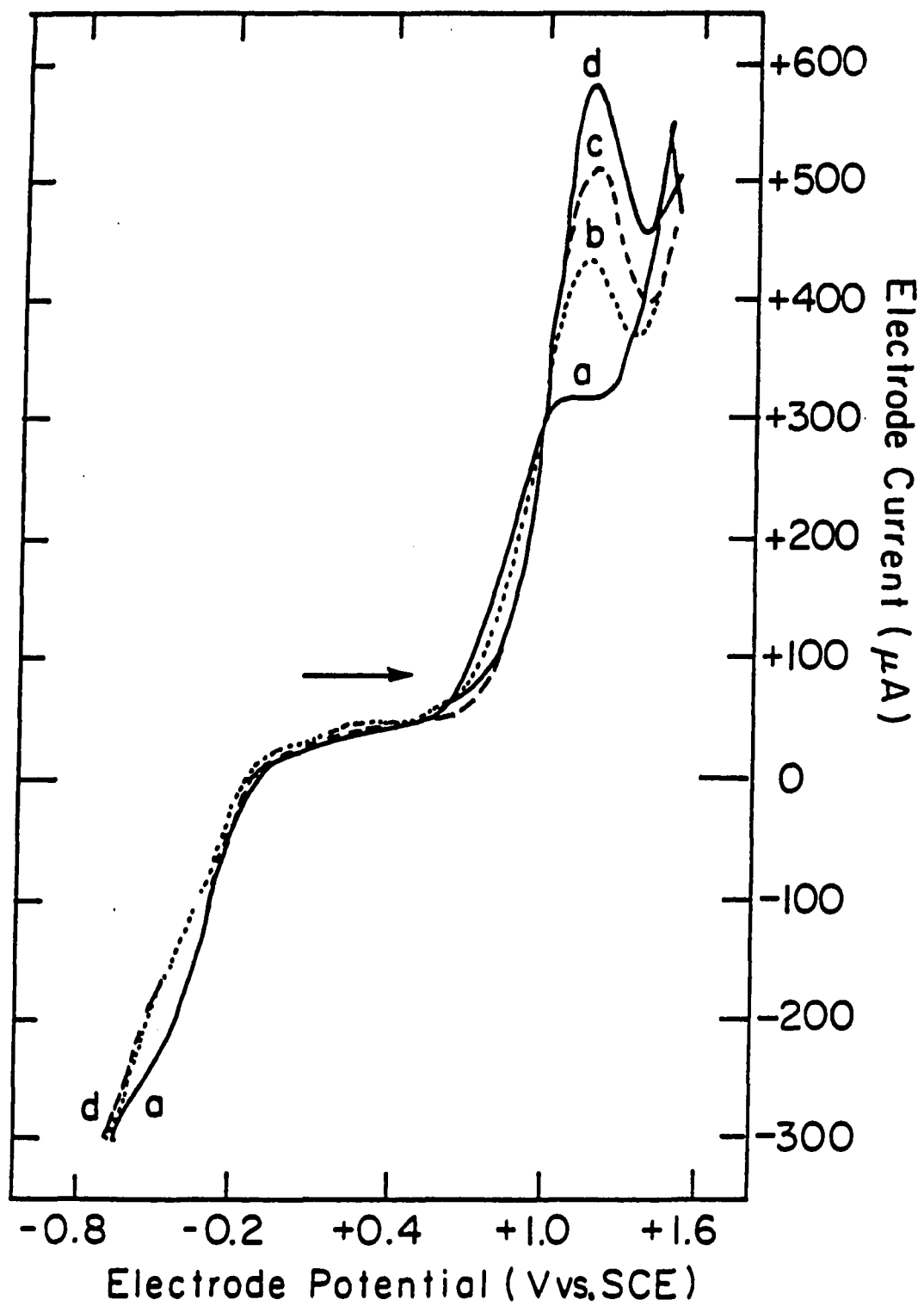
The cyclic voltammetric response for sulfur-containing pesticides on a gold rotating disc electrode was investigated. Prior adsorption of the compounds during the cathodic polarization of the electrode was found to be prerequisite for oxidation on the gold surface. Oxidation of the analyte at the positive potentials occurs

Figure VII-5. Current-potential curves in flow-injection cell with potential scans interrupted at -800 mV, during the injection of dimethoate, as a function of delay time after the sample plug has passed by the electrode

Conditions: 1.0 V/min scan rate,
0.44 ml/min flow rate,
1.0 ml samples,
only the positive scans are
shown

Curves: (a) 50% acetonitrile in acetate
buffer at pH 5.0; delay times
of 0, 15, and 35 sec

(b), (c) and (d) 2.0 mM dimethoate
in 50% acetonitrile in acetate
buffer at pH 5.0; delay times
35, 15 and 0 sec, respectively



simultaneously with gold oxide formation. Such cyclic voltammetric data are interpreted to suggest that anodic detection of sulfur-containing pesticides involves the oxide-catalyzed oxidation of the analyte molecules adsorbed on the oxide-free gold surface.

VIII. FLOW-INJECTION DETECTION OF SULFUR-CONTAINING
PESTICIDES WITH PULSED AMPEROMETRIC DETECTION
AT GOLD ELECTRODES

A. Introduction

Review of the voltammetric response of sulfur-containing pesticides at gold electrode in 50% acetonitrile/acetate buffer at pH 5.0 led to the conclusion that the majority of the anodic current comes from the oxidation of pesticide molecules that are adsorbed on the oxide-free electrode surface prior to detection, rather than from the oxidation of the molecules transported to the electrode surface by hydrodynamic convection during the actual detection process. Hence, a DC detection is not applicable for pesticide molecules at gold electrodes under these conditions, and a two-step pulsed potential waveform should be useful for amperometric detection. That is, the electrode reactivity can be maintained by applying a potential (E_{ads}) for oxide reduction and analyte adsorption followed by the step to a more positive potential (E_{det}) for anodic detection of the adsorbed analyte.

Flow-injection detection with pulsed amperometric detection was applied to investigate the possibility of an anodic process for dimethoate in the potential region 0.6 to 1.2 V. The waveforms applied were: E_{det} (500 msec), varied

over the potential region of interest, and $E_{ads} = -0.50$ V (500 msec). When these waveforms were executed, anodic current peaks were observed for dimethoate with various peak sensitivities depending upon detection potential used in the waveform.

B. Optimization of 2-Step PAD Waveform

Selection of an appropriate potential waveform is necessary in order to optimize the signal-to-noise ratio and to minimize the background. Optimization of the pulsed amperometric detection waveform required the examination of the effect from variation of the potential values (E_{det} and E_{ads}) and the associated time periods (t_{det} and t_{ads}) in the waveform corresponding to the detection and adsorption processes. This examination was performed using a flow-injection system since many factors such as electrode geometry and solution flow rate can be made identical to the ultimate chromatographic application. Furthermore, with the flow injection technique, variations in background, as well as analytical response, are easily monitored.

Plots of the amperometric response for FI-PAD of dimethoate are shown in Figure VIII-1 as a function of E_{det} , E_{ads} , t_{det} and t_{ads} . Although the maximum anodic peak current was obtained for $E_{det} = 1,000$ mV (Figure VIII-1A), the value at 900 mV was selected to avoid occasional sharp

Figure VIII-1. Optimization of two-step potential waveform for FI-PAD

Conditions: 0.1 mM dimethoate
0.8 ml/min flow rate

Curves: (A) Variation of detection potential (E_{det})

$E_{ads} = -500$ mV, $t_{det} = 400$ msec,
 $t_{ads} = 600$ msec

E_{det} (mV); (a) 800, (b) 900,
(c) 1,000, (d) 1,100, (e) 1,200

(B) Variation of adsorption potential (E_{ads})

$E_{det} = 900$ mV, $t_{det} = 400$ mV,
 $t_{ads} = 600$ msec

E_{ads} (mV); (a) 400, (b) 200,
(c) 000, (d) -200, (e) -400

(C) Variation of detection time (t_{det})

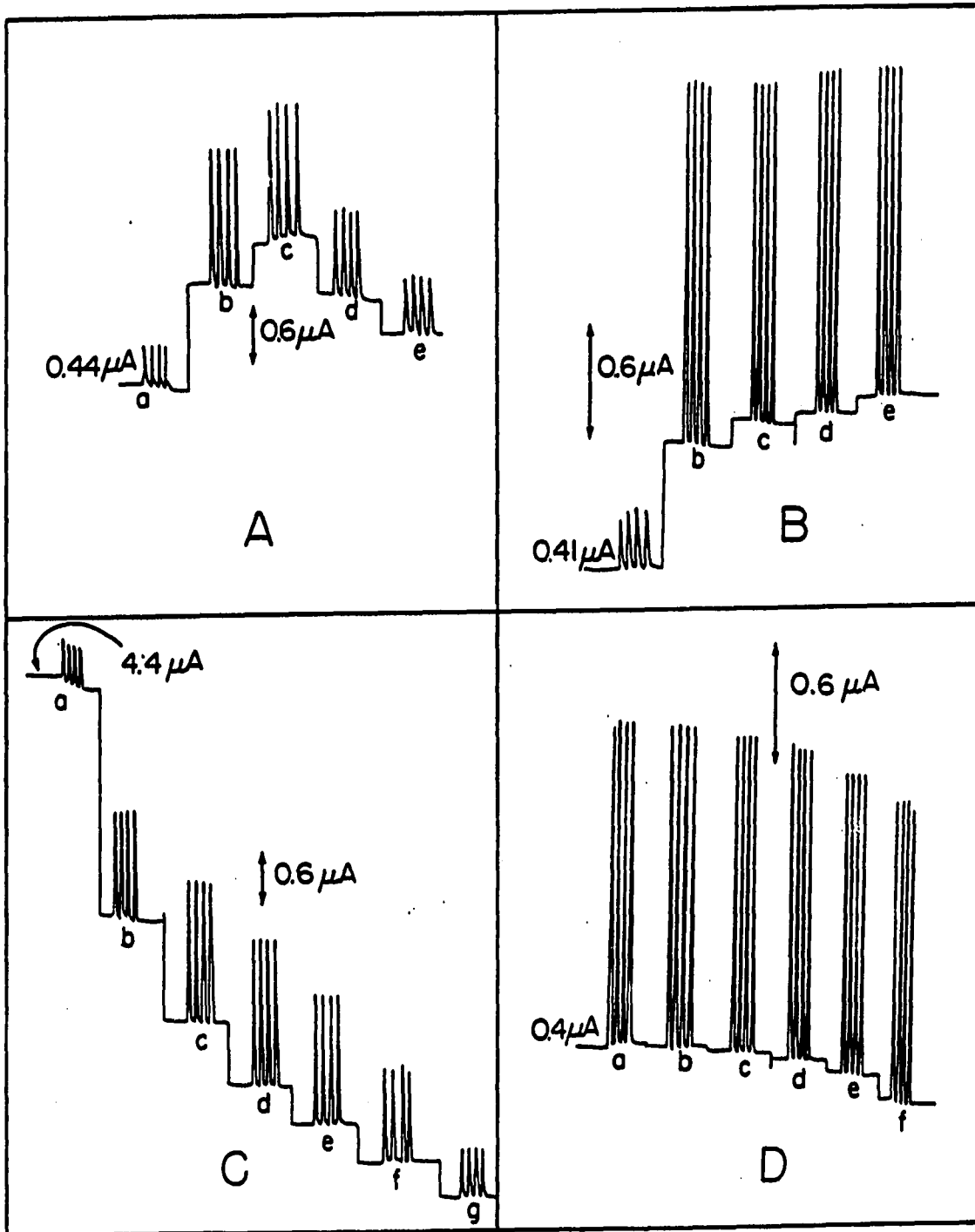
$E_{det} = 900$ mV, $E_{ads} = -200$ mV,
 $t_{ads} = 600$ msec

t_{det} (msec); (a) 100,
(b) 200, (c) 300, (d) 400,
(e) 500, (f) 700, (g) 1,000

(D) Variation of adsorption time (t_{ads})

$E_{det} = 900$ mV, $E_{ads} = -200$,
 $t_{det} = 400$ msec

t_{ads} (msec); (a) 1,000,
(b) 800, (c) 600, (d) 400,
(e) 200, (f) 100



current spikes concluded to be caused by O_2 bubbles evolved at the more positive value of potential. The observed peak current at $E_{det} = 900$ mV for dimethoate in Figure VIII-1B was independent of adsorption potential for $E_{ads} < 200$ mV. The value of $E_{ads} = -500$ mV was selected to assure the detection of all compounds.

Variation of t_{det} for application of E_{det} produced a change in sensitivity and background current as shown in Figure VIII-1C. The anodic background, resulting from the formation of gold oxide during the detection process, decreased as t_{det} was increased. Although the maximum anodic response was obtained at $t_{det} = 400$ msec, the value of $t_{det} = 1,000$ msec was chosen to obtain the lowest background signal and best peak reproducibility. The variation of t_{ads} had a much smaller effect on the amperometric response, as shown in Figure VIII-1D. It is concluded for this concentration of dimethoate (0.1 mM) that the isotherm limited surface coverage by adsorbed dimethoate is achieved for $t_{ads} > 100$ msec. The value $t_{ads} = 200$ msec was chosen for the pulsed waveform.

The optimized waveform used then: $E_{det} = 900$ mV (1,000 msec) and $E_{ads} = -500$ mV (200 msec). To verify this waveform to detection of other sulfur-containing pesticides other than dimethoate, flow injection with pulsed amperometric detection was applied for selected pesticides.

Anodic peaks were observed for all compounds studied. Examples are given in Figure VIII-2 for the detection of six sulfur-containing pesticides.

C. Calibrations

Calibration plots for dimethoate are shown in Figure VIII-3 for a concentration range of 0.02-3.0 mM. The plot of peak height vs. analytical concentration (i_p vs. C^b) is readily observed to be non-linear for $C^b > \text{ca. } 0.5 \text{ mM}$. For the region $0.02 \text{ mM} < C^b < 0.5 \text{ mM}$, the plot is linear (slope = $97.39 \pm 0.82 \mu\text{A}/\text{mM}$, $S_y = 0.23$, $r = 0.9999$) with a small non-zero intercept concluded to be the result of a systematic error (i.e., offset) which affected all data points equally. The plot of $1/i_{p, \text{corr}}$ vs. $1/C^b$ (Figure VIII-3), where $i_{p, \text{corr}} = i_p - 0.25 \mu\text{A}$, is linear (slope = $10.28 \pm 0.05 \times 10^{-3} \text{ mM}/\mu\text{A}$, $S_y = 0.002$, $r = 0.9999$) with an intercept of virtually zero ($1.15 \pm 0.65 \times 10^{-3} /\mu\text{A}$), as expected for detection of an desorbed analyte with a large energy of adsorption (121).

D. Limits of Detection for Selected Pesticides

Detection limits for flow injection with pulsed amperometric system were obtained for ten pesticides using optimized two-step waveforms and these values are given in

Figure VIII-2. Representative flow-injection detection of selected sulfur-containing pesticides by two-step PAD

Conditions: 5.0 ppm each pesticide
0.63 ml/min flow rate

Waveform: $E_{det} = 900 \text{ mV (200 msec)}$
 $E_{ads} = -500 \text{ mV (500 msec)}$

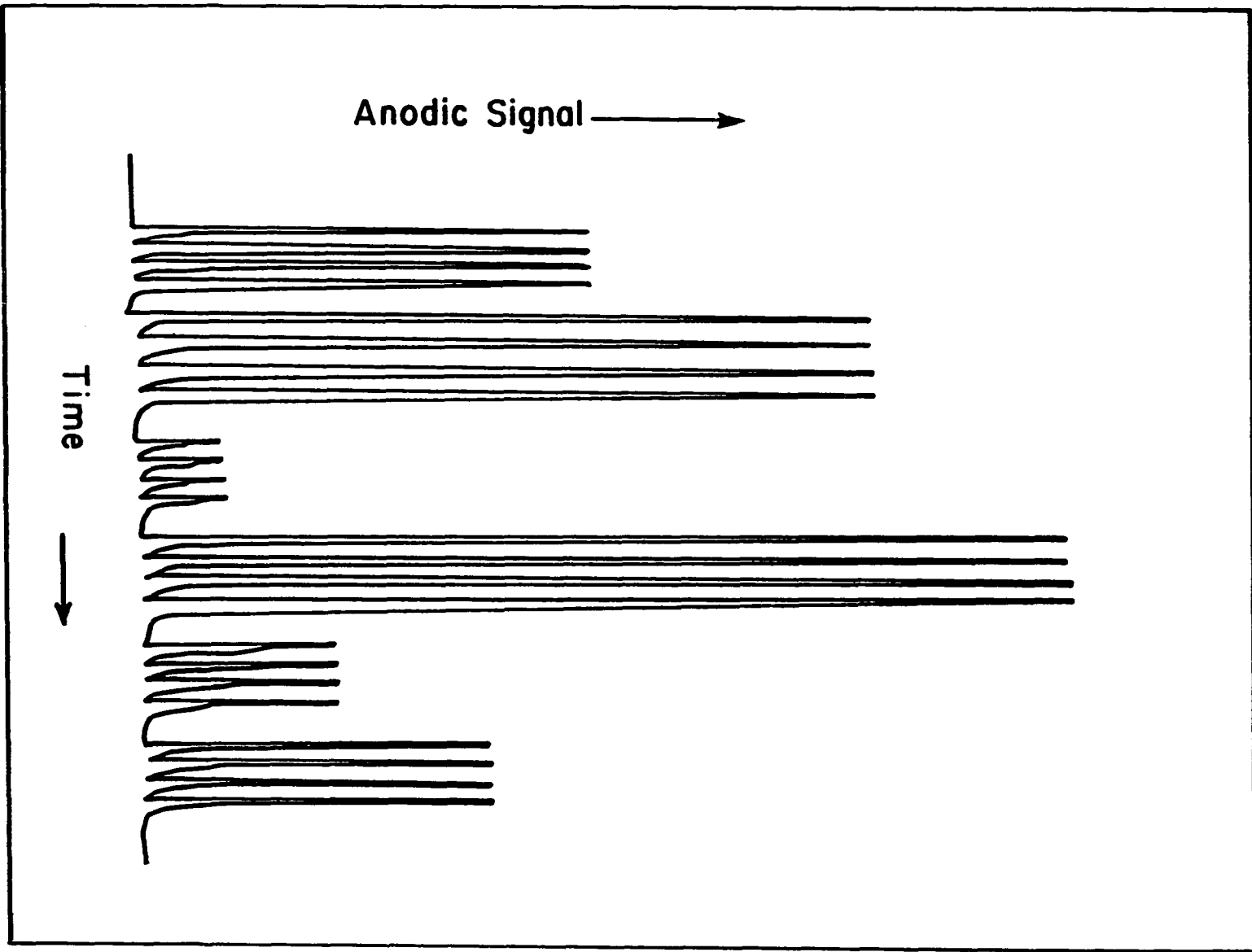


Figure VIII-3. Calibration plots for dimethoate by FI/PAD

Conditions: 0.8 ml/min flow rate

Waveform: $E_{\text{det}} = 900 \text{ mV}$, $t_{\text{det}} = 1,000 \text{ msec}$;
 $E_{\text{ads}} = -500 \text{ mV}$, $t_{\text{ads}} = 200 \text{ msec}$

Curves: (a) peak height vs. concentration (i_p vs. C^b)

(b) 1/peak height vs. 1/concentration
($1/i_p$ vs. $1/C^b$)

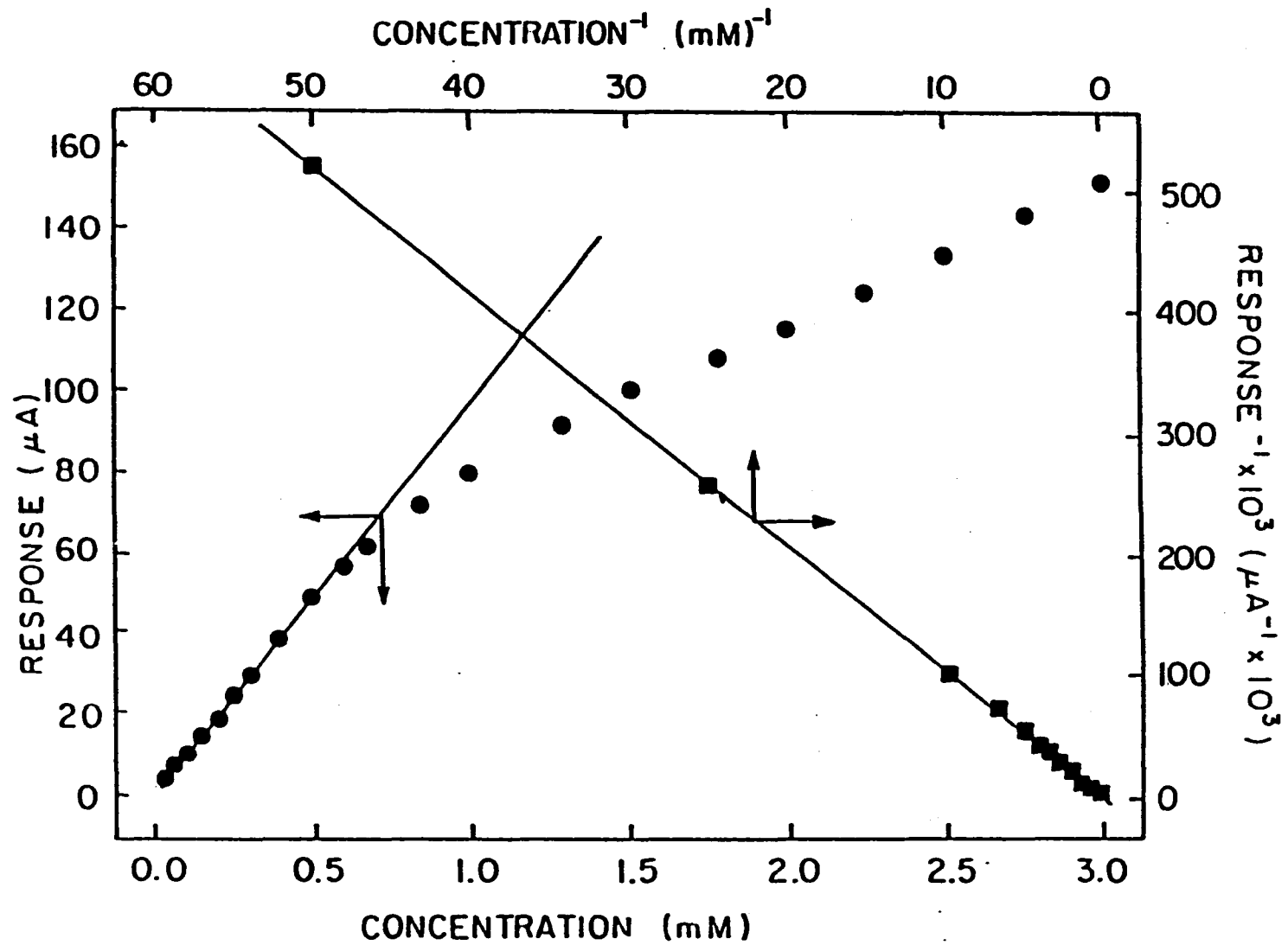


Table VIII-1. In nearly all cases, detection limits are below 100 ppb for 20- μ l injections (i.e., < 2 ng). These detection limits were found to be superior to those obtained by electrochemical detection following UV irradiation as reported by Ding and Krull (87).

It should be noted that, because of dispersion of the sample plug in the fluid stream i_p is less than the steady-state signal which would be observed for continual flow of the sample solution (C_0). The actual peak concentration (C_p) corresponding to i_p can be calculated by multiplying the analytical concentration injected by the system dispersion constant ($C_p/C_0 = \text{system dispersion constant} = 0.6$, see section III-B).

E. Electrode Fouling at Continuous Flow of Analytes

Although the electrode activity was maintained by the double-step pulsed potential waveform with subsequent injections of the analyte into the carrier stream, it was found that the electrode lost considerable activity during continuous flow of the analyte at high concentration, as shown in Figure VIII-4. This phenomenon is consistent with the observation of the distortion in peak shape for sodium thiophosphate described previously. In application where loss of electrode activity might be observed, i.e., high concentration, it is recommended that the sample volume

Table VIII-1. Limits of detection of selected sulfur-containing pesticides by FI/PAD

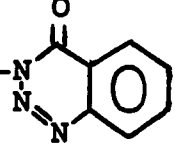
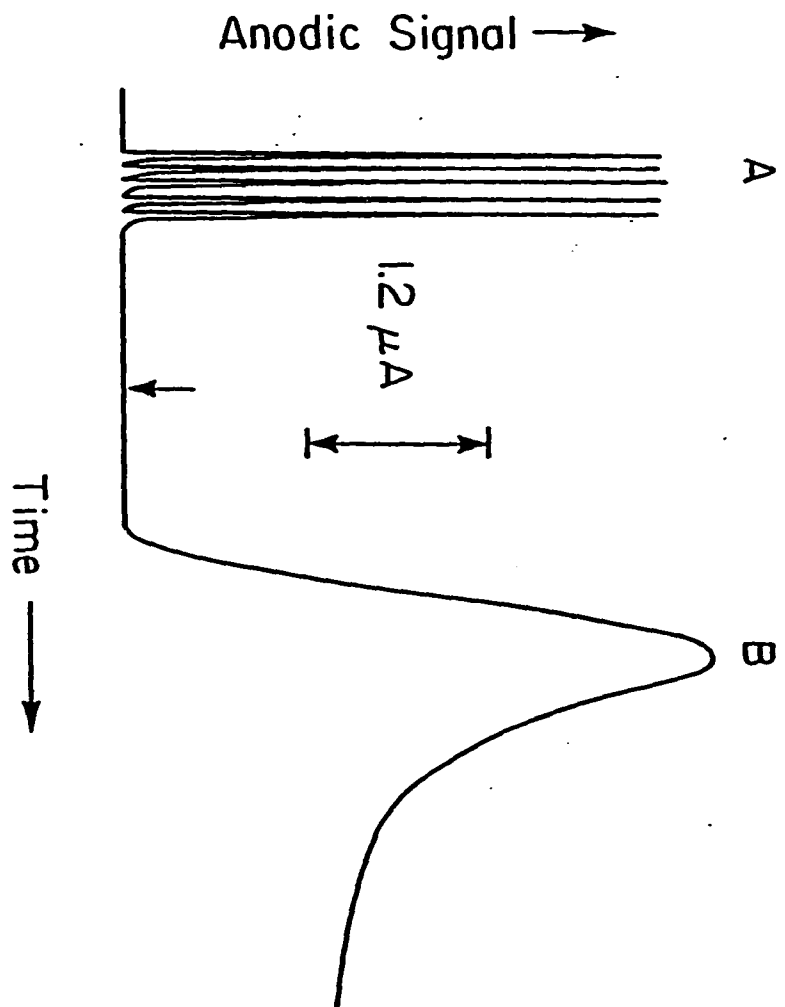
Compound	Structure	Detection limit		
		(ppb)	(ng)	(pmol)
Aldecarb	$\text{CH}_3\text{-S-C}(\text{CH}_3)_2\text{-CH=N-O-C(=O)-NH-CH}_3$	80	1.6	8.4
Dimethoate	$(\text{CH}_3\text{O})_2\text{-P(=S)-S-CH}_2\text{-C(=O)-NH-CH}_3$	40	0.8	3.5
Ethion	$(\text{C}_2\text{H}_5\text{O})_2\text{-P(=S)-S-CH}_2\text{-S-P(=S)(OC}_2\text{H}_5)_2$	20	0.4	1.0
Guthion	$(\text{CH}_3\text{O})_2\text{-P(=S)-S-CH}_2\text{-N}$ 	30	0.6	1.9
Malathion	$(\text{CH}_3\text{O})_2\text{-P(=S)-S-CH(CH}_2\text{-C(=O)-O-C}_2\text{H}_5\text{)-C(=O)-O-C}_2\text{H}_5$	20	0.4	1.2
Methomyl	$\text{CH}_3\text{-S-C}(\text{CH}_3)=\text{N-O-C(=O)-NH-CH}_3$	80	1.6	9.8
Parathion	$(\text{C}_2\text{H}_5\text{O})_2\text{-P(=S)-O-C}_6\text{H}_4\text{-NO}_2$	10	0.2	0.7
Phorate	$(\text{C}_2\text{H}_5\text{O})_2\text{-P(=S)-S-CH}_2\text{-S-C}_2\text{H}_5$	10	0.2	0.8
Thiometon	$(\text{CH}_3\text{O})_2\text{-P(=S)-S-CH}_2\text{-CH}_2\text{-S-C}_2\text{H}_5$	50	1.0	0.4
Sulprofos	$\text{C}_2\text{H}_5\text{O-P(=S)(S-CH}_2\text{-CH}_2\text{-CH}_3\text{)-O-C}_6\text{H}_4\text{-CH}_3$	120	2.4	7.4

Figure VIII-4. FI/PAD of dimethoate with consecutive injections and continuous flow

Conditions: 0.5 mM dimethoate
0.8 ml/min flow rate

Curves: (A) 100- μ L consecutive injections
(B) continuous flow



injected be decreased and/or the sample concentration be decreased by dilution. When this is not possible, e.g., chromatography with a very wide range of analyte concentrations, the waveform should be modified to a three-step waveform where electrode cleaning after detection is made more efficient by application of a large potential pulse prior to a negative step to achieve oxide reduction with subsequent analyte adsorption.

F. Conclusion

Pulsed amperometric detection was demonstrated to be applicable for detection of sulfur-containing pesticides injected into a flow stream. Detection was based on a two-step potential waveform with adsorption of the analyte during cathodic polarization and subsequent amperometric detection catalyzed by oxide formation following anodic polarization. The mechanism of the anodic detection involves prior adsorption of the sulfur compounds. Hence, the shape of the calibration curve (i_p vs. C^b) is strongly influenced by the adsorption isotherm of the analyte and, therefore, deviates from linearity at high concentrations. Calibration plots of $1/i_p$ vs. $1/C^b$ for dimethoate were linear for the range of concentration tested (0.02-3.0 mM). In most cases, detection limits were below 100 ppb for 20 μ l injection (i.e., < 2 ng).

**IX. HIGH PERFORMANCE LIQUID CHROMATOGRAPHY WITH
PULSED AMPEROMETRIC DETECTION OF
SULFUR-CONTAINING PESTICIDES**

A. Introduction

The most popular form of liquid chromatography in recent years has undoubtedly been reversed-phase liquid chromatography in which with more than 60% of the applications utilize C-18 or C-8 hydrocarbon phases chemically bonded to the silica microparticulate packing. This liquid chromatographic mode is known as "bonded-phase chromatography". The descriptions "reversed-phase" versus "normal-phase" as they pertain to liquid chromatography originate from the early history of chromatography. In reversed-phase liquid chromatography the mobile phase is polar, usually water with methanol or acetonitrile, and the bonded phase is hydrophobic, such as octadecylsilane (C-18) bonded silica. Non-polar compounds are strongly retained on the reversed-phase chromatographic columns, while very polar samples are only slightly retained.

Several advantages enhance the popularity of the reversed-phase chromatography in pesticide analysis since this mode is suitable for separation of both non-ionic and ionic compounds which are commonly found in pesticide residue and metabolites. Modern liquid chromatography is

highly efficient and usually referred to as High Performance Liquid Chromatography (HPLC). This newly developed technique is able to resolve complicated multicomponent samples in a short analysis time. Despite these advantages, HPLC of pesticides is not as successful as it should be due to the lack of a variety of highly sensitive and selective detectors. The compatibility of high performance liquid chromatography and electrochemistry can provide the answers to this drawback. Electrochemical detection is especially appropriate for use in reversed-phase liquid chromatography owing to the high polarity of the solvent mixtures which poses good electric conductivity. Sufficient ionic strength is a prerequisite and usually at least 0.05 M buffer is used.

In this section, the eventual utilization of the pulsed amperometric detection of sulfur-containing pesticides will be demonstrated in terms of detection in reversed-phase HPLC. With prior separation of pesticides by liquid chromatography, the applicability of pulsed amperometric detection has been extended to the selective determination of specific pesticides in a mixture.

Chromatographic separations were performed using the system described in Section III-4A. The eluent flow rate was varied between ca. 0.4-0.8 ml/min to optimize the separations which were all performed under isocratic

conditions. The major difficulty to be overcome was the compatibility of the eluent composition, selected to optimize the separation and ensure stability of the chromatographic column and enhance electrochemical detection. A mixture of 50% acetonitrile in aqueous acetate buffer (0.1 M) at pH 5.0 was found to be the best eluent in this study. This eluent was prepared by mixing equal volumes of acetonitrile and the acetate buffer, filtering through a 0.45 μ m filter and degassing under vacuum. Degassing of the eluent was observed to be necessary and important for a good chromatographic performance and for preventing air bubbles from entering into the electrochemical flow-through detection cell.

Standard pesticides were obtained from the Environmental Protection Agency (EPA) and were used without further purification. Values of purity labelled on the sample vials were generally in the range of 85-98%. Sample solutions were prepared freshly prior to each use by dissolving a specific amount of a compound in acetonitrile and diluting to volume with acetonitrile and acetate buffer such that the final composition is 50% in acetonitrile by volume. Due to limited amounts of samples obtained, these sample solutions were used without prior filtering and degassing.

Electrochemical detection was achieved using a two-step pulsed amperometric detection at a gold electrode. The waveform was established in the customary manner with a step from the negative potential (E_{ads}) for reduction of oxide with adsorption of the analyte to a positive potential (E_{det}) for anodic detection of the adsorbed sample. The detection potential was chosen to be sufficiently positive so that significant oxidative cleaning occurred simultaneously with the anodic oxidation of the analyte, hence, a more energetic oxidative cleaning pulse was not needed subsequent to E_{ads} .

B. Chromatography

The relative elution order for each pesticide was determined initially by individual injection of each compound into the chromatograph. Standards of single pesticides were found in several cases to give multiple peaks. Apparently as results of decomposition and contamination by impurities. No attempt was made to identify the decomposition products nor to purify the samples. The fact that these peaks were detected under these experimental conditions implies that these contaminants are also electroactive.

A representative chromatogram of a mixture of eight standard pesticides each at a concentration of 5 ppm

(ca. 100 ng) is shown in Figure IX-1. The flow rate of 0.64 ml/min was appropriate to obtain adequate chromatographic separation of the first two peaks, i.e., the minor peak for phorate and the major peak of ethion, with an acceptable overall chromatographic time of 50 min. Since all these pesticides have the same mode of action, it is unlikely that all of these pesticides will be found in one real-life sample. Hence the analysis time can be made shorter by increasing the flow rate of the eluent to achieve the optimum analysis time for a specific sample matrix.

Detection limits of pesticides obtained by high performance liquid chromatography with pulsed amperometric detection (HPLC-PAD) are expected to be higher than those obtained by flow-injection analysis with pulsed amperometric detection (FIA-PAD) due to greater dispersion of the sample plug within the chromatographic column. Deviation of the detection limits in HPLC system from those in the FIA system depends upon the capacity factor (k') of a compound. In general, a simple approximation of the detection limit of a compound in HPLC can be made if the detection limit is known in FIA according to the following equation:

$$DL_{\text{HPLC}} = DL_{\text{FIA}} \times \frac{(i_{p,\text{HPLC}}/c_{\text{HPLC}}^b)}{(i_{p,\text{FIA}}/c_{\text{FIA}}^b)}$$

Figure IX-1. Chromatogram of a mixture of eight standard pesticides using HPLC/PAD

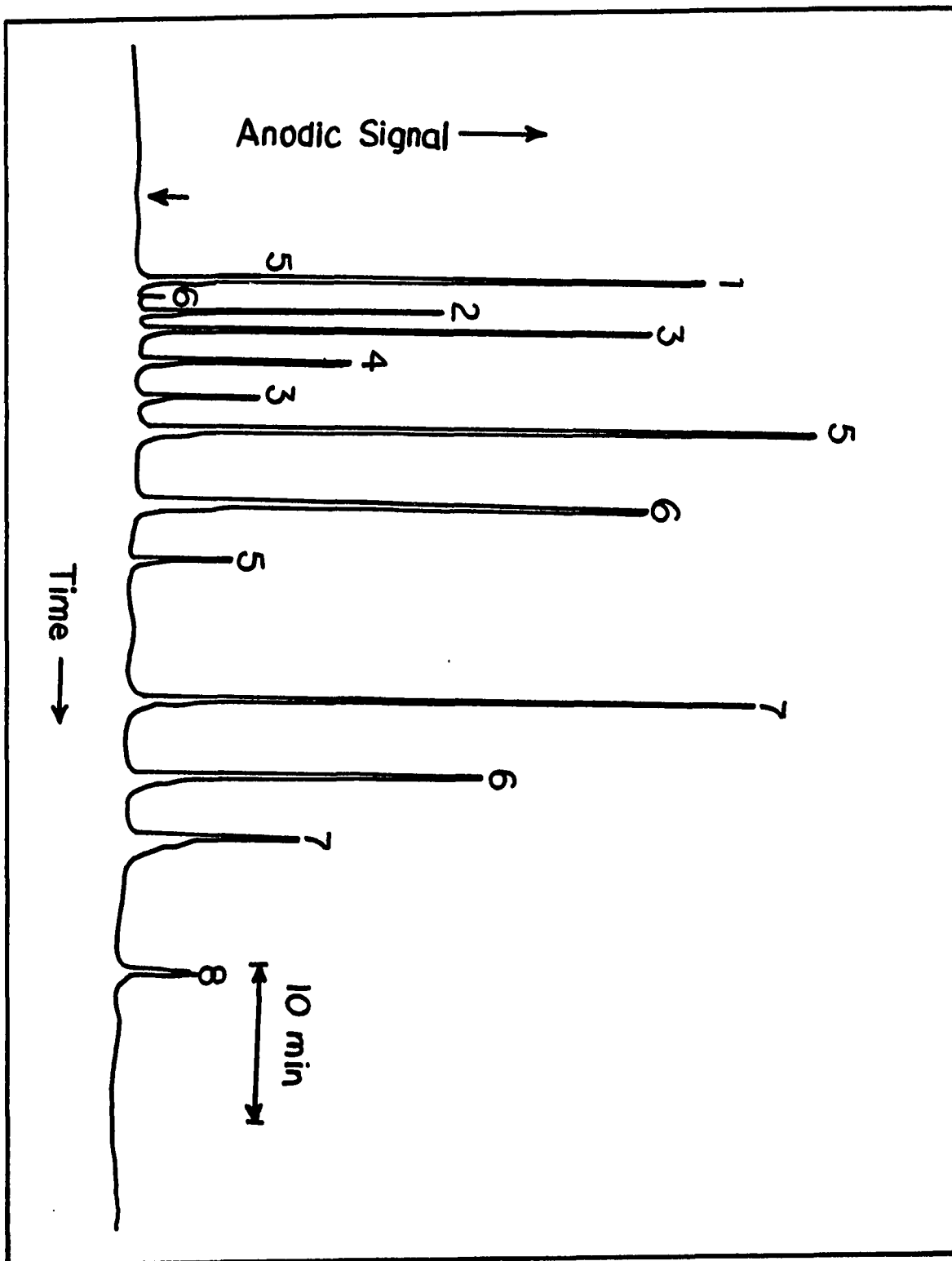
Column: C-18 reversed phase

Eluent: 50% acetonitrile in acetate buffer at pH 5.0,
0.64 ml/min flow rate

Samples: 50 μ L containing 5 ppm each pesticide

Waveform: $E_{det} = 1,000$ mV, $t_{det} = 600$ msec;
 $E_{ads} = -500$ mV, $t_{ads} = 200$ msec

Peaks: (1) Ethion, (2) Methomyl,
(3) Dimethoate, (4) Aldecarb,
(5) Phorate, (6) Thiometon,
(7) Guthion, (8) Sulprofos



Since anodic signals obtained by pulsed amperometric detection of sulfur compounds at a gold electrode do not always increase linearly with bulk concentration of the analyte, the ratio i_p/C^b is not always constant, especially at higher concentrations. Hence this approximation is not applicable unless C^b_{HPLC} and C^b_{FIA} are made to be approximately the same or are both in the linear regions of the analytical calibration.

C. Analysis of a Real-life Sample

The chromatographic separation of a water sample from a local lake (Lake Laverne, Iowa State University campus) spiked with 0.2 ppm each of dimethoate and phorate is shown in Figure IX-2. The chromatogram for the unspiked blank is shown also. It is clear that pulsed amperometric detection is capable of detection of these pesticides at concentrations commonly encountered in a real-life sample.

D. Conclusion

Pulsed amperometric detection with a two-step waveform was shown to be successful for detection of sulfur-containing pesticides in a chromatographic effluent stream. With the appropriate electrolyte used as a chromatographic, sensitive and direct detection of these pesticides

Figure IX-2. Chromatograms of a lake water sample with and without spiking with pesticides using HPLC/PAD

Column: C-18 reversed phase

Eluent: 50% acetonitrile in acetate buffer at pH 5.0, 0.71 ml/min flow rate

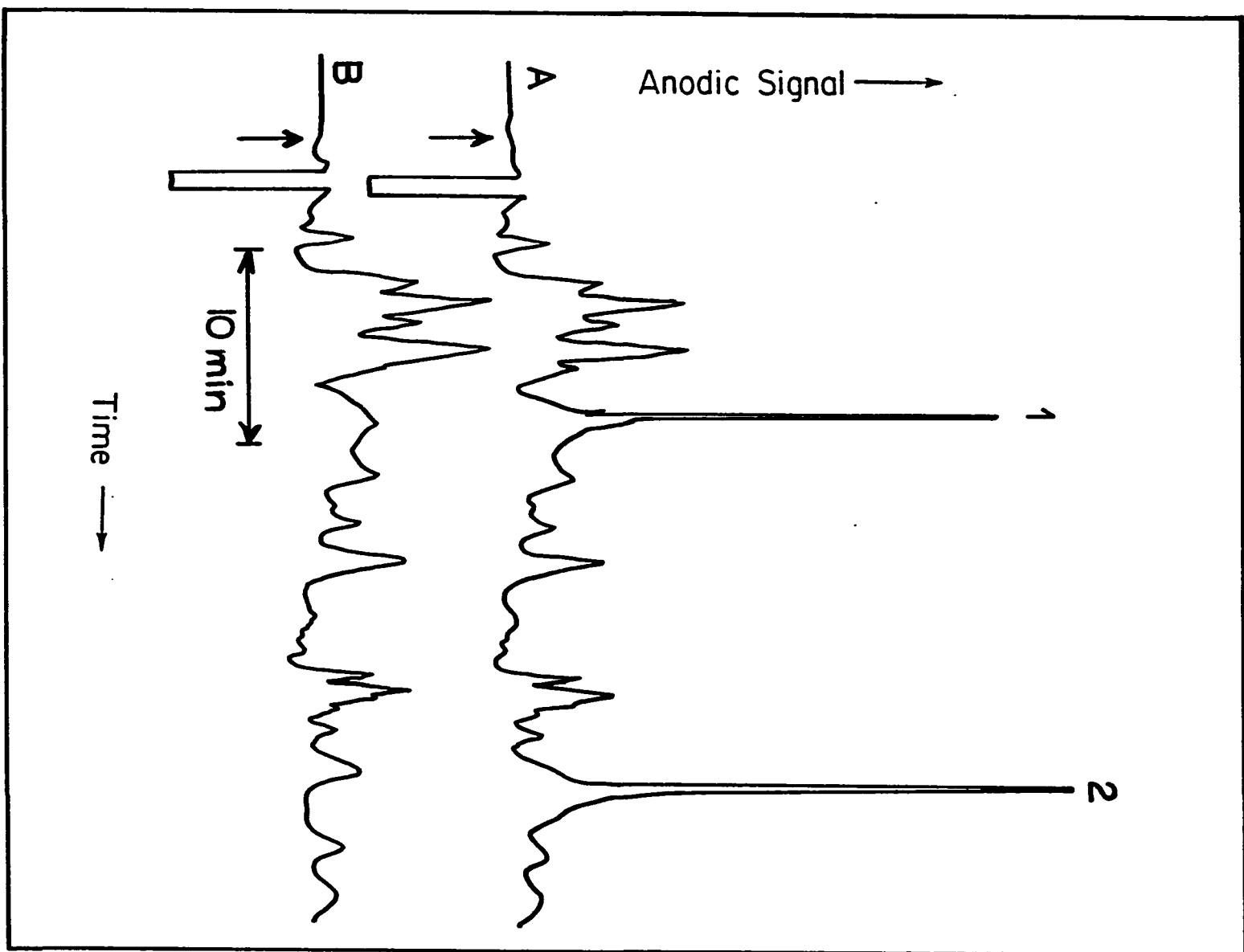
Samples: 20 μ L containing 0.2 ppm each pesticide

Waveform: $E_{det} = 1,000$ mV ($t_{det} = 500$ msec)

$E_{ads} = -500$ mV ($t_{ads} = 200$ msec)

Chromatograms: (A) Lake LeVerne water spiked with pesticides;
(1) dimethoate
(2) phorate

(B) Lake LeVerne water without spiking with pesticides



have been demonstrated with the emphasis on the electrochemical detection not on the chromatographic separation. Additional development of the chromatography is needed to obtain satisfactory resolution of all compounds in particular complex samples.

X. C-18 REVERSED PHASE TRACE ENRICHMENT OF PESTICIDES

A. Introduction

The occurrence of organothiophosphorous pesticides in the aquatic environment is mainly due to their increasing agricultural use. To assess the environmental impact of these compounds, which are potent cholinesterase inhibitors, selective and sensitive analytical methods have been developed based mainly on solvent extraction or adsorption from aqueous media. The ability of organophosphorous pesticides to undergo degradation or chemical alteration shortly after application is one of the advantages. However, the diesters formed by hydrolysis of one functional group are usually more stable, and also inhibit cholinesterase. Therefore, simultaneous determination of the parent compounds and their degradation products would indicate more reliably the amount of pesticides present in natural waters as a consequence of leaching, wash-over or contamination from aerial spray.

In contrast to the efficient accumulation of the organophosphorous parent molecules, the enrichment of the degradation products of these compounds is beset by problems as these degradation products are acidic substances which are present in water as non-volatile salts. A uniformly efficient procedure for their simultaneous isolation has not

yet been reported. Extraction with pure organic solvents results in negligible recoveries of < 1%. The formation of ion-association complexes with the tetraphenylarsonium cations promotes the efficient extraction of dialkylphosphorodithioates and can be used for selective trace enrichment of these anions (122). However, recoveries are still poor, frequently less than 80%.

Reversed-phase adsorption on octadecyl-modified silica gel (C-18) packed in commercially available cartridges has been used successfully for the isolation and concentration of a variety of organic substances from aqueous media (123-126). Adsorption on the C-18 reversed-phase cartridge is highly efficient for simultaneous enrichment of organophosphorous pesticides and their phosphorous-containing pesticides (127).

There was a doubt whether the detection limits reported for sulfur-containing pesticides (Table VIII-1) were sufficiently low such that reversed-phase HPLC with pulsed amperometric detection is applicable to environmental samples at all concentration levels routinely encountered. To assure the capability of the detection technique, a preconcentration method was developed to improve the determination of pesticides at very low concentrations. The method is based on adsorption of aqueous pesticide solutions onto a C-18 forecolumn followed by on-line backflushing with

the chromatographic eluent to elute the accumulated pesticides into the separation column for further specific quantitative determination utilizing pulsed amperometric detection at a gold electrode. Illustration was made using dimethoate as the sample pesticide.

Dimethoate (see structure on Table VII-1) is a contact and systemic insecticide effective against a broad range of insects on a wide range of crops. It is a polar compound (solubility in water: 25 g/l at 21°C) and rather stable in aqueous media at acidic or neutral pH. As a result of its mobility, it may be found not only in waste water and surface water but also in soil and ground water. In sediments, dimethoate probably only will be found near effluents from pesticide manufacturing plants (128). A number of methods for the simultaneous determination of organophosphorous pesticides in environmental samples or foodstuffs have been proposed (129-131) with poor results for dimethoate and other polar pesticides.

In this section, an effective preconcentration of dimethoate is demonstrated using the system described in section III-4B. Calibration study (signals vs. total amounts of dimethoate deposited) was performed and the accumulation recoveries were investigated to evaluate the efficiency of this trace enrichment method.

B. Determination of the Capacity of the Forecolumn

To ensure that the fore column is not overloaded by the pesticides during the loading period, the capacity of the forecolumn was determined initially by a simple breakthrough method. Although the column capacity can be estimated from the volume of the C-18 packing material inside the forecolumn, the method is not truly reliable since actual adsorption is dependent on the system conditions and mostly on the nature of the analyte being adsorbed.

The actual capacity of the forecolumn was determined by pumping a solution of dimethoate (0.5 mM in acetate buffer at pH 5.0) continuously into the forecolumn. Pulsed amperometric detection at the outlet of the forecolumn was maintained to record the change of the signal from the effluent stream as a function of time. No signal from dimethoate is expected during early loading of the compound since all dimethoate molecules should be retained onto the forecolumn. Once all adsorption sites on the forecolumn have been used up and the column becomes saturated with dimethoate, the breakthrough phenomenon occurs causing dimethoate to appear in the effluent stream and be detected. By utilizing this method, a breakthrough curve for dimethoate was obtained experimentally and the result is

shown in Figure X-1. From the concentration of dimethoate (0.5 mM), loading flow rate (0.64 ml/min) and the breakthrough time (56.3 min), (see Figure X-1) the total capacity of the forecolumn was calculated to be 18 umole (4.14 mg) of dimethoate.

C. Preconcentration and Calibration

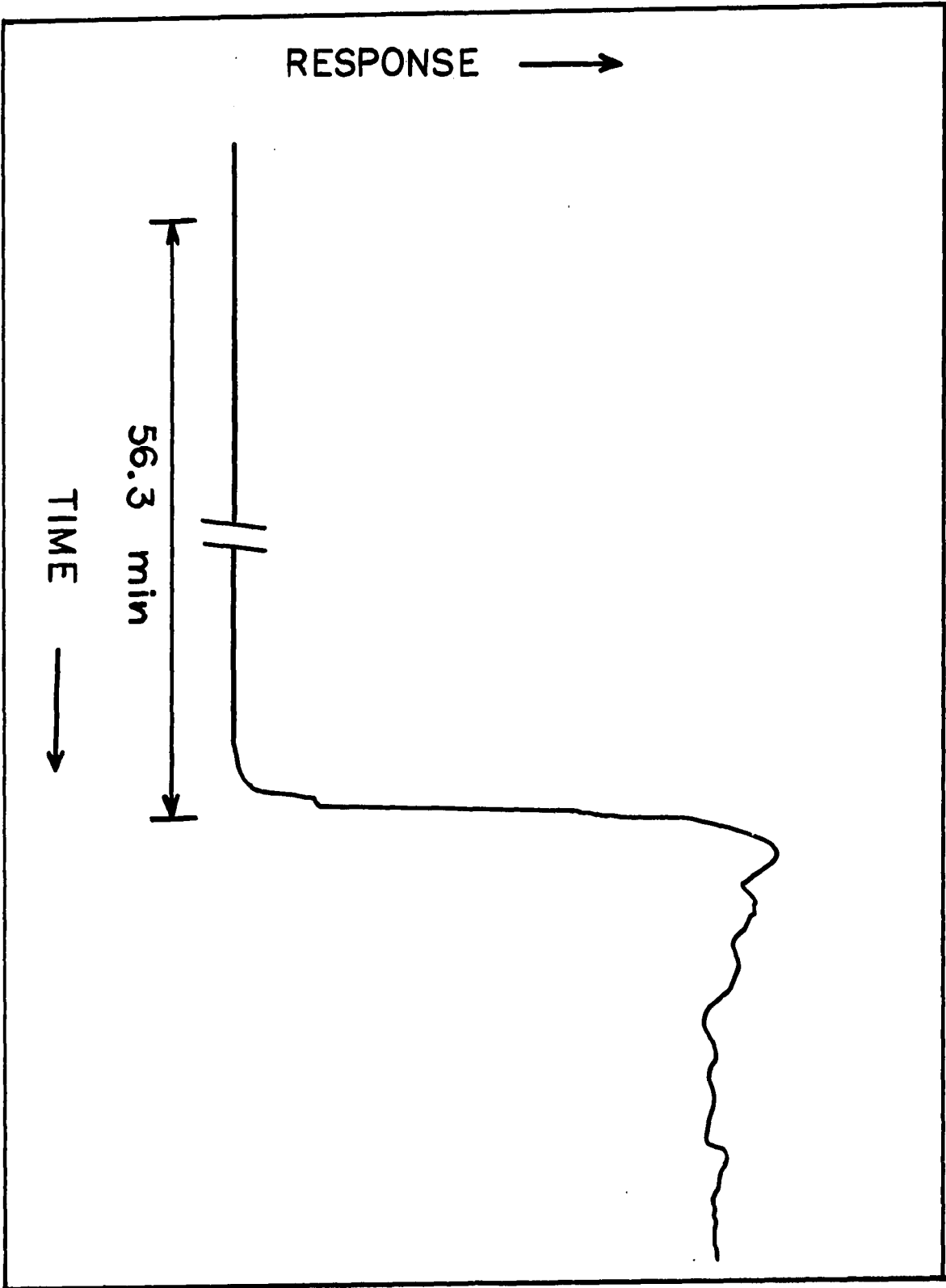
Trace enrichment of dimethoate was performed using the system described in section III-4B. The forecolumn was simply inserted as a sample loop at the injection valve of the chromatographic system. Although no chromatographic separation was necessary since only a single compound was being determined, the analytical column was needed to be present in the system to serve as a pressure regulator. Without the analytical column located between the forecolumn and the detection cell, dramatic change in baseline at the detector was observed when the injection valve was switched due to the change of pressure of the system from a low pressure (without the forecolumn) to a high pressure (with the forecolumn).

The use of two separate pumps, one serving to load pesticide onto the forecolumn, and the other serving to pump the chromatographic eluent through analytical column, allows these two procedures to be performed independently. Hence

Figure X-1. Break-through curve for dimethoate on C-18 reversed phase
forecolumn using PAD

Conditions: 0.5 mM dimethoate,
0.64 ml/min loading flow rate

Wave form: $E_{det} = 900 \text{ mV (1,000 msec)}$
 $E_{ads} = -200 \text{ mV (500 msec)}$



the chromatographic baseline was recorded simultaneously with the loading of the pesticide onto the forecolumn.

The improvement in detection sensitivity for dimethoate produced by this trace enrichment method is illustrated in Figure X-2. Without preconcentration, the peak for 50 ppb dimethoate ($0.2 \mu\text{M}$, 1 ng in 20 μl injection) is barely perceptible (Figure X-2A) as compared to that obtained following preconcentration of 50 ppb dimethoate solution for 45 minutes at a loading flow rate of 0.85 ml/min (2 μg total in ca. 38 ml sample) (Figure X-2B).

Negative peaks obtained in Figure X-2A,B was concluded to be water. Since dimethoate was prepared in aqueous solution; hence, the forecolumn was full of water after loading of pesticide solution and backflushing with chromatographic eluent caused this water to come out from the analytical column before dimethoate. The anodic peak obtained following dimethoate peak was an unknown system peak which was observed after switchings of the injection valve either in the presence or absence of dimethoate.

Calibration was performed for dimethoate by the observation of the peak heights as a function of loading time (15 to 150 sec) under the same concentration of dimethoate (0.5 mM) and loading flow rate (0.83 ml/min). Results are shown in Figure X-3. Plots of anodic peak heights vs. total amounts of dimethoate accumulated is

Figure X-2. Detection of dimethoate using PAD with and without preconcentration

Conditions: 50 ppb dimethoate in water,
0.64 ml/min flow rate

Waveform: $E_{det} = 900$ mV ($t_{det} = 1,000$ msec)

$E_{ads} = -200$ mV ($t_{ads} = 200$ msec)

Curves: (A) without preconcentration, 20 μ L injection

(B) with preconcentration, loading time of 45 min, i.e. 2 μ g of dimethoate

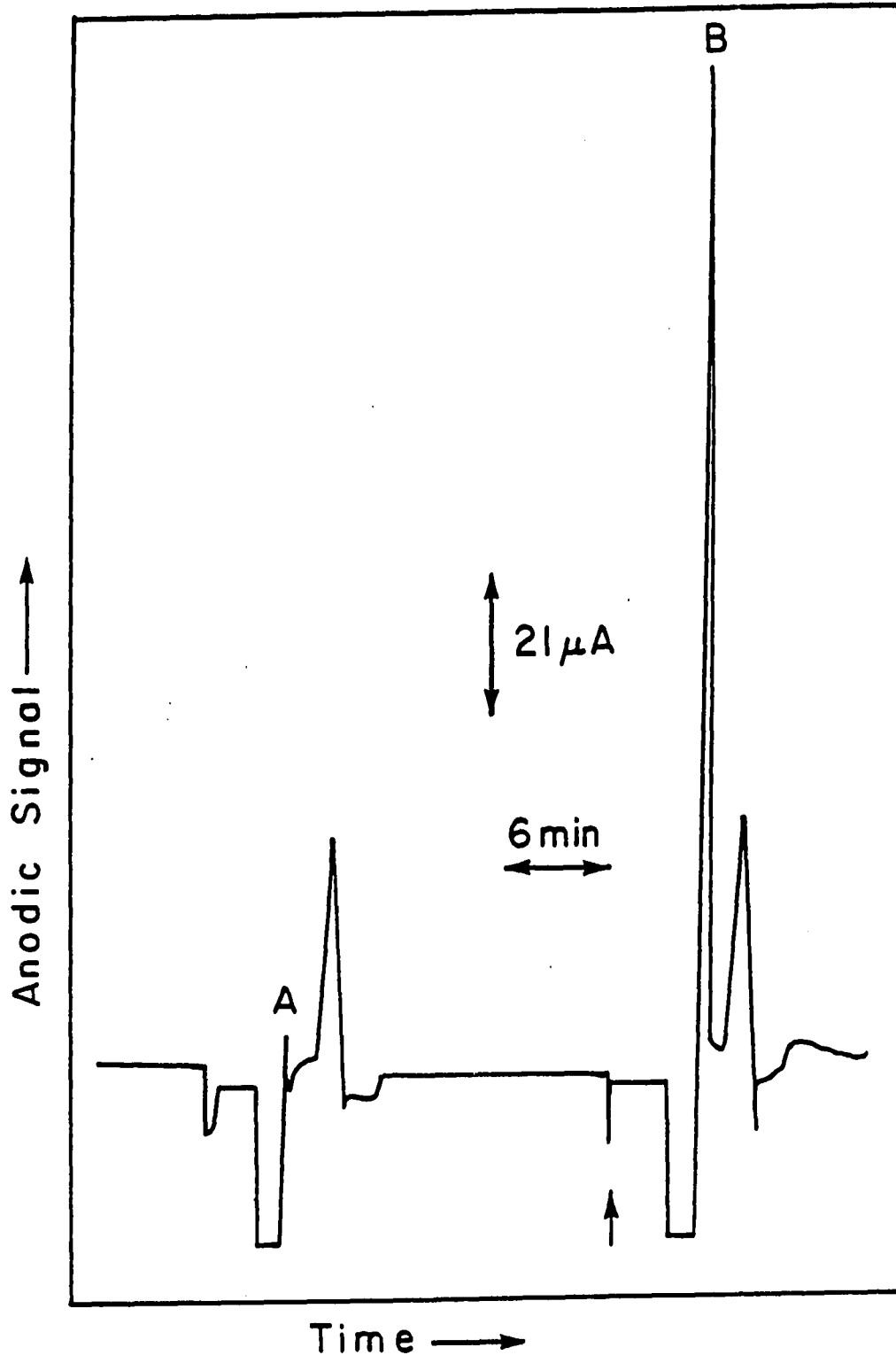
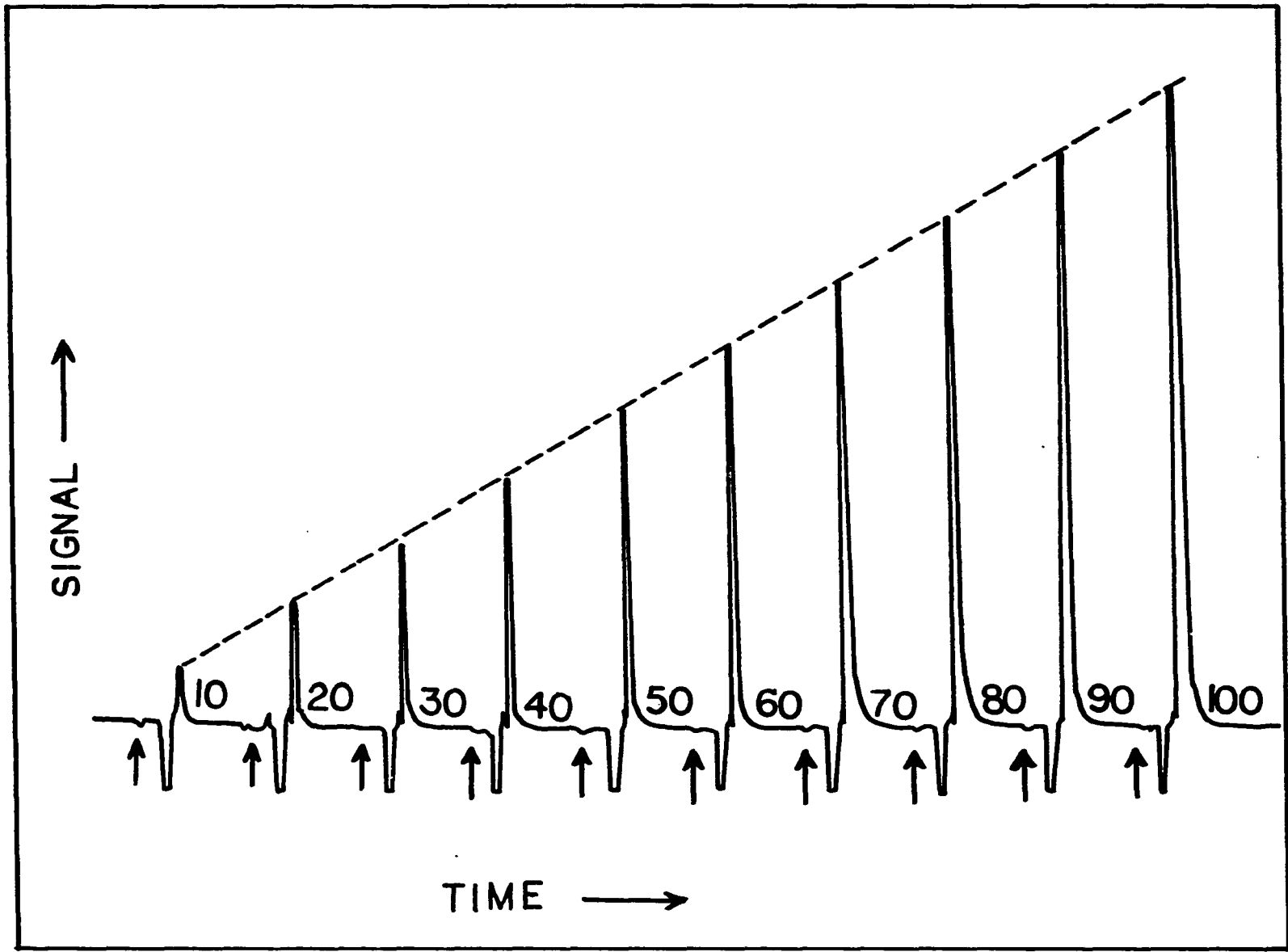


Figure X-3. Preconcentration calibration plots for dimethoate using PAD

Conditions: 0.5 mM dimethoate,
0.64 ml/min eluent flow rate,
0.83 ml/min sample loading flow rate

Waveform: $E_{det} = 900$ mV, $t_{det} = 1,000$ msec;
 $E_{ads} = -200$ mV, $t_{ads} = 200$ msec



linear with a slope of $0.04725 \pm 0.0004 \mu\text{A}/\text{ng}$, a virtually zero intercept ($-0.0076 \pm 0.0005 \mu\text{A}$) and a correlation coefficient $r = 0.9999$. The linear response of the electrochemical detection observed in this study implied that the peak concentrations of the analyte were fairly low such that the anodic signals were not influenced by the adsorption isotherm of the analyte.

D. Determination of Forecolumn Efficiency

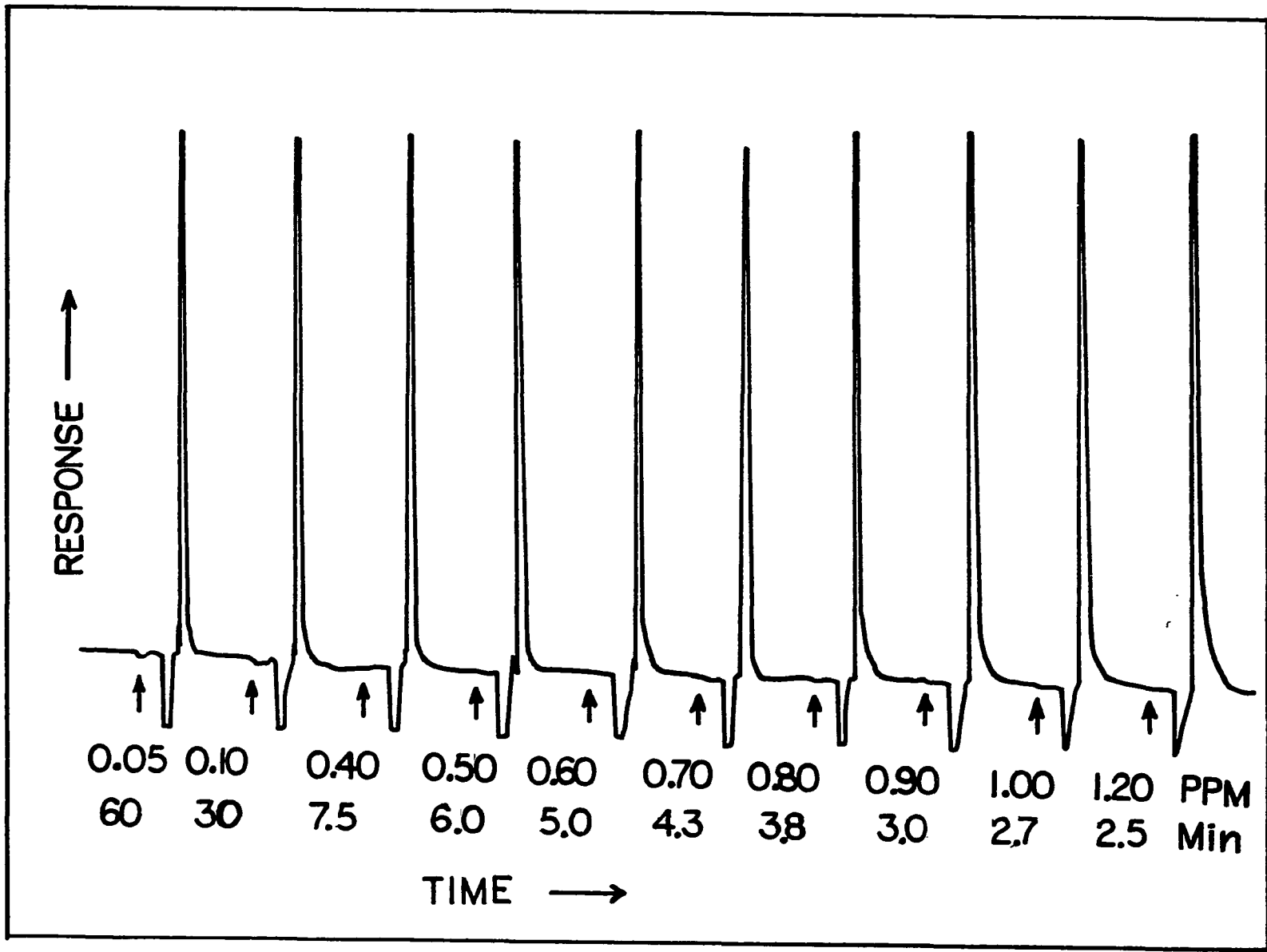
The efficiency of accumulation of traces of dimethoate from aqueous solutions was investigated by two experiments.

First, preconcentration was performed using the system described in section III-4B for ten combinations of dimethoate concentrations (0.05-1.2 ppm) and loading times (60.0-2.5 min) such that the total amount of dimethoate deposited onto the forecolumn was kept constant at 2.0 μg . Peak heights obtained from this experiment was found to be reproducible (rsd 2.1%) as shown in Figure X-4. Therefore, it was concluded that the forecolumn efficiency was constant at least under these experimental conditions where total amount of dimethoate deposited is 2.0 μg and that this efficiency was not dependent upon the pesticide concentration nor loading time.

The second experiment was performed to evaluate the absolute forecolumn efficiency using the system described in

Figure X-4. Reproducibility of efficiency of the forecolumn by PAD after preconcentrations of same absolute amount of dimethoate at different concentrations and sample loading times

Conditions: 0.64 ml/min eluent flow rate,
0.67 ml/min loading flow rate



section III-4C. The forecolumn was placed into a closed loop such that the sample volume of pesticide injected could be recycled through the forecolumn to adsorb any pesticide not adsorbed during the former pass of the sample plug. The forecolumn was backflushed into the chromatographic system following each pass of the sample plug through the forecolumn. In two separate experiments where total amount of dimethoate injected into the closed loop were 10 ng, and 90 ng, a peak for dimethoate was obtained for each experiment only for the first pass of the sample plug. Hence, the forecolumn efficiency was concluded to be 100%.

E. Conclusion

C-18 reversed-phase trace enrichment of dimethoate provides simple and rapid preconcentration of this pesticide for use in residue analysis. The efficiency of accumulation of traces of degradation products simultaneously with the parent molecules is 100% regardless of the pesticide concentrations or the loading volumes. The fact that only one peak was obtained during the desorption process implies that dimethoate was not undergone degradation, or that the chromatographic conditions were not suitable for the separation of these degradation products and the parent molecules. Hence, more development in chromatography is needed for this purpose. At the time being, the method

serves very well for determination of total dimethoate present in a sample.

XI. SUMMARY

Pulsed amperometry at a gold electrochemical detector was demonstrated for the detection of sulfur-containing pesticides. The results presented for dimethoate are representative of all compounds studied.

Oxidation of sulfur-containing pesticides on gold electrodes in 50% acetonitrile and acetate buffer at pH 5.0 yields an anodic current which decays to a negligible value within a few seconds. The mechanism for the oxidation is believed to involve preadsorption of the pesticide molecules onto the oxide-free electrode surface during cathodic polarization, followed by the oxide-catalyzed oxidation of the adsorbed molecules at anodic detection potential. Formation of a fully-developed gold oxide layer on the electrode surface inhibits adsorption of unreacted molecules and further oxidation of the analyte. The electrode fouling by surface oxide causes the anodic current to decay with time during detection at a constant potential (DC).

The properties of the oxidation of sulfur-containing pesticides on gold were utilized to design a pulsed potential waveform which can "continuously" reactivate a gold electrode involved in the oxidation of these analytes.

The resulting waveform consists of two potential steps. The faradaic signal is determined at the detection potential, E_{det} , for oxidation of the adsorbed analyte simultaneously with formation of the surface oxide. The surface of the gold electrode is then cleaned of the gold oxide by stepping the applied potential to a negative value near the negative limit for the solvent, E_{ads} , where gold oxide is reduced and adsorption of the analyte also occurs.

The use of the a two-step potential waveform has been termed "double potential pulsed amperometric detection". Execution of this waveform in flow-injection detection of sulfur-containing pesticides results in the maintenance of a high and uniform electrode activity making possible the reproducible anodic detection of these analytes. Since the mechanism of the anodic detection involves prior adsorption of the compounds, the shape of the calibration curve is strongly influenced by the adsorption isotherms of the analytes and, therefore, deviates from linearity at high concentrations. Detection limits below 100 ppb were determined for most compounds tested.

Double potential pulsed amperometric detection was applied to the detection of sulfur-containing pesticides separated by reversed phase high performance liquid chromatography (HPLC). The system utilized a C-18 reversed phase column with 50% acetonitrile in acetate buffer at pH

5.0 as the eluent. Detectability was increased significantly using preconcentration from a larger sample onto a C-18 forecolumn.

XII. SUGGESTED FUTURE RESEARCH

This research project has made possible the combination of Pulsed Amperometric Detection (PAD) and reversed phase High Performance Liquid Chromatography (HPLC). The advantage of the specificity of the separation has been achieved using a binary solvent system. Presently, separations are accomplished only by isocratic conditions. Although "gradient elution" is desirable, changing the eluent composition during the chromatographic run causes substantial drifting of the background current. The technique of Pulsed Coulometric Detection (PCD), currently being developed in this laboratory, could be applied to help elucidate this problem. PCD is able to compensate automatically for the background current; thus, a true indication of analyte oxidation is obtained upon sampling of the anodic current.

The lack of specificity in PAD is apparent. Prior separation of sulfur-containing pesticides by reversed phase HPLC is required for selective determination of specific pesticides in a mixture. The need for further work to develop chromatographic conditions suitable for the direct application of PAD is obvious.

Identification of the oxidation product of the detection reaction in PAD is an interesting problem. An inherent limitation of PAD is that only small amounts of

oxidation products are produced with the technique. Hence, it is impossible to identify and quantitate the oxidation products dissipated during the electrochemical oxidation with PAD in its present state. In this study, a prolonged oxidation of pesticide was accomplished using DC and PAD at a gold wire gauge electrode. Although sulfate ion was found as one of the oxidation products, other products containing the organic moieties are as yet unidentified. Liquid extraction with a proper organic solvent in conjunction with Mass Spectrometry and Gas Chromatography (GS/MS) should enable the identification and quantitation. It should be remembered that it always is questionable whether the oxidation products obtained in a batch cell after a prolonged electrolysis are the same as those obtained in situ during actual pulsed electrochemical detection. More research utilizing surface spectrometry should be done to elucidate this problem.

The process of oxidation of sulfur-containing pesticides could fully be understood by experimentally determining "n", the number of electron participating in the electrochemical oxidation with PAD in its present state. Chronocoulometry in a thin-layer cell developed in this research failed to answer the question. The phenomenon of electrode fouling during chronocoulometric process makes it obvious that a more detailed study of adsorption behavior of

analytes as well as their corresponding oxidation products on gold is needed. This, again, requires surface spectrophotometric techniques.

Finally, the response of the PAD technique for the detection of other sulfur-containing analytes with various electrode materials and binary solvent systems yet is remained for further investigation. Only then will the usefulness of PAD to reversed phase HPLC be accomplished to the full extent.

XIII. BIBLIOGRAPHY

1. Hanekamp, H. B.; Bos, P.; Frei, R. W. Trends in Anal. Chem. 1982, 1, 135.
2. Rucki, R. J. Talanta 1980, 27, 147.
3. Kissinger, P. T. Anal. Chem. 1977, 48, 447A.
4. Bratin, K.; Kissinger, P. T. J. Liq. Chromatogr. 1981, 4 (Suppl. 2), 321.
5. Jacobs, W. Current Separations 1982, 4, 45; Bioanalytical Systems, Inc., Newsletter, West Lafayette, IN.
6. Hartley, A. M.; Hiebert, A. G.; Cox, J. A. J. Electroanal. Chem. 1968, 17, 81.
7. Stojek, Z.; Kublik, Z. J. Electroanal. Chem. 1975, 60, 349.
8. Yoshida, Z. Bull. Chem. Soc. Jpn. 1981, 54, 562.
9. Kreuger, H. R.; O'Brien, R. D. J. Econ. Entomol. 1959, 52, 1063.
10. Umetsu, N.; Grose, H. F.; Allahyari, R.; Abu-El-Haj, S.; Fukuto, T. R. J. Agric. Food Chem. 1977, 25, 946.
11. Brooks, G. T. In "The Future for Insecticides", Metcalf, R. L. and McKelvey, J. J. Ed.; Wiley-Interscience: New York, 1976; pp. 97-143.
12. Schaeffer, C. H.; Wilder, W. H. J. Econ. Entomol. 1970, 63, 480.
13. Black, A. L., Chiu, Y. C.; Fahmy, M. A. H.; Fukuto, T. R. J. Agric. Food Chem. 1973, 21, 747.
14. Mendoza, C. E. J. Agric. Food Chem. 1969, 17, 1196.
15. McBain, J. B.; Yamamoto, I.; Casida, J. E. Life Sci. II 1971, 10 1311.
16. Wustner, D. A.; Desmarchelier, J.; Fukuto, T. R. Life Sci. II 1972, 11, 583.

17. Schrader, G. Verlag Chemie Weinheim 1963, 281.
18. Fukuto, T. R.; Metcalf, R. L.; March, R. B.; Maxon, M. G. J. Econ. Entomol. 1955, 48, 347.
19. Patchett, G. G.; Batcheldel, G. H. J. Agric. Food Chem. 1960.,8, 54.
20. Stambach, K.; Dalley, R.; Suter, R.; Szekely, G. Anal. Chem. 1963, 196, 332.
21. Aichenegg, P. C.; Gillen, L. E. U.S. Patent 3,454,679, CA.,1969, 71, 90816.
22. Crosby, D. G. Residue Rev. 1969, 25, 1.
23. Frawley, J. P.; Cook, J. W.; Blake, J. R.; Fitzhugh, O. G. J. Agric. Food Chem. 1958, 6, 28.
24. Ackermann, H. J. Chromatogr. 1968, 36, 309.
25. Okada, K.; Uchida, T. J. Agric. Chem. Soc. Jpn. 1962, 36, 245.
26. Dauterman, W. C. Bull. W. H. O. 1971, 44, 133.
27. Mitchell, T. H.; Ruzicka, J. H.; Thomson, J.; Wheals, B. B. J. Chromatogr. 1968, 32, 17.
28. Rosen, J. D. "The photochemistry of several pesticides in Environmental Toxicology of Pesticides", Matsumura, F., Boush, G. M., and Misato, T., Eds.; Academic Press: New York, 1982.
29. Niessen, H.; Teitz, H.; Frehse, H. Pflanzenschutz Nachr. Bayer 1962, 15, 129.
30. Stricks, W.; Chakravarti, S. K. Anal. Chem. 1962, 34, 508.
31. Zahradnik, R.; Zuman, P. Collect. Czech. Chem. Commun. 1959, 24, 1132.
32. Zuman, P.; Zahradnik, R. J. Phys. Chem. 1957, 208, 135.
33. Zahradnik, R. Collect. Czech. Chem. Commun. 1956, 21, 111.

34. Halls, D. J.; Townshend, A.; Zuman, P. Anal. Chim. Acta 1968, **40**, 459.
35. Kitakawa, T.; Taku, K. Bull. Chem. Soc. Jap. 1973, **46**, 2151.
36. Cauquis, G.; Lachenal, D. J. Electroanal. Chem. 1962, **34**, 508.
37. Bond, A. M.; Cassey, A. T.; Thackeray, J. R. J. Electrochem. Soc. 1973, **120**, 1502.
38. Bond, A. M.; Cassey, A. T.; Thackeray, J. R. J. Electroanal. Chem. 1973, **48**, 71.
39. Aoki, Y.; Takeda, M.; Uchiyama, M. J. Assoc. Off. Anal. Chem. 1975, **58**, 1286.
40. Mes, J.; Campbell, D. J. Bull. Environ. Contamin. & Toxicol. 1977, **16**, 53.
41. Johnson, L. D.; Waltz, R. H.; Ussary, J. P.; Kaiser, F. E. J. Assoc. Off. Anal. Chem. 1976, **59**, 174.
42. Kjolholt, J. Inter. J. Environ. Anal. Chem. 1985, **20**, 161.
43. Greenhalgh, R.; Nelson, M. A. J. Chromatogr. 1976, **128**, 157.
44. Luke, B. G.; Dahl, C. J. J. Assoc. Off. Anal. Chem. 1976, **59**, 1081.
45. Cochran, W. P. J. Chromatogr. Sci. 1979, **17**, 124.
46. Lawrence, J. F.; Turton, D. J. Chromatogr. 1978, **159**, 207.
47. Horvath, C.; Melander, W.; Molnar, I.; Molnar, P. Anal. Chem. 1975, **14**, 2295.
48. Majors, R. E. J. Chromatogr. Sci. 1977, **15**, 334.
49. Sparacino, C. M.; Hines, J. W. J. Chromatogr. Sci. 1976, **14**, 549.
50. Udenfriend, S. "Fluorescent Assay in Biology and Medicines"; Academic Press: New York, 1962; p. 461.

51. MacDougall, D. Residue Rev. 1962, 1, 24.
52. Argauer, R. J. In "Analytical Methods for Pesticides and Plant Growth Regulators"; Zwig, G. Ed.; Academic Press: New York, 1977; Vol. IX, Chapter 4.
53. Addison, J. B.; Semeluk, G. P.; Unger, I. J. Lumin. 1977, 15, 323.
54. Wustner, D. A.; Desmarchelier, J.; Fukuto, T. R. Life Sci. II. 1972, 11, 583.
55. Moye, H. A.; Wheaton, T. A. J. Agric. Food Chem. 1979, 27, 29.
56. Isshiki, K.; Tsumura, S.; Watanabe, R. J. Assoc. Off. Anal. Chem. 1980, 63, 747.
57. Frei, R. W.; Lawrence, J. F. J. Chromatogr. 1973, 83, 321.
58. Frei, R. W.; Lawrence, J. F.; Hope, J.; Cassidy, R. M. J. Chromatogr. Sci. 1974, 12, 40.
59. Polta, T. Z. Ph.D. Dissertation, Iowa State University, Ames, Iowa, 1986.
60. Uddin, Z. Ph.D. Dissertation, Iowa State University, Ames, Iowa, 1985.
61. Samec, Z.; Weber, J. Electrochim. Acta 1975, 20, 403.
62. Samec, Z.; Weber, J. Electrochim. Acta 1975, 20, 413.
63. Wierse, D. G.; Lohrengel, M. M.; Schultze, J. W. J. Electroanal. Chem. Interfacial Electrochem. 1978, 92, 121.
64. Van Huong, C. N.; Parsons, R.; Marcus, P.; Montes, S.; Ouder, J. J. Electroanal. Chem. Interfacial Electrochem. 1981, 119, 137.
65. Hamilton, I. C.; Woods, R. J. Appl. Electrochem. 1983, 13, 783.
66. Martins, M. E.; Castellano, C.; Calandra, A. J.; Aravia, A. J. J. Electroanal. Chem. Interfacial Electrochem. 1977, 81, 291.

67. Martins, M. E.; Castellano, C.; Calandra, A. J.; Aravia, A. J. J. Electroanal. Chem. Interfacial Electrochem. 1978, 92, 45.
68. Itabashi, E. J. Electroanal. Chem. Interfacial Electrochem. 1984, 177, 311.
69. Moscardo-Levelut, M. N.; Plichon, V. J. Electrochem. Soc. 1984, 131, 1538.
70. Moscardo-Levelut, M. N.; Plichon, V. J. Electrochem. Soc. 1984, 131, 1545.
71. Koryta, J.; Pradac, J. J. Electroanal. Chem. Interfacial Electrochem. 1968, 17, 177.
72. Reynaud, J. A.; Malfoy, B.; Canesson, P. J. Electroanal. Chem. Interfacial Electrochem. 1980, 114, 195.
73. Safronov, A. Y.; Tarasevich, M. R.; Bogdanovskaya, V. A.; Chernyak, A. S. Elektrokhimiya 1983, 19, 421.
74. Zakharov, V. A.; Bessarabova, I. M.; Songina, O. A.; Timoshkin, M. A. Elektrokhimiya 1971, 7, 1215.
75. Zakharov, V.A. Nov. Polyarogr., Tezisy Dokl. Vses. Soveshch. Polyarogr.; 6th 1975, 119; Chem. Abstr. 1977, 86, 10026c.
76. Buckley, A. N.; Hamilton, I. C.; Woods, R. J. Electroanal. Chem. 1987, 216, 213.
77. Finklea, H. O.; Avery, S.; Lynch, M. Langmuir 1987, 3, 409.
78. Koen, J. G.; Huber, J. F. K. Anal. Chem. Acta 1970, 51, 303.
79. Koen, J. G.; Huber, J. F. K.; Poppe, H.; den Boef, G. J. Chromatogr. Sci. 1970, 8, 192.
80. Zietek, M. Mikrochim. Acta, 1976, 463.
81. Zietek, M. Mikrochim. Acta, 1976, 549.
82. Budnikov, G. K.; Toropova, V. F.; Ulakhavich, A. N.; Viter, I. P. Z. Anal. Khimii, 1974, 29, 1204.

83. Halls, D. J.; Townshend, A.; Zuman, P. Anal. Chim. Acta, 1968, 41, 51.
84. Brand, J. D.; Fleet, B. Analyst, 1970, 95, 905.
85. Budnikov, G. K.; Supin, G. S.; Ulakhavich, N. A.; Shakurova, N. K. Z. Anal. Chimii, 1975, 30, 2275.
86. Clark, G. J.; Goodin, R. R.; Smiley, J. W. Anal. Chem., 1985, 57, 2223.
87. Ding, X. D.; Krull, I. S. J. Agric. Food Chem. 1984, 32, 622.
88. Hughes, S.; Meschi, P. L.; Johnson, D. C. Anal. Chim. Acta 1981, 132, 1.
89. Hughes, S.; Johnson, D. C. Anal. Chim. Acta 1981, 132, 11.
90. Hughes, S.; Johnson, D. C. Anal. Chim. Acta 1982, 30, 712.
91. Hughes, S.; Johnson, D. C. Anal. Chim. Acta 1983, 149, 1.
92. Edwards, P.; Haak, K. Am. Lab 1983, 4, 78.
93. Rocklin, R. D.; Pohl, C. A. J. Liq. Chromatogr. 1983, 6, 1577.
94. Neuburger, G. G.; Johnson, D. C. Anal. Chem. In Press.
95. Neuburger, G. G.; Johnson, D. C. Anal. Chem. In Press.
96. Polta, J. A.; Johnson, D. C. J. Liq. Chromatogr. 1983, 6, 1727.
97. Polta, J. A.; Johnson, D. C. J. Chromatogr. 1985, 324, 407.
98. Rocklin, R.D. Adv. Chem. Ser. 1985, 210, 13.
99. Polta, J. A.; Johnson, D. C. Anal. Chem. 1985, 57, 1373.

100. Thomas, M. B.; Sturrock, P. E. J. Chromatogr. 1986, 357, 318.
101. Ohsawa, K.; Yoshimura, Y.; Watanabe, S.; Tanaka, H.; Yokato, A.; Tamura, K.; Imaeda, K. Anal. Sci. 1986, 2, 165; Chem. Abstr. 1986, 105, 17715w.
102. Polta, T. Z.; Johnson, D. C. J. Electroanal. Chem. 1986, 209, 159.
103. Polta, T. Z.; Johnson, D. C. J. Electroanal. Chem. 1986, 209, 171.
104. Larew, L. A.; Mead, D. A.; Johnson, D. C. J. Anal. Chim. Acta, in press.
105. Welch, L. E.; Mead, D. A.; Johnson, D. C. Anal. Chim. Acta, in press.
106. Grahame, D. C. Chem. Rev. 1947, 41, 441.
107. Mohilner, D. M. Electroanal. Chem. 1966, 1, 1.
108. Payne, R. Tech. Electrochem. 1972, Chapter 2.
109. Osteryoung, R. A.; Lauer, G.; Anson, F. C. Anal. Chem. 1962, 34, 1833.
110. Osteryoung, R. A.; Lauer, G.; Anson, F. C. J. Electrochem. Soc. 1963, 110, 926.
111. Christie, J. H.; Anson, F. C.; Lauer, G.; Osteryoung, R. A. Anal. Chem. 1963, 35, 1973.
112. Bard, A. J.; Faulker, L. R. In "Electrochemical Methods"; John Wiley & Sons, Inc.: New York, 1980.
113. Anson, F. C. Anal. Chem. 1966, 38, 54.
114. Christie, J. H.; Osteryoung, R. A.; Anson, F. C. J. Electroanal. Chem. 1967, 13, 236.
115. Anson, F. C.; Christie, J. H.; Osteryoung, R. A. J. Electroanal. Chem. 1967, 13, 348.
116. Kostelitz, M.; Domange, J. L.; Oudar, J. Surf. Sci. 1973, 34, 431.

117. Meschi, P. L.; Johnson, D. C. Anal. Chim. Acta 1981, 124, 303.
118. Hoare, J. P. J. Electrochem. Soc.: Electrochemical Science and Technology, 1984, 808.
119. Eto, M. In "Organophosphorus pesticides: Organic and Biological Chemistry"; CRC Press: Cleveland, Ohio, 1974; p. 66.
120. Thomas, M. B.; Sturrock, P. E. J. Chromatogr. 1986, 357, 318.
121. Polta, T. Z.; Johnson, D. C.; Luke, G. R. J. Electroanal. Chem. 1986, 209, 171.
122. Drevenkar, V.; Frobe, Z.; Stengl, B.; Stefanac, Z. Anal. Chim. Acta 1983, 154, 277.
123. Aue, W. A.; Kapila, S.; Hastings, C. R. J. Chromatogr. 1972, 73, 99.
124. Riggin, R. M.; Howard, C. C. Anal. Chem. 1979, 51, 210.
125. Renberg, L.; Lindstrom, K. J. Chromatogr. 1981, 214, 327.
126. Bushway, R. J. J. Chromatogr. 1981, 211, 135.
127. Drevenkar, V.; Frobe, Z.; Stengl, B.; Tkalcevic, B. Mikrochimica Acta 1985, 1, 143.
128. Kjolholt, J. Intern. J. Environ. Anal. Chem. 1985, 20, 161.
129. Ault, J. A.; Schofield, C. M.; Johnson, L. D.; Waltz, R. H. J. Agric. Food Chem. 1979, 27, 825.
130. LeBel, G. L.; Williams, D. T.; Griffith, G.; Benoit, F. M. J. Assoc. Off. Anal. Chem. 1979, 62, 241.
131. Ambrus, A.; Hargitai, E.; Karoly, G.; Fulop, A.; Lantos, J. J. Assoc. Off. Anal. Chem. 1981, 64, 743.

XIV. ACKNOWLEDGEMENTS

I wish to express my gratitude to Professor Dennis Johnson for his guidance and support throughout my graduate study. His technical expertise as well as his unique ability to encourage are deeply appreciated.

The financial support from the Chemistry Department at Iowa State University in the form of a teaching assistant and the grant from Dionex Corporation are gratefully acknowledged.

I owe a great deal to everybody at the Chemistry Machine Shop at Iowa State University. Eldon Ness and his co-workers had made all "home-made" apparatus possible, especially the Coulometric flow-through cell. Their friendship, quality of work and prompt service are greatly appreciated.

I also would like to acknowledge the past and present members of the electrochemistry group for their friendship and exchange of ideas. A special thanks to Theresa Polta who gave me advice and initial guidance for my research project. I thank Andy Tang for his time and patience in helping me with technical problems in electrical instrumentation. I recognize Larry Welch, my lab mate, who made the second half of my graduate research more enjoyable with his friendship and entertainment. I thank Bill LaCourse for typing the first draft of this thesis.

I wish to recognize my two children, Daniel and Alisa, who were born in the United State while I was pursuing my Ph.D. study at Iowa State University. Daniel, who was born while I was taking my written preliminary examination, has been my "Lucky charm". Through him I have learned determination and persistence. I also thank Alisa for her cooperation and companionship while I was writing this thesis.

Lastly, to my dear husband, Preecha, I give a very special thanks. The extensive sharing of ideas has been both technically productive as well as intellectually and emotionally stimulating. I will always be indebted for his constant patience, companionship and love.